Investigating the feasibility of generating chimeric intergroup rotavirus triple-layered virus-like particles on SA11 double-layered particles

P le Roux

orcid.org/0000-0002-9106-4442

Dissertation accepted in partial fulfilment of the requirements for the degree *Master of Science in Biochemistry* at the North-West University

Supervisor: Prof AA van Dijk

Graduation May 2023

27249964

Abstract:

There remains a need for safer and more effective human rotavirus (RV) vaccines, despite the availability of several commercial rotavirus vaccines, especially given that RV is a leading cause of diarrhoea-related deaths worldwide among children younger than 5 years old. After the first 12 months following vaccination, the vaccine efficacy of the main commercially available RV vaccines was 44% in the high-mortality settings of developing countries of Africa and Asia which is lower than the 77% to 98% efficacy of the medium- to low-mortality settings of developed countries. This may also be due to the different strains of rotavirus present in developing countries of Africa and Asia compared to those strains upon which these vaccines are based. Therefore, non-replicating regional-specific vaccines may be needed in populations with partial immunity to overcome this gap in vaccine efficacy.

Baculovirus-expressed RV VP2/4/6/7 triple-layered particles (TLPs) are promising candidate dead subunit vaccines that have been shown to protect against RV infections in several animal models. However, producing these multicomponent particles using a co-infection strategy is difficult and ineffective. Our previous co-infection results visualised by transmission electron microscopy (TEM) revealed problems with the assembly of RV-TLPs. Less than 30% were fully assembled RV-TLPs when co-infected with dualcistronic recombinant baculoviruses (rBVs) expressing VP2/6 and VP4/7.

It was hypothesized that the partial assembly of RV-TLPs may have been due to a lack of calcium during assembly. Therefore, in this study, we attempted to generate fully assembled RV-TLPs using dualcistronic rBVs expressing RVA/Human-wt/ZAF/GR10924/1999/G9P[6] VP2 and VP6 co-infected with dualcistronic rBVs expressing either genotype G12P[4], G12P[6], or G12P[8] VP4 and VP7 in media supplemented to 20mM calcium. However, only RV-DLPs were formed when using a co-infection strategy despite the additional calcium supplementation.

To overcome the inherent disadvantage of co-infections, where it is impossible to control the ratios at which individual cells are infected, multi-gene baculovirus donor plasmids have previously been developed, but they have not been widely implemented.

In this study, we further investigated the feasibility of generating a single recombinant baculovirus expressing all four RVA/Simian-tc/ZAF/SA11-N5/1958/G3P5B[2] TLP proteins (VP2/6/4/7). A pFastBACquad donor plasmid containing insect cell codon-optimised open reading frames (ORFs) of all four SA11 TLP proteins was designed, purchased and used in a Bac-to-Bac Baculovirus vector expression system (BVES) to generate quadcistronic rBVs expressing SA11 VP2/6/7/4 simultaneously in the same cell. Using these quadcistronic rBVs, fully assembled SA11 RV-TLPs were generated and visualized using TEM.

Therefore, using quadcistronic rBVs in a Bac-to-Bac BVES presents a better and more cost-effective platform to investigate the formation of RV virus-like particles, than using a co-infection approach using dualcistronic rBVs, and was successful in generating fully assembled SA11 VP2/6/4/7 TLPs.

The results presented herein serve as proof of principle that quadcistronic rBVs in a Bac-to-Bac BVES may be used to investigate the extent to which SA11 VP2/6 DLPs may serve as a universal backbone for generating heterologous VP2/6/4/7 RV-TLPs with a variety of regional-specific VP4/7 outer capsids as regional-specific subunit vaccine candidates against RV. Further, chimeric RV-TLPs may be instrumental in evaluating RV structural compatibility and stability by using recombinant baculoviruses as a vector, thereby avoiding any possible known, or unknown, genetic restrictions that may affect the generation of chimeric rescued RVs generated by a reverse genetics system. Baculovirus-generated TLPs may also aid basic research into the start of the RV replication cycle by investigating viral entry into host cells.

Keywords: Rotavirus, rotavirus virus-like particles, Bac-to-Bac baculovirus expression system, multicistronic expression, SA11 VP2/6/4/7 triple-layered particles, transmission electron microscopic visualisation.

“Magna opera Domini exquisita in omnes voluntates ejus!”

Acknowledgements:

I am immensely grateful towards the following:

- Prof. Albie (A.A.) Van Dijk for years of supervision, training, advice, guidance, proofreading, mentoring, and for her academic and moral support.

- Prof. A.C. Potgieter for academic advice and resources.

- Dr. Anine Jordaan for initial electron micrographs.

- Mr. Mohammad Jaffer for electron micrographs of RV-TLPs.

- Jayme Herbert, Luan Theart, Martin Visser, Strauss Van Graan, Marno Huyzers, and Khanyisile Hlongwane for practical and technical advice during experiments, as well as creating a friendly work environment conducive to studying.

- My dear friends for their unwavering moral support. Especially for Karnu Van Heerden, Johan Koen, Liam Hugo, Jayme Herbert, Chandre Liebenberg, Annemie Calitz, Simon Brace, Job Voster, and Jaccie Zeelie.

- My parents, Ronel and Jaco le Roux, for their love and support.

- My lovely dear Anandie for all her immense love, care, prayers and support!

- The German Research Foundation (DFG), the Poliomyelitis Research Foundation (PRF) and North-West University (NWU) for their financial support.

Table of contents:

List of figures: 8
List of Tables: 10
Chapter 1: Literature review 11
1.1. The impact of rotavirus infection 11
1.2. Efficacy of commercial rotavirus vaccines 11
1.3. Rotavirus genome segments, proteins and particles 12
1.4. Rotavirus classification and nomenclature 14
1.5. Rotavirus zoonosis 17
1.6. Prevalent RV G- and P-types in Africa 17
1.7. The role of VP2, VP6, VP7 and VP4 in protection against RV diarrhoea 18
1.8. The rotavirus replication cycle 20
1.9. The role of calcium in virus propagation and formation 22
1.10. Rotavirus virus-like particles 23
1.11. Generation of chimaeric VLPs derived from consensus genome sequences of human RV strains co-circulating in Africa 25
1.12. Multicistronic baculovirus expression systems 27
1.13. Structural compatibility between the RNA-dependent RNA polymerase (VP1) of RVA and RVG 28
1.14. Problem statement 32
1.15. Aims 32
Chapter 2: Evaluating the effect of calcium supplementation on assembly of chimeric RV-VLPs with RV strain GR10924 DLPs and African strain outer capsids. 33
2.1. Introduction 34
2.2. Materials and Methods 35
2.2.1. Introduction 35
2.2.2. Rotavirus strains, plasmids, bacteria, insect cell lines, and bacmids 38
2.2.3. Design and purchase of a pFastBACdual donor plasmid for the expression of RV GR10924 VP2 and VP6 40
2.2.4. Preparation of competent bacterial cells 40
2.2.5. Propagation of donor plasmids 41
2.2.6. Purification of donor plasmids 42
2.2.7. Generation of recombinant bacmids 43
2.2.8. Purification of recombinant bacmids 43
2.2.9. Confirmation of transposition of ORFs encoding RV proteins into the recombinant bacmid via PCR 44
2.2.10. Agarose gel electrophoresis 46
2.2.11. Insect cell propagation 46
2.2.12. Generation of recombinant baculoviruses expressing RV VP2, VP6, VP4 and VP7 47
2.2.13. Quantification and purification of baculovirus stocks 48
2.2.14. Propagation of baculoviruses 49
2.2.15. Generation of amplified plaque-purified baculovirus stocks 50
2.2.16. Immuno-fluorescent monolayer assay (IFMA) 50
2.2.17. Preparation of proteins from Sf9 insect cells 52
2.2.18. Sodium dodecyl sulphate-polyacrylamide gel electrophoresis (SDS-PAGE) 52
2.2.19. Western blot analysis 53

2.2.20. Production of RV-DLPs 54
2.2.21. Production of chimaeric RV-VLPs 54
2.2.22. Verification of the production of chimaeric rotavirus-like particles using transmission electron microscopy (TEM) 54
2.3. Results and Discussion 55
2.3.1. Preparation of RVA/Human-wt/ZAF/GR10924/1999/G9P[6] DLPs 55
2.3.2. Generation of recombinant baculoviruses expressing RVA/Human-wt/ZAF/GR10924/1999/G9P[6] VP2 and VP6 58
2.3.3. Retrieval of three archived recombinant bacmids (rBacmid_G12P[4], rBacmid_G12P[6], and rBacmid_G12P[8]) 66
2.3.4. Generation of rBV_G12P[4], rBV_G12P[6], and rBV_G12P[8] 68
2.3.5. Evaluation of the assembly of baculovirus-expressed RV proteins into chimaeric RV-VLPs 72
2.4. Summary 74
Chapter 3: Investigating the possibility of generating RV-TLPs using recombinant quadcistronic VP2/6/4/7 recombinant baculoviruses. 77
3.1. Introduction 77
3.2. Materials and Methods 78
3.2.1. Design of pFastBACquad donor plasmids containing insect cell codon-optimised ORFs encoding RV VP2/6/4/7 78
3.2.2. Preparation of competent bacterial cells 80
3.2.3. Isolation of RV SA11 TLPs and verification assembly by TEM 81
3.2.4. Quantification of Rotavirus virus-like particle yield 82
3.3. Results and Discussion 83
3.3.1. Preparation of recombinant bacmids encoding RV SA11 VP2, VP6, VP4, and VP7 83
3.3.2. Generation of a quadcistronic rBV_SA11_VP2/6/4/7 85
3.3.3. TEM evaluation of the assembly of RV-VLPs from quadcistronic rBVs expressing RV SA11 VP2, VP6, VP4 and VP7 91
3.3.4. Caesium chloride isopycnic separation of RV-VLPs 94
3.4. Summary 101
Chapter 4: Concluding Discussion 102
Appendix A: Conference outputs 109
Appendix B: Abbreviations 110
Appendix C: Permissions 113
Reference list: 127

List of Figures:

Figure 1.1: Rotavirus dsRNA genome segments visualised on SDS-PAGE and cryo-EM reconstruction of the RV-TLP 13
Figure 1.2: A model of the positions of neutralization escape mutations selected by various mAbs against VP7 of RRV 19
Figure 1.3: The rotavirus replication cycle 20
Figure 1.4: Schematic representation of *in vitro* RV-TLP (VP2/6/7) assembly and disassembly by altering calcium concentration 21
Figure 1.5: A ribbon diagram of the RRV VP7 trimer and a single subunit displaying secondary structure elements 22
Figure 1.6: Electron micrographs of native SA11 DLPs, native SA11 virions, the first chimeric RV-DLPs and the first chimeric RV-TLPs 24
Figure 1.7: RV-VLPs generated in insect cells using wild-type bacmid strains directly isolated from stool samples.. 26
Figure 1.8: Maximum likelihood phylogenetic tree of RV groups and the structure of RV RdRp (RV VP1) 30
Figure 1.9: RV clade A and clade B VP1 viral (+)ssRNA recognition 30
Figure 2.1: Diagram of the Bac-to-Bac® System 37
Figure 2.2: Plasmid maps of pFastBACdual, pFastBACquad, and pFBd_GR10924_VP2-VP6 39
Figure 2.3: Schematic representation of the expected PCR amplicon sizes of transposed bacmid DNA 45
Figure 2.4: Agarose gel of PCR of bacmid DNA 57
Figure 2.5: IFMA of Sf9 insect cells infected with rBV_GR10924_VP2/6 60
Figure 2.6: SDS-PAGE of RVA/Human-wt/ZAF/GR10924/1999/G9P[6] VP2 and VP6 expressed by plaque-purified rBV_GR10924_VP2/6. 62
Figure 2.7: SDS-PAGE (I) and western blot analysis (II) of the expression of RVA/Human-wt/ZAF/GR10924/1999/G9P[6] VP2 and VP6 by plaque-purified rBV_GR10924_ VP2/6 64
Figure 2.8: Electron micrograph of RVA/Human-wt/ZAF/GR10924/1999/G9P[6] VP2/6 DLPs 65
Figure 2.9: Agarose gel of PCR of isolated bacmid DNA encoding African RV strain VP4 and VP7 (genotypes G12P[4], G12P[6], and G12P[8]) 67

Figure 2. 10: SDS-PAGE of prepared proteins from rBV_G12P[4], rBV_G12P[6], and rBV_G12P[8] before plaque purification 68
Figure 2.11: SDS-PAGE of lysed Sf9 insect cells infected with plaque-purified (I) rBV_G12P[4] and (II) rBV_G12P[8] 70
Figure 2.12: IFMA of Sf9 insect cells infected with rBV_G12P[4]_PL3, rBV_G12P[6]_PL3, and rBV_G12P[8]_PL3 71
Figure 2.13: SDS-PAGE of RV-VLPs from lysates ultracentrifuged through a 40% sucrose cushion 72
Figure 2.14: Electron micrograph of co-infected Sf9 insect cells 73
Figure 3.1: Plasmid maps of pFBq donor plasmids 79
Figure 3.2: Agarose gel of PCR of bacmid DNA encoding RV SA11 VP2, VP6, VP4 and VP7 84
Figure 3.3: IFMA of Sf9 insect cells infected with rBV_SA11_VP2/6/4/7**.....** 86
Figure 3.4: SDS-PAGE of baculovirus expressed RV proteins of plaque-purified rBV_SA11_VP2/6/4/7 88
Figure 3.5: Western blot of lysates of Sf9 cells infected with rBV_SA11_VP2/6/4/7 following ultracentrifugation through a 40% sucrose cushion. 90
Figure 3.6: SDS-PAGE of three cell lysates of Sf9 cell infected with rBV_SA11_VP2/6/4/7 92
Figure 3.7: Electron micrograph of RVA/Simian-tc/ZAF/SA11-N5/1958/G3P5B[2] RV-VLPs 93
Figure 3.8: Ultracentrifuged lysates of Sf9 cells infected with rBV_SA11_VP2/6/4/7 95
Figure 3.9: Electron micrographs of RVA/Simian-tc/ZAF/SA11-N5/1958/G3P5B[2] VP2/6/4/7 TLPs 97

List of Tables:

Table 1.1: Coding assignment of the genome segments, main functions and distinctive properties of rotavirus proteins 14
Table 1.2: Comparing the RV group with the species infected 15
Table 1.3: Whole-genome classification for some human, bovine, porcine, simian, and avian rotavirus strains 16
Table 1.4: A summary of the most prevalent RV strains detected in southern and eastern Africa between 2010 and 2015 18
Table 1.5: A description of the pFBq constructs prepared from genomic data obtained from human faecal samples containing African RV strains 26
Table 1.6: Terminal sequence of RV (+)ssRNA encoding RV VP1 29
Table 2.1: Various RV strains, relevant ORFs and encoded proteins that were used in this part of the study. 38
Table 2.2: Primer sequences as recommended in the Invitrogen® Bac-to-Bac® BEVS manual 45
Table 2.3: The titer of various rBV_GR10924_VP2/6 P1 stocks and the relevant white colony (from Fig 2.4) and recombinant bacmid. 59
Table 3.1: Rotavirus strains and genome segments used in the pFBq donor plasmids. 78
Table 3.2: The titer of various rBV_SA11_VP2/6/4/7 P1 stocks and the relevant white colony (from Fig. 3.2) and corresponding recombinant bacmids. 85
Table 3.3: The titer of rBV_SA11_VP2/6/4/7 plaque stocks at passage 4 89
Table 3.4: RV-VLP concentration and yield following ultracentrifugation 93
Table 3.5: RV-VLP concentration and yield following ultracentrifugation 96

Chapter 1: Literature review

1.1. The impact of rotavirus infection

Rotavirus (RV) was, in 2016, the primary cause of diarrhoea-related deaths worldwide among children younger than 5 years old (Troeger, Blacker*, et al.*, 2018). In 2016 the estimated mortality was 128 500, of which 104 733 were in sub-Saharan Africa (Troeger, Khalil*, et al.*, 2018). Rotavirus infects mature enterocytes of the small intestine resulting in acute gastroenteritis (AGE) in small children as well as infants (Bishop *et al.*, 1973).

Rotavirus may also be fatal to animals during the neonatal period which is deleterious to the economic stability of many animal farming ventures (Dhama *et al.*, 2009). Bovine rotaviruses (BRV) contribute to enteritis and diarrhoea in intensively reared neonatal calves (Dhama *et al.*, 2009; Malik *et al.*, 1996; Mebus *et al.*, 1977; Mebus *et al.*, 1971; Mebus *et al.*, 1973; Mebus *et al.*, 1969; Pisanelli *et al.*, 2005; Rathi *et al.*, 2007; Singh & Pandey, 1988). Rotavirus also affects piglets (Lecce *et al.*, 1976), foals (Flewett *et al.*, 1975), lambs (Snodgrass *et al.*, 1976), rabbits (Bryden *et al.*, 1976), and various other animals leading to the loss of livestock (Dhama *et al.*, 2009; Holland, 1990; Kaminjolo & Adesiyun, 1994; Malik *et al.*, 1996).

1.2. Efficacy of commercial rotavirus vaccines

In humans, live attenuated RV vaccines are administered before 15 weeks of age to prevent severe RV diarrhoea. The efficacy of two of the main commercial vaccines, RotaTeq and Rotarix, is lower in developing countries compared to that in developed countries (Burnett *et al.*, 2020; Henschke *et al.*, 2022; Jonesteller *et al.*, 2017; Page *et al.*, 2018; Tate *et al.*, 2012). Within the first year following vaccination vaccine efficacy of the main commercially available vaccines ranged from 48% to 57% (Henschke *et al*., 2022). After 12 months the vaccine efficacy in high-mortality settings of developing countries was 44% compared to the efficacy in medium- and low-mortality settings of developed countries which was 77% and 98%, respectively (Clark *et al.*, 2019).

Rotarix, RIX4414, is a live neonatal G1P[8] strain of rotavirus attenuated by successive passaging in cell culture (Richard & David, 2009). The commercial RV vaccines RotaTeq and RotaSiil are interspecies bovine-human RV reassortant vaccines. They utilize a universal bovine double-layered particle (DLP) backbone with

VP4 and VP7 from different human strains. RotaTeq is a bovine-human re-assortment containing human VP7s from G1, G2, G3, and G4 strains and the VP4 from a P[1] strain on a bovine VP2/6 double-layered particle backbone (Heaton *et al.*, 2005; Matson, 2006). The RV vaccines RotaSiil and RotaVac developed in India are becoming available. RotaSiil is a heat-stable bovine-human reassortant vaccine containing VP7s from G1, G2, G3, G4, and G9 strains and a bovine VP2/6 double-layered particle backbone (Naik *et al.*, 2017). RotaVac is a neonatal human RV vaccine derived from a naturally attenuated and reassorted RV strain, 116E, which is a G9P[11] RV strain containing a bovine VP4 (Bhan *et al.*, 1993; Bhandari *et al.*, 2014).

The low efficacy of two of the main commercial RV vaccines in developing countries compared to developed countries may be due to malnutrition, environmental enteropathy, passive transfer of maternal antibodies or genetic factors such as differences in sialic acid residues or histo-blood group antigens (HBGAs) (Desselberger, 2017). Another factor may be the result of different strains of rotavirus present in developing countries of Africa and Asia compared to those upon which these vaccines are based (Isanaka *et al.*, 2021; Jason *et al.*, 2010; Jere *et al.*, 2014; Nelson *et al.*, 2009; Varghese *et al.*, 2022). Therefore, there is a need for further development of locally rationally designed RV vaccines or vaccine booster candidates to cover the gap in the efficacy of the current RV vaccines.

In cases where live RV vaccines were administered, but only resulted in partial immunity, the gap in efficacy cannot be filled by another live RV vaccine. Live RVs must be able to replicate in an individual to a sufficient level to invoke an immune response. However, if a live attenuated vaccine against RV is given to an already vaccinated person the existing immunity will hamper its replication. Non-replicating rotavirus virus-like particles (RV-VLPs) are promising candidates as RV dead subunit boosters for humans since RV-VLPs have been shown to protect against RV infections in animal models, such as mice (Redmond *et al.*, 1993), gnotobiotic pigs (Saif & Fernandez, 1996) and rabbits (Ciarlet *et al.*, 1998). VLPs can be produced in large quantities and administered to people and animals without the need to reproduce and should effectively invoke a sufficient immune response to improve partial immunity in humans as well.

1.3. Rotavirus genome segments, proteins and particles

The RV virion is a triple-layered particle (TLP) (Flewett *et al.*, 1974). As illustrated in Fig. 1.1, the viral genome consists of eleven genome segments (GS) of dsRNA coding for twelve proteins, listed in Table 1.1, six structural and six non-structural proteins. The viral inner core consists of 60 dimers of the 94 kDa VP2 (GS2) (Labbé *et al.*, 1991). The middle layer consists of 260 trimers of the 45 kDa VP6 (GS6) (Prasad *et al.*, 1988). The outer layer consists of 780 monomers (260 trimers) of the glycosylated 37 kDa VP7 (GS9) (Prasad *et al.*, 1988) and spikes formed by 60 trimers of the protease-sensitive 87 kDa VP4 (GS4) (Dormitzer *et al.*, 2004; Settembre *et al.*, 2011). The 6 structural proteins form three layers with VP2 constituting the outer layer of the single layered-particle (SLP) which is 45 nm in diameter (Bican *et al.*, 1982; Labbé *et al.*, 1991). Rotavirus VP2 and VP6 constitute a double layered-particle (DLP) (Trask *et al.*, 2012) which is approximately 70 nm in diameter (Crawford *et al.*, 1994; Jere *et al.*, 2014; Palomares & Ramírez, 2009). If the DLP is covered by VP4 and VP7 it constitutes a TLP which is 75-80 nm in diameter (Crawford *et al.*, 1994; Jere *et al.*, 2014; Palomares & Ramírez, 2009). The outer capsid protein VP7 is glycosylated (Cohen *et al.*, 1979; Espejo *et al.*, 1981; Estes *et al.*, 1982; Mason *et al.*, 1980; Rodger *et al.*, 1977), and VP4 is protease-sensitive (Almeida *et al.*, 1978; Estes *et al.*, 1981; Matsuno *et al.*, 1977).

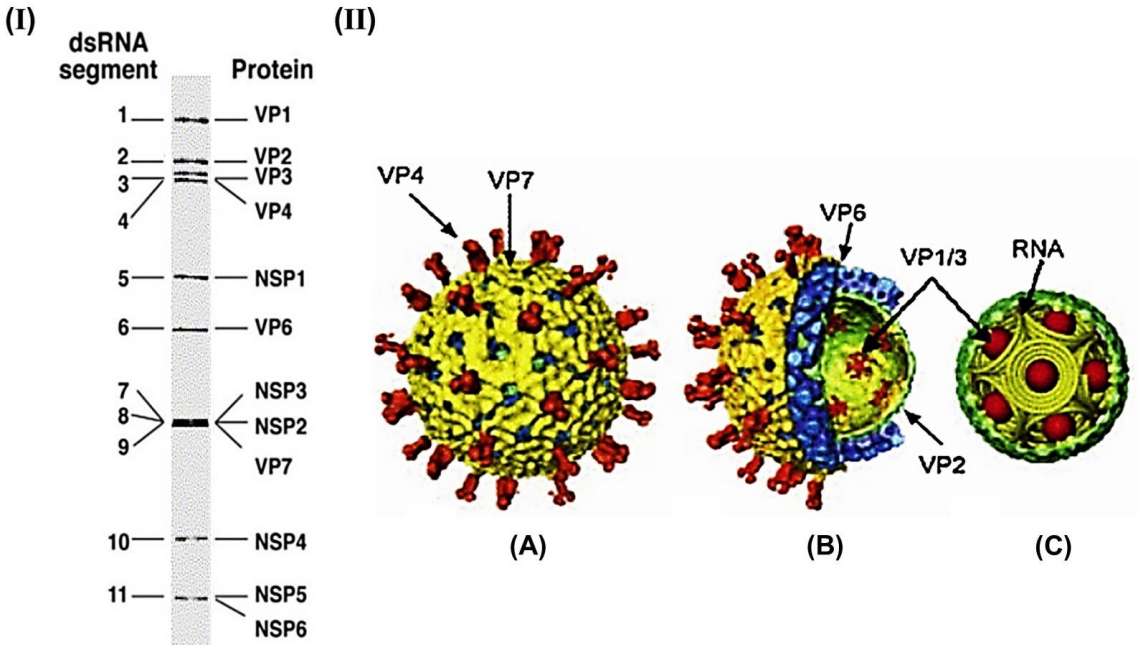

Figure 1.1: Rotavirus dsRNA genome segments visualised on SDS-PAGE and cryo-EM reconstruction of the RV-TLP. (I) SDS-PAGE displaying the 11 dsRNA genome segments comprising the rotavirus group A (RVA) genome. The genome segments are numbered on the left and the corresponding proteins they encode are denoted on the right. **(II)** Cryo-EM reconstruction of the RV-TLP. **(A)** Rotavirus TLP with VP4 (coloured orange) and VP7 (coloured yellow). **(B)** Cutaway view of

the RV-TLP showing the VP6 (coloured blue) and VP2 (coloured green) and the transcriptional enzymes (coloured red) anchored inside of the VP2 core particle. **(C)** Cutaway view of the RV core particle showing the VP2 (coloured green), the transcriptional enzymes VP1 and VP3 (coloured red) and packaged dsRNA. Figure 1.1 is adapted from Desselberger (2014) with permission.

Table 1.1: Coding assignment of the genome segments, main functions and distinctive properties of rotavirus proteins. Adapted from Attoui *et al*. (2012) with permission.

Genome segment	Protein	Molecular weight (kDa)	Number of molecules	Location	Main function
1	VP1	125	12	Core vertices	**R**NA-dependent RNA polymerase
2	VP2	94	120	Inner shell	**C**ore-shell protein
3	VP3	97	12	Core vertices	**M**ethyl-transferase
4	VP4	88	180	Surface spike	**P**rotease-sensitive
5	NSP1	59	-	Cytoskeleton	Interferon **A**ntagonist
6	VP6	45	780	Inner capsid	**I**ntermediate capsid shell
7	NSP3	37	-	Viroplasm, ER	**T**ranslation enhancer
8	NSP2	35	-	Viroplasm	**N**TPase
9	VP7	34 and 38	780	Surface	**G**lycosylated
10	NSP4	20	-	Viroplasm, ER	**E**nterotoxin
11	NSP5 & NSP6	22	-	Viroplasm, ER	P**H**osphoprotein

The denoted size of the encoded proteins was based on the simian RV strain RVA/Vervet monkey-tc/ZAF/SA11-4F/1958/G3P6[1]. The molecules were calculated per virion from structural studies of purified virions and were confirmed by X-ray crystallography studies (McClain *et al.*, 2010; Prasad *et al.*, 1994; Prasad *et al.*, 1990). The bolded and capitalized letters are used to designate the genome segment in RV classification.

1.4. Rotavirus classification and nomenclature

Rotaviruses (Latin *rota*, “wheel”) are named after their wheel-like appearance (Flewett *et al.*, 1974). Rotaviruses constitute the genus *Rotavirus*, one of the six genera of the *Sedoreoviridae* family (Matthijnssens *et al.*, 2022).

The classification of RVs into serogroups is based on antigenic differences of VP6 and was proposed in 1985 (Graham & Estes, 1985). Currently, there are 9 serogroups of RVs, namely RV groups A-D and F-J, listed with the species they infect in Table 1.2 (Ferrari *et al.*, 2022). The RVA strains (Bishop *et al.*, 1973; Malherbe & Strickland-Cholmley, 1967) are the most widely studied of the RV groups since they cause life-threatening diarrhoea in infants, mammals and avian species. RVBs (Bridger, 1980; Chen *et al.*, 1985) and RVHs (Alam *et al.*, 2007) are associated with diarrhoeal disease in older children and adults. RVC (Saif *et al.*, 1980) has thus far been associated with limited outbreaks of gastroenteritis in institutional settings and families. RVE was

isolated from diseased pigs in 1986 (Pedley *et al.*, 1986) and has subsequently not been isolated again, nor has any sequence data of RVE been produced despite various attempts (Matthijnssens *et al.*, 2019; Walker *et al.*, 2020). Therefore RVE has been removed as a RV group (Ferrari *et al.*, 2022; Matthijnssens *et al.*, 2019; Walker *et al.*, 2020). RVD (Pedley *et al.*, 1986), RVF (McNulty *et al.*, 1984), and RVG (McNulty *et al.*, 1984) have only been recovered from birds. RVI occurs in dogs (Mihalov-Kovács *et al.*, 2015). RVJ has been reported in bats (Bányai *et al.*, 2017; Ferrari *et al.*, 2022).

Table 1.2: Comparing the RV group with the species infected:

RV Group	Species in which this RV group causes diarrhoea
A	A primary cause of life-threatening diarrhoea in infants Mammalian and avian species
B	Older children and adults
C	In institutional settings, in children and families
D	Birds
F	Birds
G	Birds
H	Older children and adults
I	Dogs
J	Bats

In 1989 a binary classification system was developed. Rotaviruses were classified into P (VP4) or G (VP7) serotypes based on immunological reactivity and gene structures. This antigenic classification based on serotypes was gradually extended by a sequence-based classification system of rotaviruses into genome segment 4 (encoding VP4) or genome segment 9 (encoding VP7) genotypes (Gentsch *et al.*, 1992; Gouvea *et al.*, 1990; Iturriza-Gomara *et al.*, 1999; Iturriza-Gómara *et al.*, 2004). Currently, there are 36P- and 51G types (RCWG, 2020).

Initially, human rotavirus strains were grouped into three human rotavirus genogroups identified using RNA-RNA hybridization (Flores *et al.*, 1982), the Wa, DS-1 and AU-1 genogroups (Nakagomi *et al.*, 1989).

In 2008 whole-genome sequence-based genotyping for RV classification (Table 1.3) was introduced (Matthijnssens, Ciarlet, Heiman*, et al.*, 2008; Matthijnssens, Ciarlet, Rahman*, et al.*, 2008). Whole-genome sequence-based genotyping is reflected as Gx-

P[x]-Ix-Rx-Cx-Mx-Ax-Nx-Tx-Ex-Hx, representing the genotypes of the genome segments encoding VP7-VP4-VP6-VP1-VP2-VP3-NSP1-NSP2-NSP3-NSP4-NSP5, respectively. The capitalized letter designating each protein coincides with its main function (Fig. 1.1). The letter is followed by an Arabic number for the corresponding genotype, which is here indicated by an "x". For instance, GS6 (VP6) is designated by an "I" for "Intermediate capsid shell" followed by an Arabic number. Genome segment 2 (VP2) is designated by a "C" for "Core-shell protein" followed by an Arabic number.

Table 1.3: Whole-genome classification for some human, bovine, porcine, simian, and avian rotavirus strains (Matthijnssens, Ciarlet, Heiman*, et al.*, 2008):

			VP[7]	VP4	VP6	VP1	VP2	VP3	NSP1	NSP2	NSP3	NSP4	NSP5
→ Wa	Hu	Wa-like	G1	P[8]	I1	R1	C1	M1	A1	N1	T1	E1	H1
KU	Hu	Wa-like	G1	P[8]	I1	R1	C1	M1	A1	N1	T1	E1	H1
Dhaka16-03	Hu	Wa-like	G1	P[8]	I1	R1	C1	M1	A1	N1	T1	E1	H1
D	Hu	Wa-like	G1	P[8]	I1	R1	C1	M1	A1	N1	T1	E1	H1
P(rice)	Hu	Wa-like	G3	P[8]	I1	R1	C1	M1	A1	N1	T1	E1	H1
ST3	Hu	Wa-like	G4	P[6]	I1	R1	C1	M1	A1	N1	T1	E1	H1
IAL28	Hu	Wa-like	G5	P[8]	I1	R1	C1	M1	A1	N1	T1	E1	H1
WI61	Hu	Wa-like	G9	P[8]	I1	R1	C1	M1	A1	N1	T1	E1	H1
B3458	Hu	Wa-like	G9	P[8]	I1	R1	C1	M1	A1	N1	T1	E1	H1
RMC321	Hu	Wa-like	G9	P[19]	I5	R1	C1	M1	A1	N1	T1	E1	H1
Dhaka12-03	Hu	Wa-like	G12	P[6]	I1	R1	C1	M1	A1	N1	T1	E1	H1
Matlab13-03	Hu	Wa-like	G12	P[6]	I1	R1	C1	M1	A1	N1	T2	E1	H1
B4633-03	Hu	Wa-like	G12	P[8]	I1	R1	C1	M1	A1	N1	T1	E1	H1
Dhaka25-02	Hu	Wa-like	G12	P[8]	I1	R1	C1	M1	A1	N1	T1	E1	H1
→ DS-1	Hu	DS-1-like	G2	P[4]	I2	R2	C2	M2	A2	N2	T2	E2	H2
TB-Chen	Hu	DS-1-like	G2	P[4]	I2	R2	C2	M2	A2	N2	T2	E2	H2
B1711	Hu	DS-1-like	G6	P[6]	I2	R2	C2	M2	A2	N2	T2	E2	H2
DRC86	Hu	DS-1-like	G8	P[6]	I2	R2	C2	M2	A2	N2	T2	E2	H2
DRC88	Hu	DS-1-like	G8	P[8]	I2	R2	C2	M2	A2	N2	T2	E2	H2
69M	Hu	DS-1-like	G8	P[10]	I2	R2	C2	M2	A2	N2	T2	E2	H2
L26[a]	Hu	DS-1-like	G12	P[4]	I2	R2	C2	M1/M2	A2	N1	T2	E2	H1
N26-02	Hu	DS-1-like	G12	P[6]	I2	R2	C2	M2	A2	N1	T2	E6	H2
RV176-00	Hu	DS-1-like	G12	P[6]	I2	R2	C2	M2	A2	N2	T2	E6	H2
RV161-00	Hu	DS-1-like	G12	P[6]	I2	R2	C2	M2	A2	N2	T2	E1	H2
→ Au-1	Hu	AU-1-like	G3	P[9]	I3	R3	C3	M3	A3	N3	T3	E3	H3
T152	Hu	AU-1-like	G12	P[9]	I3	R3	C3	M3	A12	N3	T3	E3	H6
NCDV-Lincoln	Bo		G6	P[1]	I2	R2	C2	M2		N2	T6	E2	
BRV033	Bo		G6	P[1]	I2	R2	C2	M2	A3	N2	T6	E2	H3
RF	Bo		G6	P[1]	I2	R2	C2	M2	A3	N2	T6	E2	H3
Uk	Bo		G6	P[5]	I2	R2	C2	M2	A3	N2	T7	E2	H3
WC3	Bo		G6	P[5]	I2	R2	C2	M2	A3	N2	T6	E2	H3
KJ44	Bo		G5	P[1]	I1	R1	C1	M2	A1	N1	T1	E1	H1
KJ75	Bo		G5	P[5]	I1	R1	C1	M2	A1	N1	T1	E1	H1
A131	Po		G3	P[7]	I5	R1	C2	M1	A1	N1	T1	E1	H1
Gottfried	Po		G4	P[6]	I1	R1	C1	M1	A8	N1	T1	E1	H1
OSU	Po		G5	P[7]	I5	R1	C1	M1	A1	N1	T1	E1	H1
A253	Po		G11	P[7]	I5	R1	C2	M1	A1	N1	T1	E1	H1
YM	Po		G11	P[7]	I5	R1	C1	M1	A8	N1	T1	E1	H1
PO-13	Av		G18	P[17]	I4	R4	C4	M4	A4	N4	T4	E4	H4
SA11g4"O" (5N)	Si		G3	P[1]	I2	R2	C5	M5	A5	N5	T5	E2	H5
SA11-5S	Si		G3	P[1]	I2	R2	C5	M5	A5	N5	T5	E2	H5
SA11-30/19	Si		G3	P[1]	I2	R2	C5	M5	A5	N5	T5	E2	H5
SA11-30/1A	Si		G3	P[1]	I2	R2	C5	M5	A5	N5	T5	E2	H5
→ SA11-H96	Si		G3	P[2]	I2	R2	C5	M5	A5	N5	T5	E2	H5
SA11-Both	Si		G3	P[2]	I2	R2	C5	M5	A5	N2	T5	E2	H5

The Wa-, DS-1 or AU-1-like genogroup was assigned to human strains if at least seven genome segments belonged to the respective Wa-, DS-1, or AU-1-like genotype. Colours were added to visualize certain patterns or genome constellations. Green, red, and orange indicate Wa-like, DS-1-like, and AU-like genome segments, respectively. Yellow, blue, and purple indicate the avian PO-13-like rotavirus genome segments; some typical porcine VP4, VP7, and VP6 genotypes; and the SA-11-like gene segments, respectively. Figure adapted from Matthijnssens, Ciarlet, Heiman*, et al.* (2008) with permission.

Genome segment 2 (VP2) and GS6 (VP6) of the RVA/Simian-tc/ZAF/SA11-N5/1958/G3P5B[2] (SA11-N5 RVA) (Table 1.3) were used in this project. SA11-H96

was isolated in 1958 from a rectal swap of an overtly healthy vervet monkey (*Cereopithecus aethiops pygerythrus*) (Malherbe and Strickland-Cholmley, 1967).

Two VP2 and VP6 DLPs were used in this project as backbones for the assembly of VP2/6/4/7 VLPs. The VP2-VP6 (I2-C5) DLP of SA11-N5 was used (Table 1.1), and the DS-1-like VP2-VP6 (I2-C2) DLP of RVA/Human-wt/ZAF/GR10924/1999/G9P[6] (Jere *et al.*, 2011) used by Jere and co-workers (2012).

1.5. Rotavirus zoonosis

It has been experimentally demonstrated that some RV strains can cross species barriers. Animals, such as calves, monkeys and pigs have been infected with human RV which induced diarrhoeal illness (Mebus *et al.*, 1976; Torres-Medina *et al.*, 1976; Wyatt *et al.*, 1976). Conversely, animal rotavirus strains have been shown to infect humans such as the bovine nebraska calf diarrhoea virus (NCDV) and the rhesus rotavirus (RRV). This was observed during studies which evaluated the safety and efficacy of rotavirus vaccines involving volunteers and during field studies (Nakagomi *et al.*, 1987; Vesikari *et al.*, 1983; Vesikari *et al.*, 1984; Wyatt *et al.*, 1983).

With the development of whole-genome sequence-based genotyping, evidence emerged showing that human rotaviruses belonging to the Wa-like genogroup (green in Table 1.3) have a common origin with porcine rotaviruses and human rotaviruses belonging to the DS-1-like genogroup (red in Table 1.3) have a common origin with bovine rotaviruses (Matthijnssens, Ciarlet, Heiman*, et al.*, 2008).

The zoonotic effect of some rotaviruses has been determined to be due to structural conformational variation, such as strain-dependent variation in VP8* conformation for host glycan recognition (Hu *et al.*, 2015; Stencel-Baerenwald *et al.*, 2014).

1.6. Prevalent RV G- and P-types in southern and eastern Africa

A six-year surveillance period of RV strains in southern and eastern Africa utilizing G- and P- typing, showed that G1, G2, G3, G8, G9, and G12, and that P[4], P[6], and P[8] were prevalent in southern and eastern Africa, listed in Table 1.4. Of the strains, 23.8% were G1P[8], followed by G2P[4] at 11.8%, G9P[8] at 10.4%, G12P[8] at 4.9%, G2P[6] at 4.2% and G3P[6] at 3.7%. Atypical rotavirus G- and P-type combinations (such as G1P[4], G2P[8], G9P[4] and G12P[4]) were also detected at a low frequency of 2% and may have arisen through reassortment (Seheri *et al.*, 2018).

Table 1.4: A summary of the most prevalent RV strains detected in southern and eastern Africa between 2010 and 2015 Seheri *et al.* (2018):

Strain	Prevalence
G1P[8]	23.8%
G2P[4]	11.8%
G9P[8]	10.4%
G12P[8]	4.9%
G2P[6]	4.2%
G3P[6]	3.7%
Atypical rotavirus G- and P-type combinations	2%

1.7. The role of VP2, VP6, VP7 and VP4 in protection against RV diarrhoea

The correlates of protection from RV infections have not been completely defined, but many studies have implicated neutralizing antibody responses (Crawford *et al.*, 1999).

Monoclonal antibodies (MAbs) against RV VP6 have been shown to inhibit the transcription process (Ginn *et al.*, 1992) and to protect against RV infection in mice (Burns *et al.*, 1996; Mathieu, 2001) regardless of VP6 nanostructure (Tamminen *et al.*, 2020).

The P (VP4) and G (VP7) serotypes represent independently segregating neutralization epitopes eliciting antibodies capable of neutralizing rotavirus infectivity and inducing protective immunity (Fields *et al.*, 1996; Shaw *et al.*, 1986). The target of the VP4 P-type-specific (homotypic) neutralizing antibodies on VP4 is definitive of the specific P genotype/serotype. The target of the G-type-specific (homotypic) neutralizing antibodies on VP7 is definitive of the G serotype/genotype (Clarke & Desselberger, 2015). However, the conserved epitopes on VP4 and VP7 are possibly responsible for heterotypic protection (Clarke & Desselberger, 2015). A predominantly homotypic antibody response is characteristic of initial exposure to RV, in contrast to broader heterotypic responses that are induced by repeated exposure to RV even when individual infections are composed of restricted numbers of G-types (Clarke & Desselberger, 2015; O'Ryan *et al.*, 1994). The immune response against RV is initially primed against the exposed epitopes of the RV outer capsid proteins of VP7 and VP4, leading to the generation of homotypic neutralizing antibodies. However, following repeated exposure to RVs heterotypic antibodies are induced against non-

neutralizing, but conserved, epitopes of the outer capsid proteins or against different RV proteins, leading to heterotypic immunity (Clarke & Desselberger, 2015).

VP7 is the second most abundant protein in the virion. The crystal structure of the rhesus rotavirus (RRV, serotype G3) VP7 trimer has been determined in complex with the Fab fragment of neutralizing mAb 4F8 (Shaw *et al.*, 1986) as illustrated in Fig. 1.2. The 4F8 Fab binds across the trimer interface of VP7, stabilizing it even at calcium concentrations that would normally lead to dissociation. Known VP7 epitopes map either to the same region of the trimer surface as the 4F8 Fab or to a region at the inter-domain boundary within a subunit. It has been shown that the 4F8 Fab fragment neutralizes infectivity (Ludert *et al.*, 2002; Shaw *et al.*, 1986), with a half-maximal inhibitory concentration (IC_{50}) around 30- to 50-fold higher than that of the intact divalent IgG. This blocks the uncoating of RV virion and is the principal mechanism of neutralization by antibodies that recognize epitopes at the subunit interface (Trask *et al.*, 2012).

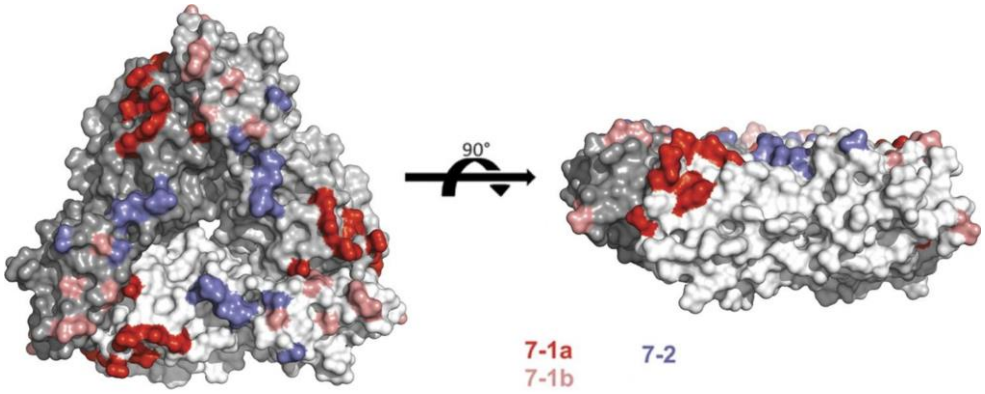

Figure 1.2: A model of the positions of neutralization escape mutations selected by various mAbs against VP7 of RRV (Aoki *et al.*, 2009). The residues roughly cluster into two regions designated as 7-1 and 7-2. Region 7-1 spans the intersubunit boundary which has been divided into 7-1a (red), on one side of the interface, and 7-1b (pink), on the other. The residues in 7-2 are in blue. The 4F8 Fab has contacts in both regions 7-1a and region 7-1b (Aoki *et al.*, 2011). The figure is taken from Aoki *et al.* (2009) with permission.

However, there is some uncertainty about which neutralization antigen is immunodominant. The results from studies of children naturally infected with human rotaviruses or bovine-human virus reassortants suggest that VP4 may be the immunodominant neutralization antigen in a homotypic response (Christy *et al.*, 1993; Ciarlet *et al.*, 1998; Ward *et al.*, 1993). However, data from another study of children suggested that VP7 is the immunodominant neutralization antigen (Ciarlet *et al.*, 1998; Ward *et al.*, 1990). In contrast, the protective efficacy of VP 2/6/7 TLPs or VP 2/6 DLPs

were poor in rabbit models, suggesting that the presence of VP4-specific intestinal IgG may be required to induce high levels of protection against RV infection (Ciarlet *et al.*, 1998). These results from experiments in rabbits suggest that both VP4 and VP7 neutralization antigens may be required in a parenteral immunogen to induce protection from rotavirus infection (Ciarlet *et al.*, 1998).

1.8. The rotavirus replication cycle

Rotavirus infects mature enterocytes of the small intestine resulting in acute gastroenteritis (AGE) in young children, and infants (Bishop *et al.*, 1973) as well as a variety of animals. The RV replication cycle is illustrated in Fig. 1.3.

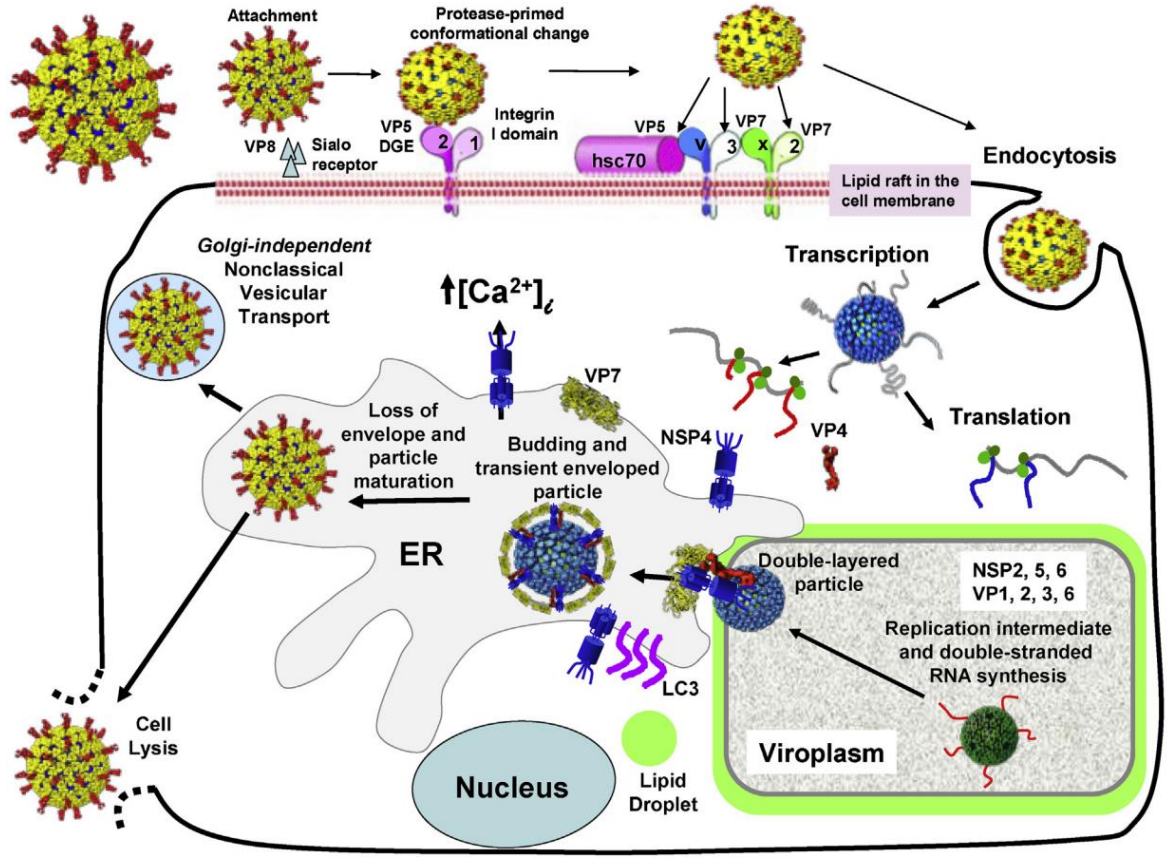

Figure 1.3: The rotavirus replication cycle. The RV-TLPs initially attach to sialoglycans (or histo-blood group antigens) on the host cell surface, thereafter the RV-TLP interacts with the other cellular receptors, including integrins and Hsc70. Via receptor-mediated endocytosis, the RV particle is internalized. Lowered calcium concentrations in the endosome result in the uncoating of the outer layer, resulting in the release of transcriptionally active DLPs into the cytoplasm. These DLPs initialise rounds of mRNA transcription, which subsequently are used to translate viral proteins. Following sufficient viral protein synthesis, the RNA genome is replicated and packaged into newly generated DLPs in the viroplasms, which interact with lipid droplets. Newly generated DLPs bind to NSP4, which serves as an endoplasmic reticulum (ER) receptor, and bud into the ER. Further, NSP4 acts as a viroporin to release calcium from intracellular stores. Transiently enveloped particles are visualised in the ER. As RV outer capsid proteins (VP4 and VP7) assemble, the transient membranes are removed, resulting in the formation of mature TLPs. Progeny virions are released via cell lysis. In polarized epithelial cells, particles are released via a non-classical vesicular transport mechanism. The figure is taken with permission from Desselberger (2014).

The replication cycle consists of several steps. The attachment of the virus to the cell is mediated by VP4 and VP7. Once the VP4 spikes of RV-TLPs come into contact with the cellular receptor of the host cell, conformational changes occur such that the lipophilic domains of VP5* that are normally hidden below VP8* become exposed on the surface of the TLP in the form of a 'post-penetration umbrella' conformation (Kim *et al.*, 2010; Settembre *et al.*, 2011). Treatment of RV particles with trypsin seems to cause this necessary protease-primed conformational change (Crawford *et al.*, 2001; Espejo *et al.*, 1981; Mason *et al.*, 1980).

Following the binding of the TLP via VP4, the exact mechanism of penetration of RV particles is unclear. Most likely viral entry occurs by endocytosis. After entry, both outer capsid proteins, VP4 and VP7, are removed from the TLP to yield a DLP. The VP7 trimers are stabilized by calcium (Cohen *et al.*, 1979). Lowering the calcium concentration during endocytosis causes the uncoating of the TLPs and the release of the transcriptionally active DLPs into the cytoplasm (Salgado *et al.*, 2018), as illustrated in Fig. 1.4.

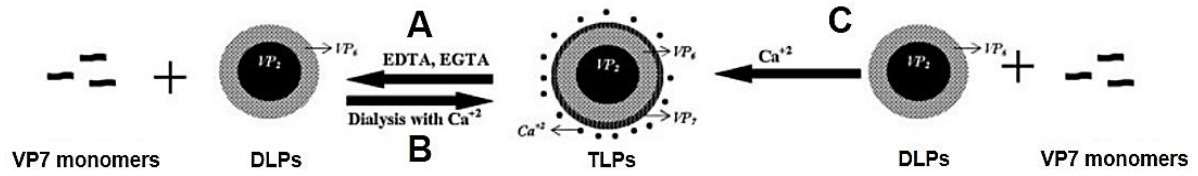

Figure 1.4: Schematic representation of *in vitro* RV-TLP (VP2/6/7) assembly and disassembly by altering calcium concentration. Rotavirus TLP (VP2/6/7) disassembly by decreasing calcium (**A**), reassembly of VP7 monomers onto DLPs by the addition of calcium (**B**), and the experimental procedure of RV assembly (**C**). The figure was taken with permission from Mellado *et al.* (2009).

DLP release is followed by plus-strand ssRNA, (+)ssRNA, synthesis mediated by VP1, VP3, and VP2. Thereafter the viroplasm is formed which mediates (+)ssRNA packaging, minus-strand RNA synthesis (replication) and DLP formation. NSP4 is a transmembrane glycoprotein located on the membrane of the endoplasmic reticulum (ER) (Au *et al.*, 1989; Chasey, 1980; Petrie *et al.*, 1982; Petrie *et al.*, 1984) and is an intracellular receptor for the new DLPs located at the periphery of the viroplasms. NSP4 interacts with VP6 during their budding towards the lumen of the ER (Maass & Atkinson, 1990; Taylor *et al.*, 1996). In the ER, DLPs are coated with VP7 and VP4 in the presence of a high concentration of calcium to form TLPs. The mature RVs are then released from the cell via various pathways (Gardet *et al.*, 2006; McNulty *et al.*, 1976).

1.9. The role of calcium in virus propagation and formation

Rotaviruses alter and utilize calcium signalling to control replication, morphogenesis, and pathogenesis (Greenberg & Estes, 2009). Rotavirus infections cause at least a 3-fold increase in intracellular calcium concentrations, and up to a 10-fold increase in the uptake of calcium into cells (Brunet *et al.*, 2000; Ruiz *et al.*, 2000).

As illustrated in Fig. 1.5, calcium bound to VP7 monomers stabilizes VP7 trimers (Aoki *et al.*, 2009; Cohen *et al.*, 1979). There are two Ca^{2+} ions bound at each subunit interface in the VP7 trimer (Trask *et al.*, 2012). Lowering the calcium concentration during endocytosis causes the uncoating of the TLP and the release of the DLP (Salgado *et al.*, 2018). The ER is a store of calcium in the cell (LaFerla, 2002). Rotavirus NSP4 contains a viroporin domain (VPD) which conducts calcium ions from the ER to the intracellular compartment (Hyser *et al.*, 2010; Hyser *et al.*, 2012; Pham *et al.*, 2017) which releases calcium from the intracellular stores (Tian *et al.*, 1994) thereby elevating the intracellular calcium concentration which is needed to stabilize the VP7 outer layer of progeny TLPs. Interaction of NSP4 with the cellular calcium sensor molecule STIM1 is necessary for viroporin function (Hyser *et al.*, 2013). DLPs are coated in the ER with VP7 and VP4 in the presence of high concentrations of calcium to form TLPs (Adams & Kraft, 1967; Altenburg *et al.*, 1980; Holmes *et al.*, 1975; Lecatsas, 1972; McNulty *et al.*, 1976; Poruchynsky *et al.*, 1991; Ruiz *et al.*, 2000; Saif *et al.*, 1978). *In vitro* assembly of VP7 onto VP6 has been shown to be calcium dependent (Ready *et al.*, 1988).

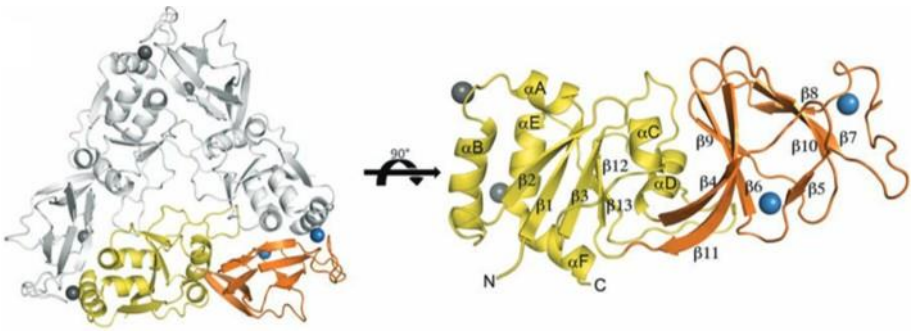

Figure 1.5: A ribbon diagram of the RRV VP7 trimer and a single subunit displaying secondary structure elements. The RRV VP7 trimer (left), viewed along its three-fold axis (i.e., as if looking onto the surface of the virion) with one subunit and one pair of Ca^{2+} ions in colour and the other two subunits in grey. The Rossmann-fold domain (domain I) is in yellow, the β-barrel domain (domain II) is in orange,

and the Ca^{2+} ions are in blue. Right is a single subunit, inside view with secondary structure elements labelled. The figure is taken from Aoki *et al.* (2009) with permission.

1.10. Rotavirus virus-like particles

Virus-like particles (VLPs) are self-assembling viral complexes of the native viral capsid but do not contain genetic material. Thus, they cannot reproduce, however, they can elicit protective immune responses similar to that of the wild-type rotavirus. Most RV-VLPs have been prepared for developing rotavirus vaccine candidates (Crawford *et al.*, 1994; Istrate *et al.*, 2008).

The advantages of RV-VLPs for vaccine purposes are that they are (i) non-infectious as they do not contain genomic material and thus cannot replicate adding to the safety of using RV-VLPs as vaccines (Charlton Hume *et al.*, 2019; Crawford *et al.*, 1994); (ii) are highly immunogenic when formulated with the appropriate adjuvants (Istrate *et al.*, 2008) as the viral proteins are in their natural conformation (Brussow *et al.*, 1990); (iii) can be genetically manipulated to provide broader protection by incorporating several RV serotypes (Crawford *et al.*, 1994; Kim *et al.*, 2002); and (iv) are amenable to large-scale production (Jere *et al.*, 2014; Vieira *et al.*, 2005). Also, RV-VLPs can induce homotypic and heterotypic protection from RV challenges (Crawford *et al.*, 1999; Redmond *et al.*, 1993).

Baculovirus expression systems have been utilized for the production of SLPs (VP2) and DLPs (VP2/6) of RV-VLPs (Fig. 1.6) since 1991 (Labbé *et al.*, 1991) and for TLPs (VP2/6/7 or VP2/6/7/4) (Fig. 1.6) since 1994 (Crawford *et al.*, 1994). Baculovirus-produced VP2, VP6, VP4 and VP7 have been shown to auto-assemble *in vitro* (Crawford *et al.*, 1994; Estes *et al.*, 1984; Ready *et al.*, 1988; Redmond *et al.*, 1993). RV-VLPs are promising candidates for human RV vaccines as they have been shown to protect against rotavirus infections in animal models, such as mice (Redmond *et al.*, 1993), gnotobiotic pigs (Saif & Fernandez, 1996), and rabbits (Ciarlet *et al.*, 1998).

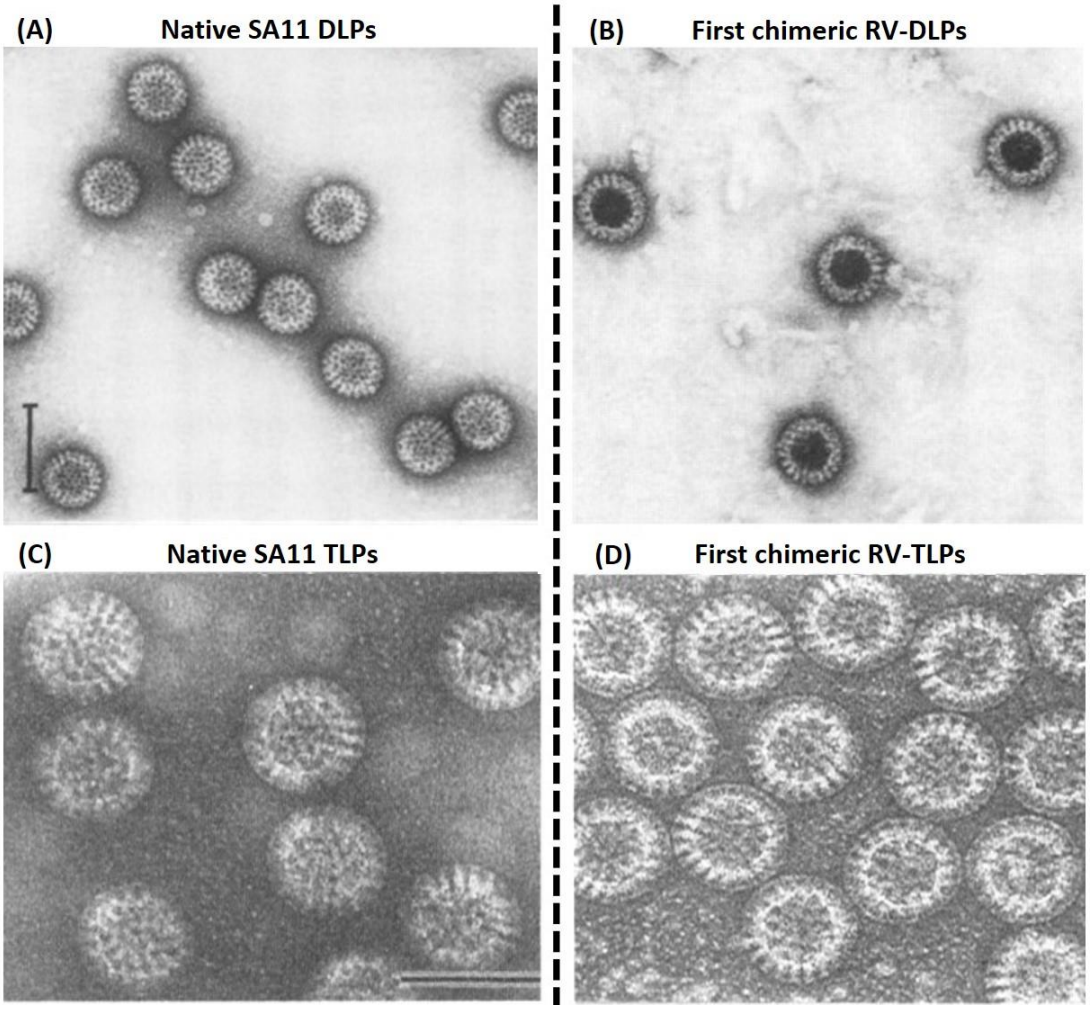

Figure 1.6: Electron micrographs of native SA11 DLPs, native SA11 virions, the first chimeric RV-DLPs and the first chimeric RV-TLPs. (A) Native double-layered SA11 virus particles purified from SA11-infected MA104 cells (Labbé *et al.*, 1991). **(B)** First chimeric DLPs were formed by coexpression of heterologous SA11 RV strain VP2 and RF RV strain VP6 in Sf9 (*S. frugiperda* 9) insect cells (Labbé *et al.*, 1991). Figures (A) and (B) were taken from Labbé *et al.* (1991) with permission. **(C)** Native triple-layered SA11 virus particles purified from SA11-infected MA104 cells (Crawford *et al.*, 1994) **(D)** First chimeric TLPs (VP2/6/7 or VP2/6/7/4) were formed in Sf9 insect cells (Crawford *et al.*, 1994). Figures (C) and (D) were taken from Crawford *et al*. (1994) with permission.

RV-VLPs generated from non-human rotavirus strains have been shown to induce protective immunity against rotavirus challenges in mice (Zhou *et al.*, 2011). Mice that were immunised with RV-TLP experimental vaccines containing VP2/4/6/7 proteins that were generated from strain SA11 elicited serum-neutralising antibodies (Crawford *et al.*, 1999). Further, several RV-VLPs prepared from bovine rotaviruses have been utilized to induce immune responses in various animal models (El-Attar *et al.*, 2009; Kim *et al.*, 2002; Madore *et al.*, 1999; Parez *et al.*, 2006; Vieira *et al.*, 2005).

Also, RV-VLPs may serve as part of multimeric dead subunit vaccines against rotavirus and other viruses. Rotavirus VP6 is a strong adjuvant in mouse models

(Blazevic *et al.*, 2016; Malm *et al.*, 2017; Tamminen *et al.*, 2020) and has been proposed as a candidate for a multivalent dead subunit vaccine against rotavirus, enterovirus, and norovirus (Blazevic *et al.*, 2016; Heinimäki *et al.*, 2019; Malm *et al.*, 2017; Tamminen *et al.*, 2020, 2021). Rotavirus VP6 elicits a stronger immune response against enterovirus (Heinimäki *et al.*, 2019) and norovirus (Blazevic *et al.*, 2016; Malm *et al.*, 2017) when RV VP6 is used with viral structural proteins of these viruses (Heinimäki *et al.*, 2019; Tamminen *et al.*, 2020).

RV-VLPs have other applications than vaccine candidates. RV-VLPs may have applications in nanotechnology. Due to their natural epithelial cell tropism (Bishop *et al.*, 1973) they can efficiently transfer bioactive molecules to other specific target tissues. RV-VLPs have been demonstrated to be useful as potential drug delivery systems to the gut as novel nanocarriers (Cortes-Perez *et al.*, 2010). RV-VLPs may be used in understanding the interaction between rotaviruses and their hosts. Also, important for this project, is their application in basic research to understand the structural conformation of rotavirus particles, and the functions of the structural proteins (Crawford *et al.*, 1994; Labbé *et al.*, 1991; Mathieu, 2001).

1.11. Generation of chimaeric VLPs derived from consensus genome sequences of human RV strains co-circulating in Africa

Transcapsidated chimaeric RV-VLPs were generated of regional specific outer capsid proteins onto a RVA/Human-wt/ZAF/GR10924/1999/G9P[6] (GR10924) (Jere *et al.*, 2011) VP2 and VP6 DLP backbone. The consensus genome sequences of African RVs (G2, G8, G9 or G12 strains associated with either P[4], P[6] or P[8] genotypes) were characterised directly from human stool samples (Jere *et al.*, 2014). This removed the need for the extremely time-consuming endeavour of tissue-adapting rotaviruses (Ward *et al.*, 1984; Ward *et al.*, 1988; Ward *et al.*, 1991). This novel approach of Jere and co-workers (2014) may be instrumental in speeding up vaccine research and development.

The codon-optimized sequences for insect cell expression of genome segments 4 (VP4) and 9 (VP7) were cloned via restriction digestion into pFBq donor plasmids, listed in Table 1.5, and used in a Bac-to-Bac Baculovirus expression system to generate RV-VLPs, Fig. 1.7.

Table 1.5: A description of the pFBq constructs prepared from genomic data obtained from human faecal samples containing African RV strains. The highlighted pFBq were those selected for this project. The table was taken from Jere *et al.* (2012).

Cloning strategy	pFBq constructs
Monocistronic: with one gene coding for VP7	pFBqG2 [a], pFBqG8 [a], pFBqG12 [a, ¥]
Monocistronic: with one gene coding for VP4	pFBqP[4] [b, ¥], pFBqP[8] [b, ¥]
Dualcistronic: with two genes coding for VP4 and VP7	pFBqG2P[6] [c, ¥], pFBqG2P[4] [c], pFBqG2P[8] [c], pFBqG8P[4] [d], pFBqG8P[8] [d, ¥], pFBqG12P[4] [e, ¥], pFBqG12P[8] [e, ¥], pFBqG8P[6] [f], pFBqG12P[6] [f, ¥], pFBqG9P[4] [f, ¥], pFBqG9P[8] [f, ¥], pFBqG9P[6] [f, ¥, †]

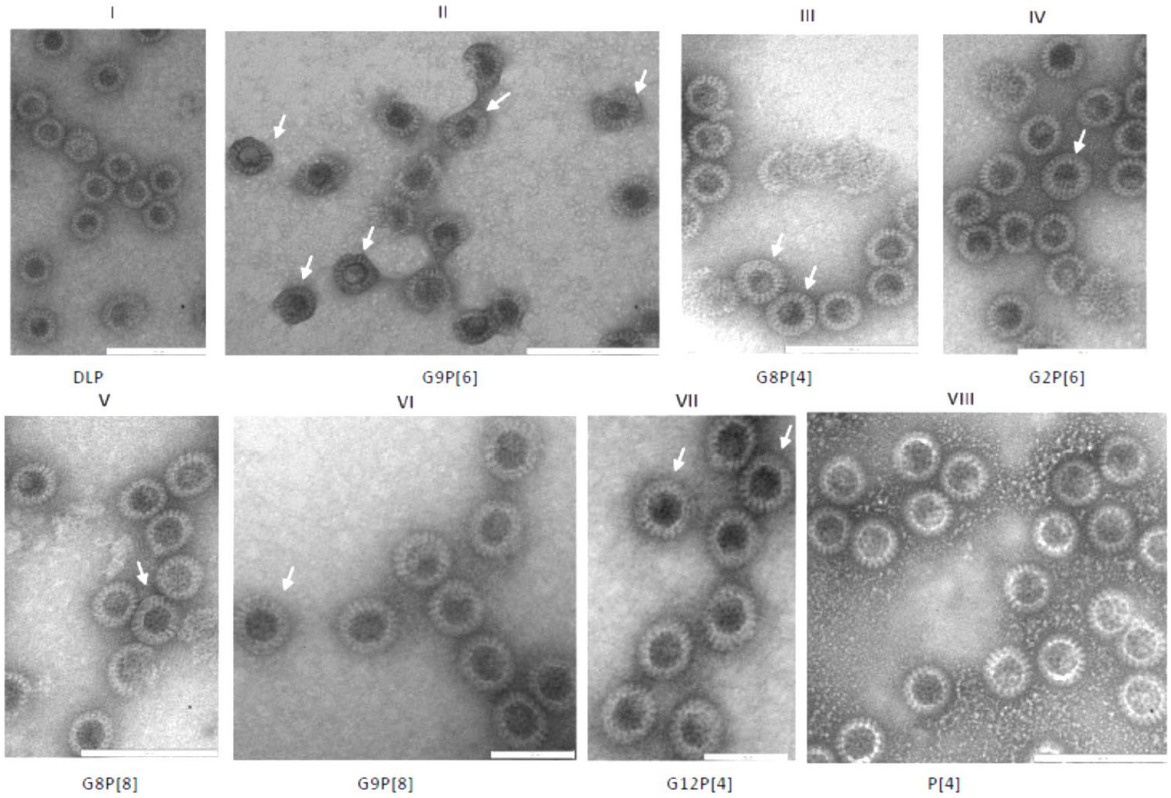

Figure 1.7: RV-VLPs generated in insect cells using wild-type bacmid strains directly isolated from stool samples. (I) RV-DLPs were produced by infecting High Five insect cells with recombinant baculoviruses (rBVs) containing ORFs encoding VP2 (C2) and VP6 (I2). Scale bar 200 nm. **(II)** RV-TLPs were produced by infecting Sf9 insect cells with rBVs containing ORFs encoding VP2 (C2), VP4 (P[6]), VP6 (I2) and VP7 (G9). Scale bar 200 nm. **(III)** Chimaeric RV-TLPs were produced by infecting High Five® cells with rBVs containing ORFs encoding VP2 (C2), VP4 (P[4]), VP6 (I1) and VP7 (G8) proteins. Scale bar 200 nm. **(IV)** Chimaeric RV-TLPs were produced by infecting Sf9 cells with rBVs containing ORFs encoding VP2 (C2), VP4 (P[6]), VP6 (I1) and VP7 (G2) proteins. Scale bar 200 nm. **(V)** Chimaeric RV-TLPs were produced by infecting High Five cells with rBVs containing ORFs encoding VP2 (C2), VP4 (P[8]), VP6 (I2) and VP7 (G8) proteins. Scale bar 200 nm. **(VI)** Chimaeric RV-TLPs were produced by infecting High Five cells with rBVs containing ORFs encoding VP2 (C2), VP4 (P[8]), VP6 (I2) and VP7 (G9). Scale bar 100 nm. **(VII)** Chimaeric RV-TLPs were produced by infecting Sf9 cells with rBVs containing ORFs encoding VP2 (C2), VP4 (P[4]), VP6 (I2) and VP7 (G12). Scale bar 100 nm. **(VIII)** Chimaeric RV-TLPs were produced by infecting High Five cells with rBVs containing ORFs encoding VP2 (C2), VP4 (P[4]) and VP6 (I2). Scale bar 200 nm. Arrows point towards RV-TLPs with a smooth extra outer ring. The figure is taken from Jere *et al*. (2014) (open-access article).

Co-infections done by Jere and co-workers (2014) (Fig. 1.7) generated RV-VLPs of which about 30% were TLPs when VP2, VP4, VP6 and VP7 from the same strain (GR10924) were used. When DLPs (DS-1) were co-expressed with outer capsid RV proteins VP4s (with P[4], P[6] or P[8] genotypes) and VP7s (with G2, G8 or G12 genotypes) derived from heterologous strains only about 10-20% of the assembled particles were TLPs (Jere *et al.*, 2014). The partial assembly of RV outer capsid proteins onto the DLPs may have been due to insufficient calcium supplementation in the TC-100 media used by Jere and co-workers (2012) (personal communication of M.K. Estes, S.E. Crawford and B.V. Prasad to A.A. Van Dijk, 2018).

1.12. Multicistronic baculovirus expression systems

Initial baculovirus expression of a single heterologous gene was achieved in 1983 (Smith *et al.*, 1983). However, baculovirus expression speedily developed towards the usage of multicistronic systems. Various assembly strategies to generate RV-VLPs have been attempted ranging from monocistronic (Jiang *et al.*, 1998; Kim *et al.*, 2002) to multicistronic (Jere *et al.*, 2014; Peixoto *et al.*, 2007; Roldão *et al.*, 2007) recombinant baculovirus expression strategies.

Co-infection strategies utilize recombinant baculoviruses that are monocistronic (expressing a single protein), dualcistronic (expressing two proteins) or multicistronic (expressing more than two proteins).

A tricistronic VP2/6/7 baculovirus expression system has been reported to yield larger quantities of RV VP7 compared to co-infection strategies (Roldão *et al.*, 2007; Vieira *et al.*, 2005). This increased VP7 expression by tricistronic baculovirus expression strategies has been reported to lead to increased RV-VLP yield (Vieira *et al.*, 2005). However, defective VP7 assembly has also been reported during the same study (Roldão *et al.*, 2007), possibly due to VP7 being expressed too early and under the control of a *p10* promoter (Roldão *et al.*, 2007; Vieira *et al.*, 2005) instead of a late polyhedrin promoter.

Although multicistronic approaches may hold certain challenges, the usage of a multicistronic recombinant baculovirus system may be beneficial. The likelihood of simultaneously infecting cells with an equal ratio of recombinant baculoviruses drastically decreases the more recombinant baculoviruses are needed to infect a

single cell at a comparable ratio. This may be significant, since the theoretical percentage of individual cells receiving an equal ratio of recombinant baculoviruses are 12.78, 1.88, 0.29 and 0.05%, respectively, when infected with 2, 3, 4 or 5 different recombinant baculoviruses each at a MOI of 5 (Belyaev *et al.*, 1995). Therefore, co-infection strategies may result in an unbalanced synthesis of expressed proteins in cells (Roldão *et al.*, 2007; Roy *et al.*, 1997). Thus, the population of cells optimally expressing recombinant proteins decreases drastically the more recombinant baculoviruses, expressing different proteins, are used during co-infection (Belyaev *et al.*, 1995). Therefore, using multicistronic baculovirus expression strategies may be advantageous over monocistronic baculovirus expression strategies when a single cell must express multiple proteins at specific ratios (Belyaev *et al.*, 1995; Roy, 2004; Vieira *et al.*, 2005). Further, the logistical load of simultaneously maintaining various baculoviruses of known titers and comparable levels of expression is extremely taxing (Berger *et al.*, 2004). Thus, using a single multicistronic baculovirus greatly simplifies virus handling and increases the reproducibility of expression experiments (Berger *et al.*, 2004).

One multicistronic baculovirus system is the MultiBac system (Berger *et al.*, 2004), which uses Cre-loxP and Tn7 transposition technologies for the production of multicistronic baculoviruses that have been reported to simultaneously express up to five subunits of a single protein that correctly assembled (Berger *et al.*, 2004). This multicistronic baculovirus strategy uses the Cre-loxP and Tn7 transposition sites that operate on independent recombination systems, to allow for the simultaneous integration of two transfer vectors, that contain multiple genes, into the same viral genome (Roy, 2004). A baculovirus-silkworm multigene expression system has been reported that used the MultiBac system to generate recombinant tricistronic baculoviruses that expressed RV-TLPs composed of RV VP2, VP6 and VP7 in silkworms (Yao *et al.*, 2012).

1.13. Structural compatibility between the RNA-dependent RNA polymerase (VP1) of RVA and RVG

In our laboratory, RV SA11 is used as a reverse genetics backbone. The SA11-based reverse genetics projects aim to rationally design safety features into rescued SA11 viruses for vaccine development. One such safety feature is the usage of genetic restrictions to reassortment between RV groups (described below), however the

structural compatibility between RV groups A and G is unknown, and therefore presents an opportunity to use a Bac-to-Bac baculovirus expression system to evaluate structural compatibility between RVA SA11 VP2/6 and RVG 03V0567 VP4/7.

The RVA SA11 strain and the RVG 03V0567 strain differ genetically in their 3' terminal sequences of their (+)ssRNA encoding RV VP1 (RNA-dependent RNA polymerase, RdRP), Table 1.6. The structure of RV RdRP is illustrated in Fig. 1.8. Conservation of the UGUG sequence of the 3' terminal sequence of RV (+)ssRNA encoding RV VP1 in Clade A RVs suggests a conserved (+)ssRNA recognition mechanism. Clade B does not have this conserved 3' terminal UGUG sequence. The extreme 3'-terminal sequence, ACCC, is conserved among clade B viruses. This suggests that Clade B RV RdRP employs a different mechanism of (+)ssRNA recognition than clade A RVs (Ogden *et al.*, 2012).

Table 1.6: Terminal sequence of RV (+)ssRNA encoding RV VP1. The table is taken from Ogden *et al.* (2012) with permission.

Clade	Species	Strain	5′ End[a]	3′ End[a]
A	RVA	SA11	GGCUAUUAAA	AGAUGUGACC
A	RVA	RRV	GGCUAUUAAA	AGAUGUGACC
A	RVA	UK	GGCUAUUAAA	AGAUGUGACC
A	RVA	ETD	GGCUAUUAAA	CGAUGUGACC
A	RVA	PO-13	GGCUAUUAAA	AGAUAUGACC
A	RVA	02V0002G3	GGCUAUUAAA	CGAUGUGACC
A	RVC	Bristol	GGCUAAAAAA	UAUUGUGGCU
A	RVD	05V0049	GGCAAUUAAA	ACUUGUGACC
A	RVF	03V0568	GGCAAUUAAU	UAAUGUGACC
B	RVB	Bang373	GGCACAAUAU	AUAAAAACCC
B	RVB	DB176	GGCAAUAAUG	GUAAAAACCC
B	RVG	03V0567	GGCAUAUAUU	AUAAAGACCC
B	RVH	B219	GGCACUAUGG	UAAUAUACCC
B	RVH	J19	GGCACUAUGG	UAAUAUACCC

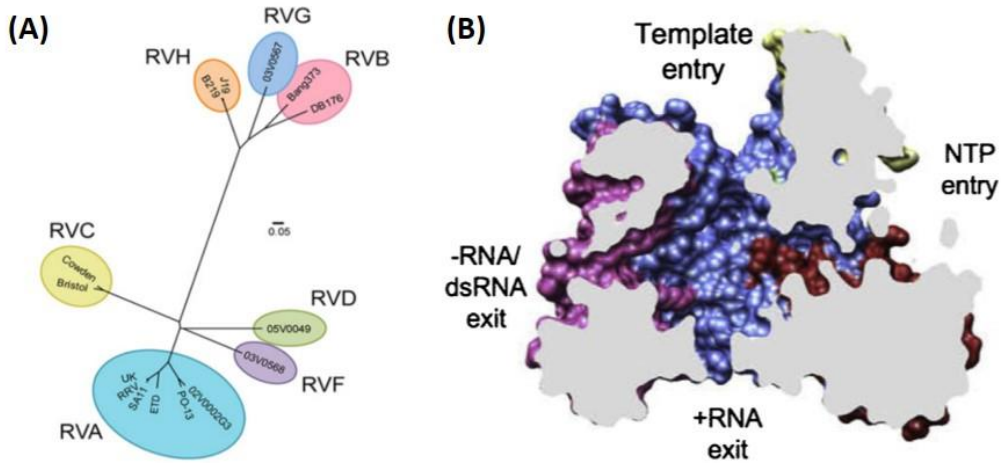

Figure 1.8: Maximum likelihood phylogenetic tree of RV groups and the structure of RV RdRp (RV VP1). (A) Maximum likelihood phylogenetic trees comparison of the deduced amino acid sequences of RV RdRP VP1. Figure adapted from (Ogden *et al.*, 2012) with permission. **(B)** The structure of RV RdRp (RV VP1). A sagittal cutaway of a surface rendering of a complete RV RdRp polypeptide chain. The N-terminal domain is coloured yellow, the C-terminal (bracelet) domain is coloured pink, and the C-terminal plug is coloured cyan. The four tunnels extending into the central cavity are shown (Desselberger, 2014; Lu *et al.*, 2008). The figure is taken from Lu *et al.* (2008) with permission.

The RdRP of SA11 (RVA) and 03V0567 (RVG) differ, since 03V0567 (RVG) has a narrower template entry tunnel than the SA11 strain (RVA) as illustrated in Fig. 1.9. This is due to an insertion of 3 amino acids (Fig. 1.9) in Clade B RVs which would narrow and alter the shape of the template entry tunnel in a region that is important for specific interaction with the G4 and U5 bases in the RVA (Clade A) RdRP. These genetic and structural differences between Clade A and Clade B RV may restrict reassortment (Ogden *et al.*, 2012).

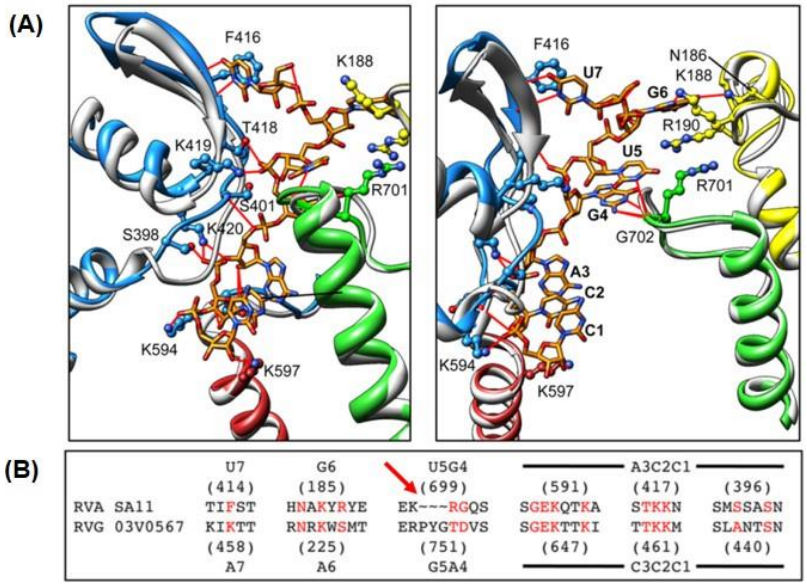

Figure 1.9: RV clade A and clade B VP1 viral (+)ssRNA recognition. (A) A close-up model of the template entry tunnel of RVA SA11 VP1 (coloured ribbon) with RNA oligonucleotide (orange sticks) bound in two different views. (Ogden *et al.*, 2012) used PDB2R7W to make the images. The RNA bases are denoted in a 3' to 5' direction. RVA SA11 VP1 subdomains are coloured as follows: N-terminal is

yellow, C-terminal is pink and polymerase subdomains: fingers are blue, the palm is brick red and thumb is green. The side chains of RV VP1 residues that interact with the RNA are depicted and labelled. The predicted structure of the RVG strain 03V0567 VP1 (grey ribbon) is overlayed on the SA11 RVA structure (coloured ribbon). For clarity parts of the structure have been omitted. **(B)** Structure-based sequence alignment of specific regions of VP1 (made by (Ogden *et al.*, 2012) via PDB2R7Q) and the homology model of RVG 03V0567. RVA SA11 residues that interact with RNA, and the aligning residues of the RVG VP1 model, are coloured red. Above the alignment, the initial amino acid number in the series and the RNA nucleotide with which the RVA SA11 VP1 residues interact are denoted. Below the alignment, the identities of the aligning amino acids and aligning nucleotides for RVG 03V0567 are denoted. Figure adapted from Ogden *et al.* (2012) with permission.

Rotavirus replication is an integral part of RV reverse genetics. Reverse genetics requires the RV VP1 to recognise the (+)ssRNA of the 11 genome segments encoding the 12 RV proteins during RV replication. However, as described above, Clade A and Clade B RVs may use different mechanisms for (+)ssRNA recognition. This may restrict RV replication genetically when reassorting these Clade A or Clade B VP1s with RV genome segments encoding other RV proteins from a different clade. This restriction would hamper RV replication unless the 3' ends of the (+)ssRNA are matched with the corresponding RV VP1. Generating rescued SA11 virions with the Clade A VP1 and terminal sequences exchanged for those of Clade B may serve as a safety feature as this would restrict reassortment with other Clade A RVs.

However, determining the structural compatibility between SA11 DLPs and Clade B RV outer capsids may aid in shedding light on the possibility of reassortment between this novel SA11 and native Clade B RVs. Since RVB (Bridger, 1980; Chen *et al.*, 1985) and RVH (Alam *et al.*, 2007) are Clade B RVs that infect humans, there exists a potential for reassortment between these clade B RVs and this novel SA11. Also, future reverse genetics projects that reassort Clade A and B RVs may potentially be hampered by other unknown genetic restrictions or structural incompatibility between the outer capsid and DLP. Therefore, using a Bac-to-Bac Baculovirus expression system may side-step possible genetic restrictions, since a baculovirus vector would be used, and allow for the evaluation of the structural compatibility of the RV proteins. Therefore, the generation of RV-VLPs may aid reverse genetics research endeavours, by purely focusing on the structural compatibility of the various structural proteins.

1.14. Problem statement

The partial assembly of RV VP7 on DLPs observed in a previous study in our laboratory is problematic and probably due to a lack of calcium supplementation during assembly (see Section 1.11).

The extent of structural compatibility between SA11 VP2/6 DLPs and VP4 and VP7 of various RV groups is not known. It has been shown that there are structural and genetic differences between VP1 of SA11 and RVG which may affect reassortment (see Section 1.13). A reverse genetics (RG) system utilizes all 12 RV proteins to generate recombinant RVs. However, the VP1 and (+)ssRNA recognition mechanisms differ between RV clades (Ogden *et al.*, 2012). Our laboratory uses SA11, a Clade A RV, as a reverse genetics backbone. When exchanging the VP1 and terminal sequences of RVA SA11 (Clade A) with that of clade B RVs, to implement safety features into rescued SA11 virions for vaccine development, elucidation of the structural compatibility between SA11 DLPs and Clade B RV outer capsids may partly be important to determine the potential of future reassortment between this novel SA11 and native Clade B RVs.

The use of a baculovirus expression system to generate RV-VLPs would circumvent any possible genetic restriction. Only VP2/6/7/4 are needed for VLP production. A baculovirus expression system uses baculoviruses as the vector, circumventing the usage of RV VP1 and RV (+)ssRNA recognition. This allows for the investigation of the structural compatibility of RVA SA11 VP2/6 and RVG 03V0567 VP4/7 without the possible bottleneck due to genetic restrictions.

1.15. Aims

The first aim of this study was to use the Bac-to-Bac baculovirus vector expression system (BVES) with a co-infection approach to:

- Generate fully assembled chimeric rotavirus virus-like particles with DS-1-like DLPs and an outer capsid from African strains using 20 mM calcium supplementation of the medium during assembly.
- Investigate the possibility of generating chimeric RV-VLPs using SA11 DLPs and RVG VP4 and VP7.

The second aim was to use the Bac-to-Bac BVES with a multicistronic approach to generate quadcistronic recombinant baculoviruses expressing all four RV-TLP proteins (VP2/6/4/7) to:

- Generate RV SA11 VP2/6/4/7 TLPs, as proof of principle.
- Generate transcapsidated fully assembled chimeric RV-TLPs composed of either DS-1-like VP2/6 and African strain VP4/7 or SA11 VP2/6 and RVG VP4/7.

Chapter 2: Evaluating the effect of calcium supplementation on assembly of chimeric RV-VLPs with RV strain GR10924 DLPs and African strain outer capsids.

2.1. Introduction

The two main commercially available RV vaccines, RotaTeq and Rotarix, have lower efficacy in developing countries compared to developed countries (Burnett *et al.*, 2020; Henschke *et al.*, 2022; Jonesteller *et al.*, 2017; Tate *et al.*, 2012). This may in part be due to differences in strains circulating in developing countries.

Since the 1990s baculovirus expression systems have been used for the production of rotavirus VP2 single-layer particles (SLPs), VP2/6 double-layer particles (DLPs) and VP2/6/7 or VP2/6/7/4 triple-layer particles (TLPs) (Crawford *et al.*, 1994; Labbé *et al.*, 1991). Rotavirus VLPs are promising candidate dead-subunit vaccines (Crawford *et al.*, 1994; Istrate *et al.*, 2008; Jere *et al.*, 2014) as they have been shown to protect against RV infections in mice (Bertolotti-Ciarlet *et al.*, 2003; Redmond *et al.*, 1993), gnotobiotic pigs (Saif & Fernandez, 1996), and rabbits (Ciarlet *et al.*, 1998). Rotavirus strains SA11 and rhesus rotavirus (RRV) have been instrumental in studies on RV-VLP assembly (Crawford *et al.*, 1994; Labbé *et al.*, 1991) and immunology (Bertolotti-Ciarlet *et al.*, 2003; Crawford *et al.*, 1994).

Thus, transcapsidated RV-VLPs composed of circulating RV strain outer capsid proteins on a universal backbone may prove effective as a region-specific dead-subunit vaccine. Jere and co-workers (2014) applied a novel approach that may be instrumental in speeding up vaccine research and development. Chimaeric RV-VLPs were generated from consensus genome sequences of African RV G2, G8, G9 or G12 strains associated with either P[4], P[6] or P[8] genotypes obtained directly from human stool samples (Jere *et al.*, 2014). These consensus genome sequences were insect cell codon-optimized and used for baculovirus expression of homologous and heterologous RV-VLPs. This approach bypassed the need for the intermediate step of adapting RVs to cell culture (Jere *et al.*, 2014). These chimeric RV-VLPs used RVA/Human-wt/ZAF/GR10924/1999/G9P[6] (GR10924) (Jere *et al.*, 2011) as a double-layered particle (DLP) backbone and various African RV strain outer capsids.

To generate the chimeric RV-VLPs, Jere and co-workers (2012, 2014) co-expressed RV proteins using different baculovirus co-infection strategies. Various baculovirus expression strategies are available, ranging from monocistronic (Jiang *et al.*, 1998; Kim *et al.*, 2002) to multicistronic strategies (Jere *et al.*, 2014; Peixoto *et al.*, 2007;

Roldão *et al.*, 2007). In these co-infection strategies, multiple recombinant baculoviruses expressing various RV proteins simultaneously infect the same insect cell to co-express the various RV proteins, leading to the generation of RV-VLPs.

Of the RV-VLPs, generated via co-infecting Sf9 and High Five insect cells with recombinant baculoviruses, by Jere and co-workers (2012, 2014) about 30% of homologous RV-VLPs (VP2/6/4/7 of RV GR10924) were TLPs. Heterologous RV-VLPs only generated about 10-20% RV-TLPs when DLPs were co-expressed with outer capsid RV proteins VP4s (with P[4], P[6] or P[8] genotypes) and VP7s (with G2, G8 or G12 genotypes) derived from heterologous strains (Jere *et al.*, 2014). The TC-100 Insect Medium (Sigma-Aldrich, St. Louis, MO) used by Jere and co-workers (2012) contained 8,83 mM calcium (Ca^{2+}) which is hypothesised to be an insufficient concentration of calcium for the assembly of VP7 onto DLPs. This may explain the partial assembly of VP7s onto the RV-DLPs obtained by Dr. K.C. Jere. As discussed in Section 1.9, calcium is needed during viral assembly for coating the DLP with VP7. Supplementing the media to 20 mM calcium may improve the assembly of VP7 on the DLP (personal communication of M.K. Estes, S.E. Crawford and B.V. Prasad to A.A. Van Dijk, 2018).

In this investigation, the Bac-to-Bac baculovirus expression system will be used to repeat some of the heterologous co-infections done by Jere and co-workers (2012, 2014). The recombinant bacmids generated by Dr. K.C. Jere will be used to generate recombinant baculoviruses expressing RV African strain VP7 (G12), and RV African strain VP4s (P[4], P[6], and P[8]). Co-infection of recombinant baculoviruses expressing African RV strain VP4 and VP7 (genotypes G12P[4], G12P[6], and G12P[8]) outer capsids with recombinant baculoviruses expressing RV GR10924 DLPs, as used by Dr. K.C. Jere, will be repeated. Complete assembly of VP7 on the DLP will be attempted by co-infecting recombinant baculoviruses expressing RV GR10924 DLPs (VP2/6) with recombinant baculoviruses expressing African RV strain VP4 and VP7 in media supplemented with 20 mM calcium.

2.2. Materials and Methods

2.2.1. Introduction

Baculovirus expression systems (BVES) have been used for decades in protein expression (see Sections 1.10, 1.11, 1.12 and 2.1). The Bac-to-Bac BVES (Fig. 2.1) allows for rapid and efficient generation of recombinant baculoviruses (Ciccarone *et al.*, 1998). The term Bac-to-Bac refers to bacteria to baculoviruses. The expression system utilizes *E. coli* bacteria containing the baculovirus shuttle vector (bacmid) in the form of a large plasmid of roughly 140 000 bp (Luckow *et al*., 1993). Rapid modification of the bacmid is done in *E. coli* bacteria via site-specific transposition of the expression cassette from a donor plasmid into the baculovirus shuttle vector (bacmid) (Luckow *et al*., 1993). This greatly reduces the overall speed of generating recombinant baculoviruses, by allowing for the selection of recombinant bacmids before transfection (Luckow *et al*., 1993). The recombinant bacmid DNA once transfected into susceptible lepidopteran insect cells can be read and expressed without the need for foreign proteins (Kaba *et al*., 2004; Luckow *et al*., 1993). Thus, transfecting the recombinant bacmid DNA into susceptible lepidopteran insect cells, such as Sf9 insect cells, results in the generation of recombinant baculoviruses expressing the transpositioned ORFs. Recombinant baculoviruses expressing the transpositioned ORFs can thus be produced within two weeks, compared to previous methods such as generating recombinant baculovirus via homologous recombination that required four to six weeks (Luckow *et al*., 1993). Further, chitinase and v-cathepsin promote liquefaction of the baculovirus host during the late stages of infection (Hawtin *et al.*, 1997). The integrity of secreted recombinant proteins was increased by the deletion of the chitinase and v-cathepsin genes (ΔCC) from the baculovirus *Autographa californica multiple nucleopolyhedrovirus* (Ac) bacmid (BAC) in the generation of AcBACΔCC *E. coli* cells (Kaba *et al.*, 2004).

In the Bac-to-Bac expression system (Fig. 2.1) recombinant bacmids are generated by transforming AcBACΔCC *E. coli* cells (Kaba *et al.*, 2004) with recombinant donor plasmids containing the ORFs encoding the proteins of interest between the mini Tn7 elements (the Tn7L and Tn7R sites) for site-specific transposition. The relevant ORFs encoding the genes of interest are placed under the control of either a p10 *Autographa californica* multi-capsid nucleopolyhedrosis virus (AcMNPV) promoter or a stronger polh (polyhedrin) promoter.

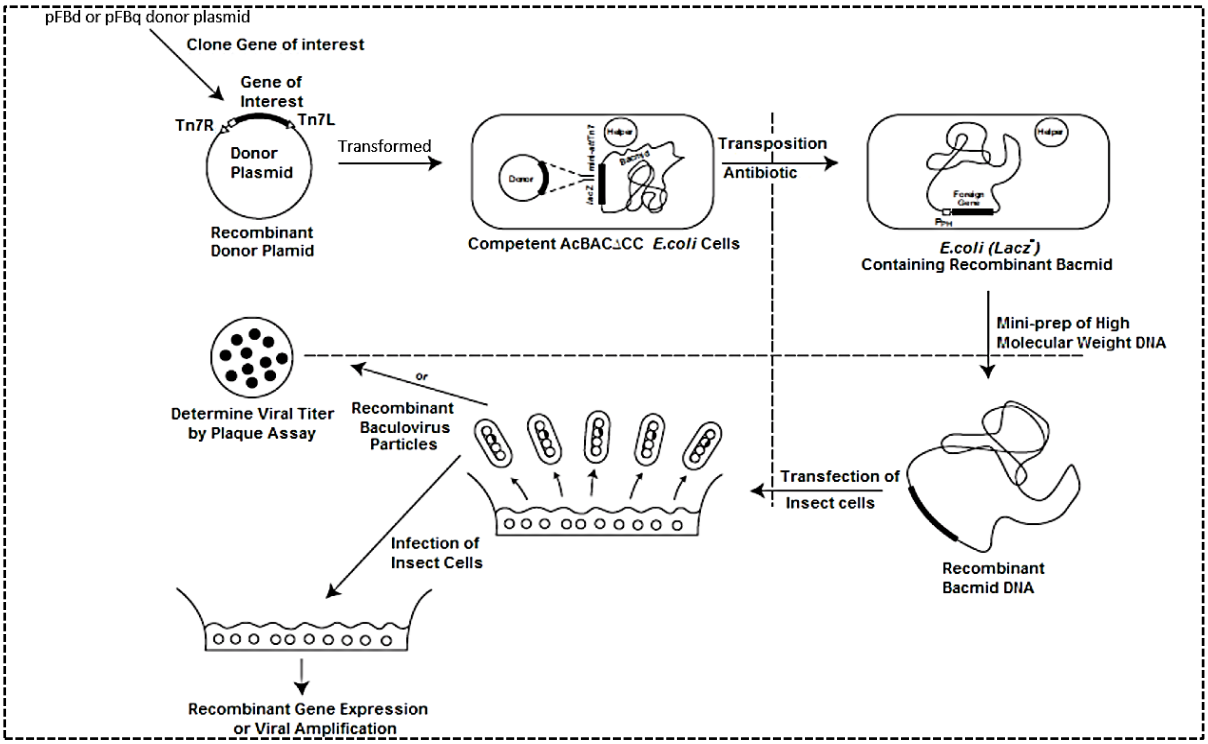

Figure 2.1: Diagram of the Bac-to-Bac® System. The generation of recombinant baculovirus and the expression of the gene of interest using the Bac-to-Bac® Baculovirus Expression System are illustrated. Adapted from Bac-to-Bac® Baculovirus Expression System manual: an efficient site-specific transposition system to generate baculovirus for high-level expression of recombinant proteins. Catalogue no. 10359-016 (Life Technologies, Grand Island, NY).

The mini Tn7 elements (Tn7L and Tn7R sites) on the various donor plasmids and the mini-*att*Tn7 attachment site on the AcBACΔCC bacmid facilitate site-specific transposition of the gene of interest from the donor plasmids (pFastBACdual or pFastBACquad) into the bacmid (Luckow *et al*., 1993). The helper plasmid (Fig. 2.1) expresses *in trans* tnsABC+D (and tnsE) genes. Transposition of the gene of interest present on the donor plasmid into the mini-*att*Tn7 attachment site results in the disruption of the LacZ operon. This disrupts the expression of the LacZα peptide, allowing for white-blue colony selection of the recombinant AcBACΔCC *E. coli* cells. Isopropyl β-D-1-thiogalactopyranoside (IPTG) inducer is added to trigger transcription of the LacZ operon. Colonies with an intact LacZ operon will have a functional beta-galactosidase capable of hydrolysing X-Gal, 5-bromo-4-chloro-3-indolyl-beta-D-galacto-pyranoside (Horwitz *et al.*, 1964), into galactose (colourless) and 4-chloro-3-brom-indigo an intense blue precipitate. Therefore, colonies of empty AcBACΔCC *E. coli* cells result in blue colonies. Colonies in which transpositioning was successful are white (Luckow *et al*., 1993).

The helper plasmid, pMON7124 (Barry, 1988), present in AcBACΔCC *E. coli* cells, contains a tetracycline resistance gene (Luckow *et al*., 1993). The bacmid in AcBACΔCC *E. coli* cells contains a kanamycin resistance gene (Luckow *et al.*, 1993). The segment between the mini Tn7 elements (Tn7L and Tn7R) of the pFBqs and pFBds contains a gentamicin resistance gene.

Recombinant bacmids are transfected into susceptible lepidopteran insect cells (Kaba *et al.*, 2004; Luckow *et al.*, 1993), such as Sf9 insect cells, resulting in recombinant baculoviruses expressing the proteins encoded by the transpositioned ORFs (Fig. 2.1).

Following transfection, the generated recombinant baculoviruses are purified and propagated in insect cells to generate purified viral stocks with higher titers. These amplified and purified recombinant baculovirus stocks are used for protein expression (Fig. 2.1).

2.2.2. Rotavirus strains, plasmids, bacteria, insect cell lines, and bacmids

To attempt the generation of fully assembled RV-VLPs by repeating the co-infection experiments of Jere and co-workers (2012, 2014), the pFBq_GR10924_VP2-VP6 donor plasmid, designed by Prof. O'Neill and used by Jere and co-workers (2012) was selected and sought. However, this plasmid was lost from the -80°C archives. Therefore, a pFastBACdual (pFBd) donor plasmid, pFBd_GR10924_VP2-VP6 (Fig. 2.2), was *in silico* designed to contain the open reading frames (ORFs) encoding RV GR10924 VP2 and VP6 (see Table 2.1). The pFBd_GR10924_VP2-VP6 was designed and ordered from GenScript, described in the text in Section 2.2.3.

Table 2.1: Various RV strains, relevant ORFs and encoded proteins that were used in this part of the study.

Strain	Genome segment	Encoded protein	Genbank accession number	Donor plasmid or recombinant bacmid [a]

RVA/Human-wt/ZAF/GR10924/1999/G9P[6]	GS2	VP2	FJ183354	pFBd_GR10924_VP2-VP6
RVA/Human-wt/ZAF/GR10924/1999/G9P[6]	GS6	VP6	FJ183358	pFBd_GR10924_VP2-VP6
RVA/Human-wt/ZAF/3176WC/2009/G12P[6]	GS9	VP7 (G12)	HQ657165	rBacmid_G12P[4] rBacmid_G12P[6] rBacmid_G12P[8]
RVA/Human-wt/ZAF/3133WC/2009/G12P[4]	GS4	VP4 (P[4])	HQ657174	rBacmid_G12P[4]
RVA/Humanwt/ZAF/GR10924/1999/G9P[6]	GS4	VP4 (P[6])	HQ657152	rBacmid_G12P[6]
RVA/Human-wt/ZAF/2371WC/2009/G9P[8]	GS4	VP4 (P[8])	JN013994	rBacmid_G12P[8]

[a] The recombinant bacmid stocks were generated by Dr. K.C. Jere and stored at -80°C (Jere *et al.*, 2012). Each recombinant bacmid contains insect cell codon optimised ORFs encoding a VP4 (P[4], P[6], or P[8]) and a VP7 (G12).

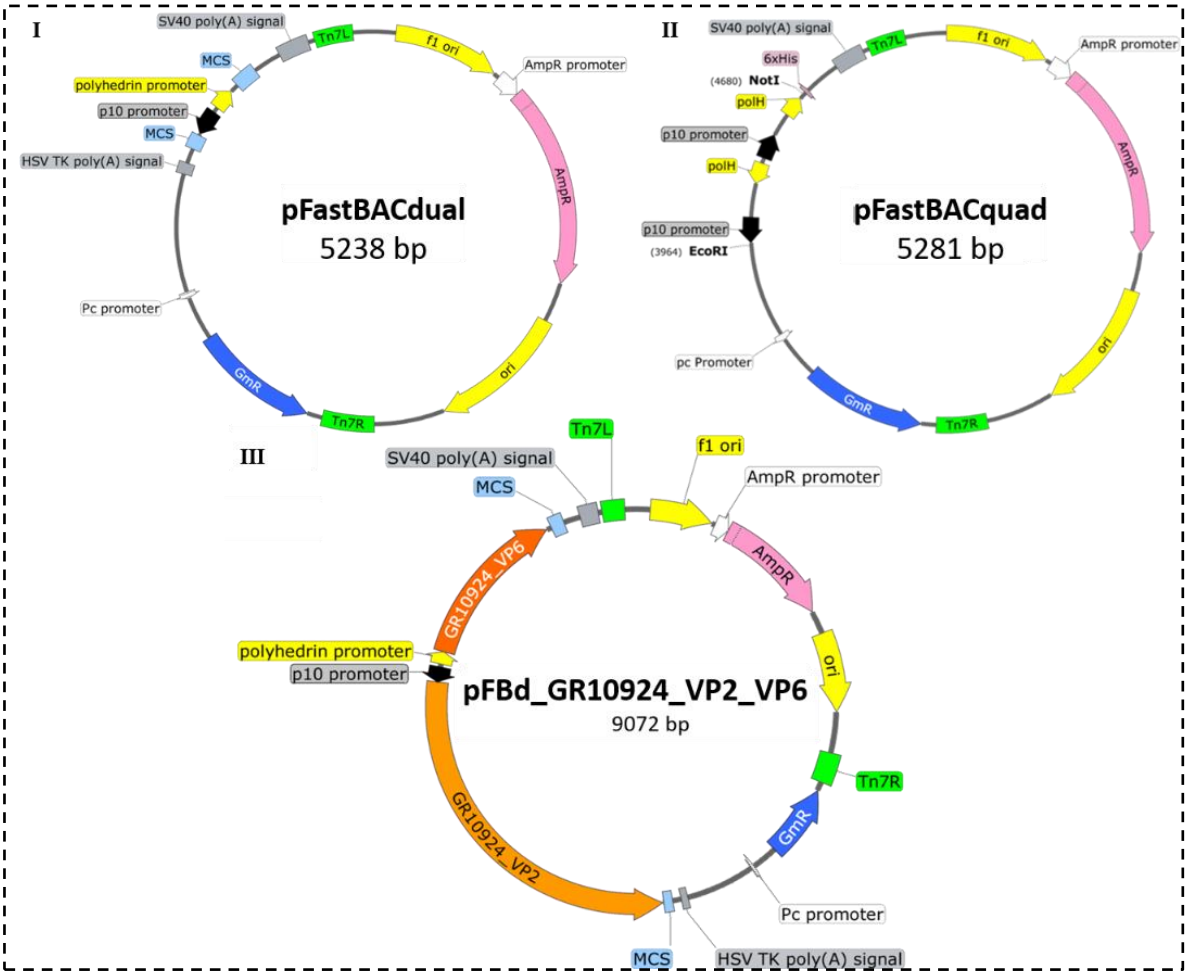

Figure 2.2: Plasmid maps of pFastBACdual, pFastBACquad, and pFBd_GR10924_VP2-VP6. Plasmid maps of **(I)** empty pFastBACdual (5238 bp), **(II)** empty pFastBACquad (5281 bp), and **(III)** pFBd_GR10924_VP2-VP6 (9072 bp) containing ORFs encoding RV GR10924 VP2 and VP6 prepared at GenScript. The 2640 bp codon optimised nucleotide sequence of the VP2 ORF (Table 2.1) was designed under the control of the p10 promoter of the pFBd. The 1194 bp codon optimised nucleotide sequence of the VP6 ORF (Table 2.1) was designed under the control of the polh promoter of the pFBd. Selection of the *E. coli* JM109 cells that acquired the pFBd_GR10924_VP2-VP6 were selected through resistance to ampicillin conferred by the ampicillin gene (selectable marker).

Prof. A.C. Potgieter generated the pFastBACquad (pFBq) (Fig. 2.2) (Jere *et al*., 2012). The multiple cloning site (MCS) of pBacgus4x-1 (Novagen, Merck Chemicals Ltd., Nottingham, UK) was incorporated into pFastBac™ (Invitrogen, Life Technologies, Grand Island, NY) (Jere *et al.*, 2012). The pBacgus4x-1 MCS permits the cloning and

co-expression of a total of four target genes under the control of two polh- or two p10 promoters.

E. coli JM109 cells (see Section 2.2.4) were selected to propagate the donor plasmids (see Section 2.2.5). AcBACΔCC *E. coli* cells (Kaba *et al.*, 2004) (see Section 2.2.1) were selected to generate and propagated recombinant bacmids containing the transposed expression cassettes (see Sections 2.2.1 and 2.2.7).

The original pFastBACquads (pFBqs) (see Table 1.6) and recombinant bacmids used by Jere and co-workers (2012) to generate recombinant baculoviruses expressing the African RV outer capsid proteins were sought from the -80°C archives. Only three of the recombinant bacmids encoding African RV VP4 and VP7 outer capsids (genotypes G12P[4], G12P[6], and G12P[8]) generated by Jere and co-workers (2012, 2014) were retrieved (Jere *et al.*, 2012; Jere *et al.,* 2014) (Table 2.1). These recombinant bacmids (rBacmid_G12P[4], rBacmid_G12P[6], and rBacmid_G12P[8]) were archived at -80°C as glycerol stocks of recombinant AcBACΔCC *E. coli* cells (Jere *et al.*, 2012).

Sf9 insect cells are clonal isolates of *Spodoptera frugiperda* Sf21 cells (IPLB-Sf21-AE) (Vaughn *et al.*, 1977). The cells were used to prepare, amplify, purify, and titrate recombinant baculoviruses as well as to produce RV-VLPs. The Sf9 insect cells used in this study were kindly provided by Prof. Vida van Staden from the University of Pretoria.

2.2.3. Design and purchase of a pFastBACdual donor plasmid for the expression of RV GR10924 VP2 and VP6

A donor plasmid, pFBd_GR10924_VP2-VP6 (Fig. 2.2), containing the ORFs (Table 2.1) encoding RVA/Human-wt/ZAF/GR10924/1999/G9P[6] (GR10924) (Jere *et al.*, 2011) VP2 and VP6 was *in silico* designed and ordered form GenScript (GenScript USA Inc. New Jersey, NJ). The ORFs were codon-optimized for expression in insect cells by GenScript using the OptimumGene™ algorithm (GenScript USA Inc. New Jersey, NJ). The ORF encoding RV GR10924 VP2 was inserted under the control of the p10 promoter and RV GR10924 VP6 was inserted under the control of the polh promoter.

2.2.4. Preparation of competent bacterial cells

For nucleic acids to traverse the outer and inner membranes of bacteria, bacteria first need to be made competent (Sambrook & Russell, 2001). There is a variety of chemical (Chung *et al.*, 1989; Hanahan, 1983; Mandel & Higa, 1970) and physical (Neumann & Rosenheck, 1972) methods of generating competent bacteria (Sambrook & Russell, 2001).

Chemical-competent *E. coli* JM109 cells and AcBACΔCC *E. coli* cells were prepared using a one-step preparation method (Chung *et al.*, 1989); cells were stored and transformed in the same solution. This method utilizes PEG-mediated transformation of *E. coli* strains (Chung *et al.*, 1989). The cells were revived from glycerol stocks, streaked out on Luria Bertani (LB) agar plates and incubated overnight at 37°C. LB agar plates and LB broth used to generate competent *E. coli* JM109 cells contained no antibiotics, and those used to generate competent AcBACΔCC *E. coli* cells were supplemented with 50 µg/ml kanamycin and 10 µg/ml tetracycline. Single colonies were picked and cultured overnight in 5 ml LB at 37°C and shaking at 225 rpm. Thereafter, 1.2 ml of overnight cell culture was added to 50 ml LB. The cells were grown at 37°C and shaken at 225 rpm to early log phase (OD_{600} = 0.5, Biochrom Libra S12 UV/Vis Spectrophotometer, Harvard Bioscience, UK), roughly 3 hours, followed by centrifugation at 4000 x g, 4°C for 10 minutes and the supernatant was removed. The cells were resuspended in 5 ml ice-cold TSS (LB supplemented with 10% PEG 6000, 5% DMSO and 50 mM $MgCl_2$) (Chung *et al.*, 1989) and incubated on ice for 20 min before adding glycerol to a final concentration of 15%. Thereafter, 200 µl aliquots of the cells were added into ice-cold microcentrifuge tubes and snap-frozen in liquid nitrogen. The newly competent *E. coli* JM109 cells and competent AcBACΔCC *E. coli* cells were archived at -80°C.

2.2.5. Propagation of donor plasmids

To generate larger amounts of donor plasmid DNA, the various donor plasmids, received from GenScript, were transformed into competent (see Section 2.2.4) *E. coli* JM109 cells.

In short, 20 ng of the donor plasmid DNA was diluted in 10 µl dH_2O and mixed with a 200 µl aliquot of chemically competent *E. coli* JM109 cells (see Section 2.2.4). The transformation mixture was incubated on ice for 30 min, before incubation at 42°C for 90 seconds. Thereafter, the mixture was transferred onto ice for 2 minutes. Followed

by the addition of 800 µl of SOC medium (Sambrook & Russell, 2001) pre-warmed to 37°C and incubated at 37°C, shaking at 225 rpm, for an hour. The transformed bacteria were plated on LB agar plates containing 50 µg/ml of carbenicillin.

2.2.6. Purification of donor plasmids

DNA isolation via alkaline lysis with detergent SDS (Birnboim & Doly, 1979) uses the exposure of the bacterial suspension to a strong anionic detergent at a pH of 12.0-12.5 to disrupt the bacterial cell walls, denatures the linear chromosomal DNA but not the covalently closed circular DNA (ccc-DNA, such as a plasmid or bacmid), and causes the release of plasmids (or the bacmid) into the supernatant (Birnboim & Doly, 1979). Large enmeshed complexes of bacterial proteins, disrupted cell walls and denatured chromosomal DNA are coated with dodecyl sulphate (Sambrook & Russell, 2001). Following the replacement of sodium ions with potassium ions these complexes of a high molecular weight are efficiently precipitated using centrifugation (Ish-Horowicz & Burke, 1981). The plasmid DNA (of a lower molecular weight compared to the large enmeshed complexes) remains suspended in the supernatant and can be precipitated via centrifugation in the presence of sufficient ethanol/isopropanol (Alloway, 1932; Crouse & Amorese, 1987; Green & Sambrook, 2016; Zeugin & Hartley, 1985).

Colonies from the plated transformed *E. coli* JM109 cells were picked from the LB-agar carbenicillin plates and cultured overnight in 5 ml LB broth (Condalab, Madrid, Spain, Cat no. 1551.00), supplemented with 50 µg/ml carbenicillin, in 15 ml conical centrifuge tubes. Overnight cell cultures were incubated at 37°C and shaken at 225 rpm.

The donor plasmid DNA was isolated using a QIAprep® Miniprep Kit (QIAGEN, Cat no. 27104) according to the manufacturer's instructions (QIAprep® Miniprep Handbook). The amount of DNA and purity were determined using a NanoDrop One spectrophotometer (Thermo Scientific, Waltham, MA, USA). This is done using the ratio between the measured absorbance at 280 nm (A_{280}) and 260 nm (A_{260}) (Warburg, 1942). The A_{260}/A_{280} ratio indicates sample purity (Glasel, 1995; Warburg, 1942; Wilfinger *et al.*, 1997), the closer the sample is to an A_{260}/A_{280} ratio of 2.0 the purer it is. Further, using the ratio between measured absorbance at 260 nm (A_{260}) and 230 nm (A_{230}) indicates the presence of contaminants such as phenols, thus, the

lower the A_{260}/A_{230} ratio is the more contaminants such as phenols are present. The expected A_{260}/A_{280} ratio is 1.8 or higher, and the expected A_{260}/A_{230} ratio is roughly 2.0-2.2 (Gallagher & Desjardins, 2006).

2.2.7. Generation of recombinant bacmids

Recombinant bacmid DNA was generated according to the instructions of the manufacturer (Bac-to-Bac Baculovirus Expression System, Invitrogen) as illustrated in Fig. 2.1. Instead of the manufacturer's recommended DH10Bac^{TM} cells, chemically competent AcBACΔCC *E. coli* cells (Kaba *et al.*, 2004) were used (see Section 2.2.1). The donor plasmid DNA was transformed into competent AcBACΔCC *E. coli* cells to generate recombinant bacmids.

In short, 20 ng donor plasmid DNA was diluted in 10 µl dH_2O and mixed with 200 µl chemically competent AcBACΔCC *E. coli* cells. The transformation mixture was incubated on ice for 30 min. Cells were then heat-shocked at 42°C for 45 seconds, thereafter, the tubes were transferred onto ice for 2 minutes, before adding 800 µl Recovery Medium for Expression (Sigma-Aldrich, CAS Number: CMR0001K-12ML) pre-heated to 37°C. Thereafter, the transformation mixture was incubated for 4 hours at 37°C and shaken at 225 rpm.

Serial dilutions of the transformation mixtures of 1:1, 1:10 and 1:100 were plated on LB agar plates containing 50 µg/ml kanamycin, 7 µg/ml gentamicin, and 10 µg/ml tetracycline. 14 µl of 20% (w/v) IPTG (Melford, Bildeston Road, Chelsworth, USA, CAS Number: 367-93-1) and 80 µl of 2% (w/v) X-Gal was spread across each plate. To facilitate blue-white colony selection, tetracycline was used at a higher concentration (14 µg/ml) than the recommended 7 µg/ml (A.C. Potgieter, personal communication). This helps the bacmid-containing cells retain the helper plasmid for transposition (see Section 2.1). The plates were incubated for 48 hours at 37°C.

White colonies were selected, incubated, bacmid isolated (see Section 2.2.8), and the size of the insert was confirmed using PCR with M13 primers (Table 2.2) (see Section 2.2.9). Bacteria were archived at -80°C by adding glycerol to a final concentration of 15% glycerol.

2.2.8. Purification of recombinant bacmids

Isolation of recombinant bacmids from transformed AcBACΔCC *E. coli* cells was done according to the method obtained from Prof Just Vlak's laboratory in Wageningen as described in Petrus Jansen van Vuren's MSc (Jansen van Vuren, 2006). This isolation method is based on the same principles of alkaline lysis with detergent SDS (Birnboim & Doly, 1979), described in Section 2.2.6.

The bacmids were propagated in overnight cell culture of 5 ml LB media (Condalab, Madrid, Spain, Cat no. 1551.00) containing 50 µg/ml kanamycin, 10 µg/ml tetracycline and 7 µg/ml gentamicin at 37°C and 225 rpm for ~16 hours. A 1.5 ml volume of the overnight cell culture was centrifuged for 1 minute at 8 000 x g to collect cells in a 1.5 ml microcentrifuge tube. Following the removal of the supernatant, this step was repeated. The AcBACΔCC *E. coli* cells were resuspended in 200 µl GTE buffer (50 mM glucose, 10 mM EDTA, 25 mM Tris/HCL pH 8, 0,1 mg/ml RNase). Then 400 µl 0.2 M NaOH/1%SDS solution was added to every sample, mixed, and incubated for 5 minutes. Following the addition of 300 µl chilled Kac solution (60 ml 5 M potassium acetate pH 4.8-5.2, 28.5 ml ddH_2O, and 11.5 ml glacial acetic acid) the tubes were inverted multiple times and put on ice for 5-10 minutes. Centrifugation at 14 000 x g in a benchtop centrifuge for 5 minutes followed. The supernatant was transferred to a new tube containing 800 µl isopropanol (at room temperature) to precipitate the DNA. The precipitated DNA was recovered via centrifugation for 15 minutes at 14 000 x g. The pelleted DNA was washed twice with 500 µl of 70% ethanol. This was followed by air-drying for 5 minutes and then dissolved in 40 µl ddH_2O. The amount of DNA and purity were determined using a NanoDrop One spectrophotometer (Thermo Scientific, Waltham, MA, USA) (see Section 2.2.7).

2.2.9. Confirmation of transposition of ORFs encoding RV proteins into the recombinant bacmid via PCR

The polymerase chain reaction (PCR) utilizes primers and a DNA polymerase to amplify specific stretches of a DNA sequence. To confirm successful transpositioning, M13 primers were used. Successful transpositioning would result in the ORFs of interest encoding the recombinant proteins, as well as the rest of the cassette between the Tn7 elements in the donor plasmids, to be located between the M13 forward (-40) and M13 reverse regions (Fig. 2.3) of the bacmid. The M13 primers (Table 2.2) were synthesized by TIB Molbiol (Berlin, Germany).

Table 2.2: Primer sequences as recommended in the Invitrogen® Bac-to-Bac® BEVS manual (Life Technologies, Grand Island, NY).

Primer name	Primer sequence	Number of bases	Tm
Bacmid PCR primers			
M13 Forward (-40)	5'- GTTTTCCCAGTCACGAC -3'	17 bases	55 °C
M13 Reverse	5'- CAGGAAACAGCTATGAC -3'	17 bases	55 °C

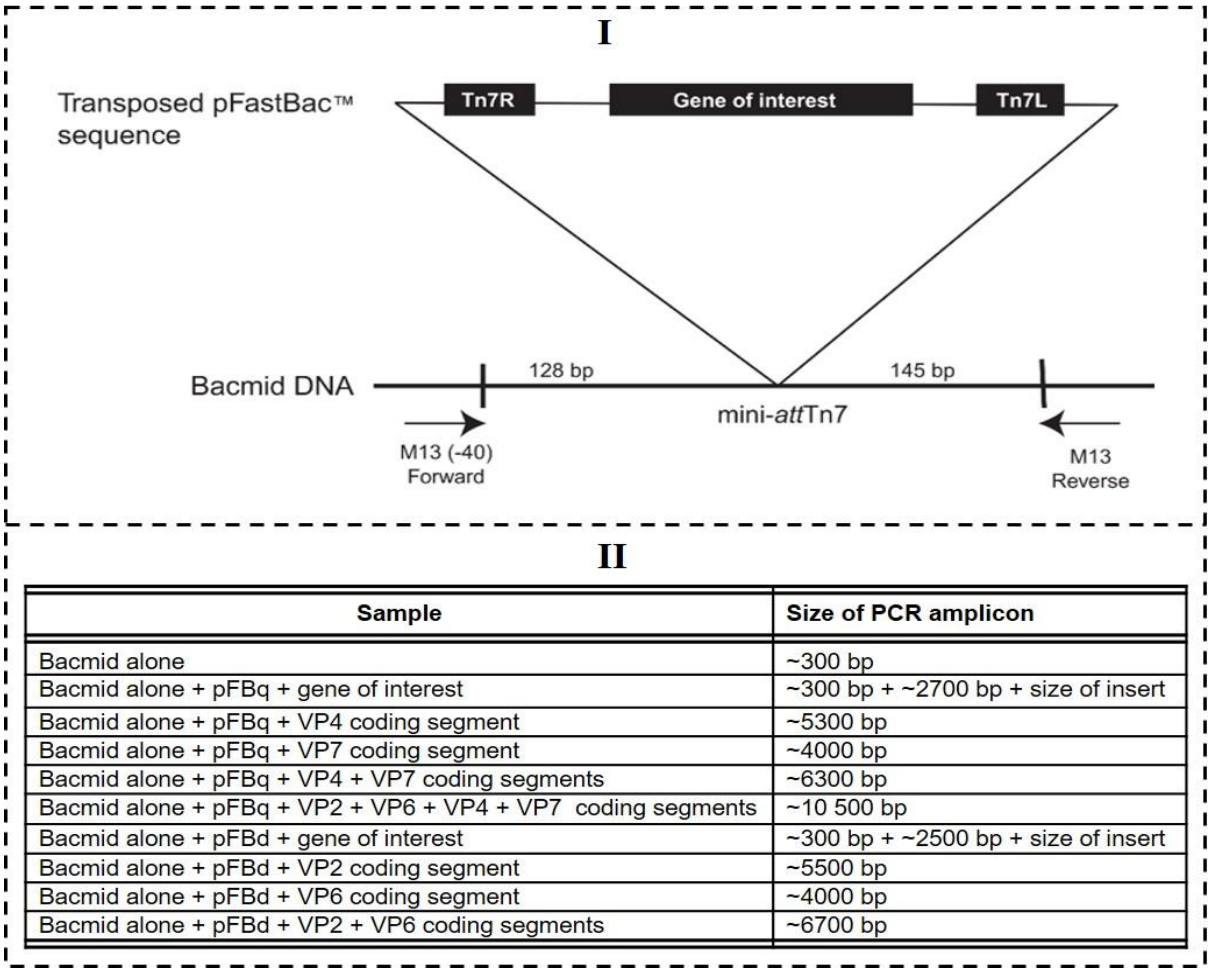

Sample	Size of PCR amplicon
Bacmid alone	~300 bp
Bacmid alone + pFBq + gene of interest	~300 bp + ~2700 bp + size of insert
Bacmid alone + pFBq + VP4 coding segment	~5300 bp
Bacmid alone + pFBq + VP7 coding segment	~4000 bp
Bacmid alone + pFBq + VP4 + VP7 coding segments	~6300 bp
Bacmid alone + pFBq + VP2 + VP6 + VP4 + VP7 coding segments	~10 500 bp
Bacmid alone + pFBd + gene of interest	~300 bp + ~2500 bp + size of insert
Bacmid alone + pFBd + VP2 coding segment	~5500 bp
Bacmid alone + pFBd + VP6 coding segment	~4000 bp
Bacmid alone + pFBd + VP2 + VP6 coding segments	~6700 bp

Figure 2.3: Schematic representation of the expected PCR amplicon sizes of transposed bacmid DNA. (I) The M13 forward (-40) and M13 reverse priming sites that flank the mini-attTn7 site within the lacZα-complementation in the bacmid which facilitates PCR analysis. **(II)** The expected PCR product of the bacmid DNA respectively transposed with pFBq and pFBd expression cassettes, Invitrogen® Bac-to-Bac® BEVS manual (Life Technologies, Grand Island, NY). Adapted from Jere *et al.* (2012).

Q5 High-fidelity DNA polymerase was used according to the protocol of New England Biolabs (240 County Rd, South Hamilton, United States). The following 50 µl reaction mixture was prepared: 10 ng DNA template, 10 µl 5X Q5 reaction buffer, 1 µl 10 mM dNTPs, 2.5 µl 10 mM M13 (-40) forward primer, 2.5 µl 10 mM M13 reverse primer, 0.5 µl (1.0 unit/50 µl reaction) Q5 High-fidelity DNA polymerase, and the reaction was filled up to 50 µl with nuclease-free water. The reaction was initially run for 3 minutes at 98°C to disassociate the double-stranded DNA into single strands. Followed by 30 cycles of a denaturation step for 45 seconds at 94°C. Then, an annealing step for 45

seconds at 60°C to allow for the annealing of the primers to the denatured single strands of template DNA (60°C instead of the typical 55°C was found to reduce non-specific amplification, results not shown). Thereafter the DNA was elongated by the polymerase for 5 minutes at 72°C. The PCR ends with a final elongation step for 7 minutes at 72°C and the samples were stored at 4°C.

Following PCR, 5 µl of the amplicons were run on a 1% agarose gel (see Section 2.2.10) to establish whether the amplicons were the correct size.

2.2.10. Agarose gel electrophoresis

Agarose gel electrophoresis is used to determine the size of DNA fragments by utilizing the negative charge of the DNA sugar-phosphate backbone in a directional electrical field. This results in migration tempos indirectly proportional to the size of the migrating DNA molecules through a three-dimensional mesh of agarose channels. The gelation of agarose forms a three-dimensional mesh of channels with diameters ranging from 50 nm to >200 nm (depending on the concentration of the agarose). This three-dimensional mesh of agarose channels results from alternative D- and L-galactose joined by α-(1→3) and β-(1→4) glyosidic linkages. These form helical fibres via anhydro bridges that aggregate in the supercoiled structures of the three-dimensional mesh (Norton *et al.*, 1986; Sambrook & Russell, 2001).

1% agarose (Melford, Bildeston Road, Chelsworth, USA, CAS Number: 9012-36-6) gels were prepared in Tris-Acetate-EDTA (TAE) buffer, containing ethidium bromide (0.5 µg/ml) as described in Sambrook and Russell (2001). Ethidium bromide (EtBr) intercalates with DNA (Elliott, 1963; LePecq & Paoletti, 1967; Waring, 1965) and was used to visualise DNA at 254-or 366-nm (LePecq & Paoletti, 1967; Sharp *et al.*, 1973). QIAGEN GelPilot loading dye (QIAGEN, 19300 Germantown Road Germantown, USA, Cat no. 239901) was used with every sample. GeneRuler 1kb DNA Ladder (Thermofisher Scientific™, Catalogue number: SM0311) was used as the DNA size marker. 10x7x0,5 cm 1% agarose gels were run for 90 minutes at 70 V and 20x14,5x0,5 cm 1% agarose gels for 90 minutes at 120 V using a Bio-Rad PowerPac Basic system. Gels were visualized using a Bio-Rad ChemiDoc™ Imaging System (Bio-Rad, California, USA).

2.2.11. Insect cell propagation

Sf9 insect cells are a clonal isolate of *Spodoptera frugiperda* Sf21 cells (IPLB-Sf21-AE) (Vaughn *et al.*, 1977). Insect cells were propagated as per the Gibco® Growth and Maintenance of Insect Cell Lines User Guide (Bio-Sciences, Dublin, Ireland). Sf9 insect cells were propagated in Gibco® (Bio-Sciences, Dublin, Ireland) TC-100 Insect Medium (Catalogue number: 13055025) supplemented with 10% foetal bovine serum (FBS, Gibco®, Catalogue number: 10270106), 1% antibiotic-antimycotic (Gibco®, Catalogue number: 15240112) and calcium chloride to a final concentration of 20 mM.

The insect cells were initiated from frozen stocks and archived as frozen stocks according to the methods described in the Gibco® Growth and Maintenance of Insect Cell Lines User Guide (Bio-Sciences, Dublin, Ireland). When initiating Sf9 insect cells from frozen stocks, cells were resuspended in 10 ml supplemented TC-100 Insect Medium pre-warmed to 28°C in a 75 cm^2 flask. The cells were incubated for an hour at 28°C to attach and thereafter the medium was replaced with fresh supplemented TC-100 Insect Medium. When freezing the cells, the procedure was as follows. The cells were dislodged using the sloughing method. The detached cells were transferred to a 50 ml centrifuge tube and centrifuged for 5 minutes at 300 x g. The supernatant was removed, and the cells were resuspended in 1 ml freezing media of 4°C (80% Grace's Insect Medium, 10% FBS, 10% DMSO) and transferred to a 1 ml cryotube at a concentration of 1 X 10^7 cells/ml. The cryotubes were stored at -20°C for 1 hour, followed by -80°C either for permanent storage or after an hour, moved to liquid nitrogen storage.

2.2.12. Generation of recombinant baculoviruses expressing RV VP2, VP6, VP4 and VP7

To generate recombinant baculoviruses, fresh recombinant baculovirus plasmid (bacmid) DNA encoding the transpositioned ORFs encoding RV VP2, VP6, VP4 and VP7 needs to be transfected into Sf9 insect cells. Transfecting recombinant bacmid DNA into susceptible lepidopteran insect cells (Kaba *et al.*, 2004; Luckow *et al.*, 1993) such as Sf9 insect cells, results in recombinant baculoviruses expressing the transpositioned ORFs encoding RV VP2 and VP6 or RV VP4 and VP7. For this study, Promega FuGENE HD Transfection Reagent (Promega, Madison, USA, Catalogue number: E2311) was selected to transfect bacmid DNA into Sf9 insect cells. The benefit of the Promega FuGENE HD Transfection Reagent is the minimal effect thereof on cell health (Roest *et al.*, 2016) while maintaining equal transfection efficacy

as other transfection reagents, such as Cellfectin™ (Invitrogen), or Insect GeneJuice™ (Novagen/EMD Biosciences) (Buchs *et al.*, 2009).

To transfect Sf9 insect cells with the bacmid DNA the manufacturer's instructions described in the Promega FuGENE HD Transfection Reagent protocol (Promega, Madison, USA, Cat no. E2311) were followed. In brief, the Sf9 insect cells were seeded into a six-well plate at a density of 1 x 10^6 cells/ml. The transfection mixture was prepared by mixing 37 µl of bacmid DNA (prepared as described in Section 2.2.8) diluted in dH_2O with 10 µl FuGENE HD Transfection Reagent, and 60 µl of Opti-MEM™ Reduced Serum Medium (Thermofisher Scientific™, Catalogue number: 31985062). The mixture was incubated for 5-15 minutes at room temperature and added to the Sf9 insect cells. The transfected cells were incubated for 5-6 days in a humidified box at 28°C. Thereafter, the cells were harvested and centrifuged at 500 x g for 2 minutes. The supernatant was stored in the dark at 4°C as a P1 viral stock, and used for subsequent infections.

To determine transformation efficacy, 1 µg of pmaxGFP plasmid (Lonza, Basel, Switzerland) (kindly provided by Professor A.C. Potgieter, Deltamune, RSA) was transfected using the FuGENE HD Transfection Reagent according to manufacturer's instructions (Promega, Madison, USA, Cat no. E2311), as listed in the text above. Transfection efficacy was determined by visualizing and photographing expressed green fluorescent protein (GFP) in successfully transfected cells using a Nikon Eclipse TE2000-S fluorescent microscope (Nikon Instruments Inc. Melville, NY, USA). The expressed green fluorescent protein (GFP, from Copepod Pontellina sp.) emits a green light within the excitation range (Ex) of approximately 482 nm, and the emission (Em) is approximately 502 nm (Shagin *et al.*, 2004) (Lonza, Basel, Switzerland).

2.2.13. Quantification and purification of baculovirus stocks

To effectively express proteins, the recombinant baculoviruses (rBVs) needed to be plaque-purified and the titer quantified. Baculoviruses (BVs) were purified and quantified using the viral plaque assay method described in the Bac-to-Bac® Baculovirus Expression Systems manual (Life Technologies, Grand Island, NY, USA). Plaque-purification decreases the risk of contaminating wild-type BVs, allows for the isolation of rBVs, and the screening of recombinant baculovirus (rBV) plaques for plaques with greater protein expression.

In short, two six-well plates were seeded at 8 x 10^5 cells/ml. A viral dilution ranging from 10^{-1} - 10^{-9} dilution was prepared with the initial dilution prepared by diluting 100 µl of viral stock in 900 µl Gibco® TC-100 Insect Medium (Thermofisher Scientific™, Catalogue number: 13055025) supplemented insect cell media. The Sf9 insect cells were incubated for 1 hour with 900 µl of inoculum on a shaker platform. Thereafter, the supernatant was removed and 2 ml of a low-gelling agarose plaque overlay was added to each well and left for 20 min before moving it to the incubator for ~10-14 days at 28°C. The plaque overlay had a final concentration of 1% low-gelling agarose (Sigma-Aldrich, CAS Number: 39346-81-1, A9045-25G), in 50% 2X Grace's Insect media (Thermofisher Scientific™, Catalogue number: 11605086), 1% antibiotic-antimycotic (Gibco®), and 10% FBS (Gibco®). Baculovirus purification or titer determination was done roughly 10-14 days post-infection (d.p.i). To visualise recombinant baculovirus plaques, viable cells were stained with neutral red staining (0.1% (w/v) neutral red in cell-culture grade water).

2.2.14. Propagation of baculoviruses

To increase baculovirus titers for protein expression analysis, recombinant baculoviruses were propagated in Sf9 cells as per the method described in the Bac-to-Bac® Baculovirus Expression Systems manual (Life Technologies, Grand Island, NY). The P1 virus stocks were isolated following transfection (see Section 2.2.12).

To increase the titer of baculovirus stocks, Sf9 insect cells were seeded in six-well plates at 1 x 10^6 cells/ml and infected at a MOI of 0,01-0,1. The infected cells were incubated for five days in a humidified box at 28°C. Thereafter, the cells were harvested and centrifuged at 500 x g for 2 minutes. The supernatant was stored in the dark at 4°C as an amplified viral stock, and used for subsequent infections.

To visualise expressed proteins on immuno-fluorescent monolayer assay (IFMA), sodium dodecyl sulphate-polyacrylamide gel electrophoresis (SDS-PAGE) or western blot, Sf9 cells were seeded in six-well plates at 1 x 10^6 cells/ml and infected with baculovirus stocks at a MOI of 1-10. The infected cells were incubated for five to six days in a humidified box at 28°C. Thereafter, the cells were harvested and centrifuged at 500 x g for 2 minutes. The proteins were prepared for SDS-PAGE or western blot as described in text in Section 2.2.17.

2.2.15. Generation of amplified plaque-purified baculovirus stocks

To increase viral yields of plaque-purified recombinant baculovirus, stocks were passaged on Sf9 cells. Baculovirus plaques were picked using the plaque purification method described in the Bac-to-Bac® Baculovirus Expression Systems manual (Life Technologies, Grand Island, NY). A sterile filter pipette was used to carefully pick a clear baculovirus plaque. The agarose plug (containing the baculovirus) was transferred to a 1,5 ml microcentrifuge tube containing 500 µl of supplemented Gibco® TC-100 Insect Medium and mixed by vortexing. Thereafter, the agarose plug solution was left overnight to allow sufficient dilution of the baculoviruses before adding 100 µl of the agarose plug solution to a well in a six-well plate seeded at a density of 1 x 10^6 cells/ml. The infected Sf9 cells were incubated at 28ºC in a humidified box for 72-120 hours. The medium was collected, added to a 2 ml microcentrifuge tube, and centrifuged for 5 minutes at 500 x g. The supernatant containing the baculovirus was recovered and stored at 4°C in the dark (as purified P2 rBV stocks).

To generate an amplified plaque-purified baculovirus stock, Sf9 insect cells at a density of 1 x 10^6 cells/ml in a six-well plate were infected with purified P2 rBV stocks at a MOI of 0,1. After CPE was complete (roughly five days post-transfection) the Sf9 cells were detached, added to a 2 ml microcentrifuge tube, and centrifuged for 5 minutes at 500 x g. The supernatant containing the amplified plaque-purified baculovirus was recovered, added to a microcentrifuge tube, and stored (as purified P3 stocks) at 4°C in the dark.

Amplified plaque-purified recombinant baculovirus stocks were quantified using a plaque assay, as described in Section 2.2.13. To generate larger 50 ml plaque-purified recombinant baculovirus stocks, 50 ml Sf9 cell shaker cultures, at a density of 2 x 10^6 cells/ml, were infected with a MOI of between 0.01-0.1 of purified P3 baculovirus stocks and incubated at 28°C, shaking at 98 rpm, for 72 hours. The amplified plaque-purified baculovirus stocks were used to produce RV-VLPs (see Section 2.12). The titer of these larger amplified plaque-purified recombinant baculovirus stocks was quantified using plaque assay, as described in Section 2.2.14.

2.2.16. Immuno-fluorescent monolayer assay (IFMA)

To determine the expression of VP2 and VP6 of RV SA11-N5 and RV GR10924, and the expression of VP4 and VP7 genotypes G12P[4], G12P[6], and G12P[8],

immunofluorescent monolayer assay (IFMA) was used (Bishop, 2016; Theart, 2022; Van Gennip *et al.*, 2012). The expression of RV SA11 VP2, VP6, VP4 and VP7 was verified using an immunofluorescent monolayer assay (IFMA) (Bishop, 2016; Van Gennip *et al.*, 2012).

The primary antibody used to detect VP2 and VP6 of RV SA11-N5, and RV GR10924 was a polyclonal rabbit anti-RV VP2/6 DLP IgG (serum kindly provided by Professor A.C. Potgieter, Deltamune, RSA) raised against RV SA11 DLPs. The primary antibody used to detect RV VP4 and VP7 was a polyclonal rabbit anti-RV SA11 TLP (raised against caesium chloride purified SA11 TLPs, serum kindly provided by Professor A.C. Potgieter, Deltamune, RSA). The secondary antibody was a fluorescently labelled (Alexa Fluor 488) goat anti-rabbit IgG conjugate (Thermofisher Scientific™).

For IFMA, Sf9 cells were seeded in a six-well plate at 1 X 10^6 cells/ml. The cells were infected with recombinant baculoviruses at a MOI of 1 and incubated at 28ºC in a humidified box for 72-120 hours. Thereafter, the media was removed. The Sf9 cells were fixed to the bottom of the six-well plate, and all the proteins were precipitated, by the addition of 1 ml of an ice-cold fixing solution (1:1 methanol: acetone), followed by 30 minutes of incubation at -20°C. Using organic solvents, e.g. methanol/acetone, for fixing cells makes a separate permeabilization step unnecessary. Organic solvents dissolve the lipids from cellular membranes thereby permeabilizing the cells, allowing access for the antibodies, and causing the coagulation and fixation of proteins in the Sf9 cells (Jamur & Oliver, 2010a; Jamur & Oliver, 2010b). This allows for the effective interaction of the primary antibodies with the precipitated proteins. The fixed Sf9 insect cells were washed with washing buffer (1x PBS with 0.05% Tween-20). Blocking buffer (1x PBS, 0.05% Tween-20 and 1% (w/v) tryptone) was added and incubated for 60 minutes at 37°C. Unspecific binding of the various antibodies was prevented by the blocking buffer coating the tissue flask with tryptone. The blocking buffer was removed, the primary antibody solution (serum-containing rabbit anti-RV IgG diluted 1:2000 in blocking buffer) was added, and incubated for 60 minutes at 37°C. The primary antibody binds to the specific antigenic epitopes of any RV proteins present. The primary antibody solution was removed, and the fixed Sf9 cells were washed three times with washing buffer to remove the excess primary antibody before adding the secondary antibody solution (anti-rabbit goat IgG conjugated diluted 1:2000 in blocking buffer). Following the addition of the secondary antibody solution, the six-well

plate was incubated for 60 minutes at 37°C. The secondary antibody binds specifically to the constant region of the rabbit antibodies. The bound secondary antibody was conjugated with an Alexa Fluor® 488 fluorescent complex. After the removal of the secondary antibody solution, the fixed cells were washed with PBS twice to remove all excess antibodies from the fixed monolayer.

The presence of RV proteins was visualized and photographed using a Nikon Eclipse TE2000-S fluorescent microscope (Nikon Instruments Inc. Melville, NY, USA). The conjugate emits a green light of which the excitation range (Ex) is approximately 495 nm and emission (Em) is approximately 519 nm.

2.2.17. Preparation of proteins from Sf9 insect cells

Sf9 cells were lysed using RIPA lysis buffer (150 mM sodium chloride, 1.0% NP-40, 0.5% sodium deoxycholate, 0.1% SDS, 50 mM Tris pH 8) supplemented with 0,025 U/µl Pierce™ Universal Nuclease for Cell Lysis (Thermofisher Scientific™ Inc., Waltham, MA, Cat no. 88701) prior to use. One tablet of Pierce™ EDTA-free protease inhibitor mini-tablets (Thermofisher Scientific™ Inc., Waltham, MA, Cat no. A32955) was added per 10 ml of RIPA lysis buffer.

Lysis of infected Sf9 insect cells was done by detaching the Sf9 insect cells from the six-well plate. Transferring the supernatant to a 2 ml microcentrifuge tube, followed by 5 minutes of centrifugation at 500 x g. The supernatant was removed and the cell pellet was lysed using 200 µl RIPA lysis buffer for 1 hour. For 50 ml shaker cultures, 10 ml RIPA lysis buffer was used. Following lysis, the total fraction (TF) was obtained by collecting lysate before centrifugation. The soluble fraction (SF) was obtained by centrifugation at 13 000 x g for 5 minutes and the supernatant was collected.

2.2.18. Sodium dodecyl sulphate-polyacrylamide gel electrophoresis (SDS-PAGE)

SDS-PAGE (Davis, 1964; Laemmli, 1970; Ornstein, 1964) was done as per the method described in Sambrook and Russell (2001). In short, a 12% acrylamide

revolving gel (0.25 M Tris pH 8.8, 1% (w/v) SDS, 1% (w/v) ammonium persulfate, 0,04% TEMED, and 12% acrylamide mix) and a 5% acrylamide stacking gel (126 mM Tris pH 6.8, 1% (w/v) SDS, 1% (w/v) ammonium persulfate, 0.1% TEMED, and 5% acrylamide mix) was used. The samples were run at 130 V for 90 minutes in TGS buffer (25 mM Tris, 250 mM Glycine, 0.1 % (w/v) SDS pH 8.3).

Proteins were visualised by staining the gel with Coomassie brilliant blue R-250 staining solution (0.25 g Coomassie brilliant blue R-250 per 100 ml of methanol: H_2O: glacial acetic acid solution in a 5:4:1 ratio) for 4 hours at room temperature. The gel was rinsed with water and de-stained for 4 hours at room temperature with methanol: H_2O: glacial acetic acid solution (5:4:1 ratio). The gels were visualized using a Bio-Rad ChemiDoc™ Imaging System (Bio-Rad, California, USA).

2.2.19. Western blot analysis

To verify the expression of RV proteins, western blot analysis (Burnette, 1981; Towbin & Gordon, 1984; Towbin *et al.*, 1979) was used. Western blot was performed according to the method described by Jere and co-workers (2012). The proteins (see Section 2.2.17) were separated by SDS-PAGE (Section 2.2.18) and then electro-blotted onto the nitrocellulose membrane (Whatman® GmbH. Dassel, Germany) while submerged in transfer buffer (25 mM Tris, 192 mM glycine, 20% methanol, pH 8.3) at 100 V for 1 hour. The membranes were stained with Ponceau S solution (Sigma-Aldrich, St. Louis, MO) to confirm the transfer of the proteins. The membranes were blocked by submergence for 3.5 hours at 4°C in 5% non-fat skim milk (Nestle (Pty) Ltd, Randburg, South Africa) in TNT buffer (0.05% Tween, 0.2 M NaCl and 0.05 M Tris-HCl (pH 7.4)). Thereafter, the membranes were washed three times with TNT buffer. Followed by incubation for 8 hours at 4°C with polyclonal rabbit anti-RV VP2/6 DLP IgG (serum kindly provided by Prof A.C. Potgieter, Deltamune, RSA) which was diluted to a 1:1000 ratio in blocking buffer (5% non-fat skim milk in TNT buffer). Primary antibodies bind to the RV VP2 and VP6 proteins. Then the membranes were washed three times with TNT buffer (5 minutes each) and then incubated in secondary antibody, donkey horseradish peroxidase-conjugated anti-rabbit IgG (Abcam San Francisco, CA) diluted 1:500 in TNT buffer for 1 hour. The secondary antibody conjugated with horse radish peroxidase (Sternberger *et al.*, 1970) binds to the constant region of the primary antibody. Thereafter the membranes were washed

three times with TNT buffer, followed by incubation with AEC buffer (0.03% 3-amino-9-ethylcarbazole (AEC) in 100% dimethylformamide, 0.2% H_2O_2 in 50 mM Sodium acetate buffer, pH 5.2) until bands were visible. AEC (3-amino-9-ethylcarbazole) was used which forms a red-coloured chromogen (Burstone, 1960; Graham *et al.*, 1965) with a distinct water-insoluble precipitate used as the substrate for the horse radish peroxidase (Koretz *et al.*, 1987). The reaction was stopped by washing with H_2O.

2.2.20. Production of RV-DLPs

To generate RV-DLPs, plaque-purified amplified recombinant dualcistronic baculovirus expressing RV VP2 and VP6 were used to infect Sf9 cells at a MOI of 5.

Infected cultures were incubated at 28°C and 100 rpm in Gibco® TC-100 Insect Medium supplemented with 20 mM calcium and 1 tablet of Pierce™ Protease Inhibitor Mini Tablets, EDTA-free (Thermofisher Scientific™ Inc., Waltham, MA, Cat no. A32955) until CPE was reached in approximately 95% of the infected cell culture (roughly five days post-infection).

2.2.21. Production of chimaeric RV-VLPs

To generate RV-TLPs using the co-infection approach, Sf9 cells were co-infected with plaque-purified recombinant baculoviruses. The method of Jere and co-workers (2012) was used for co-infection.

Plaque-purified rBV stocks confirmed to express RV proteins were used to infect Sf9 cells at a MOI of 5. To generate chimeric RV-TLPs consisting of RV GR10924 DLPs and African strain outer capsids, Sf9 cells were simultaneously co-infected with dualcistronic rBVs that were verified to express RV GR10924 VP2 and VP6 with dualcistronic rBVs confirmed to express African RV VP4 and VP7.

Infected cultures were incubated at 28°C and 100 rpm in Gibco® TC-100 Insect Medium supplemented with 20 mM calcium and 1 tablet of Pierce™ Protease Inhibitor Mini Tablets, EDTA-free (Thermofisher Scientific™ Inc., Waltham, MA, Cat no. A32955) until CPE was reached in approximately 95% of the infected cell culture (roughly five days post-infection).

2.2.22. Verification of the production of chimaeric rotavirus-like particles using transmission electron microscopy (TEM)

To verify the assembly of RV-VLPs, the cell lysates were ultracentrifuged for 2 hours at 135121.5 x g (28 100 rpm) through a 40% sucrose cushion using a Sorvall WX Ultra Series centrifuge (Thermo Fisher Scientific Inc., Waltham, MA) and a Sorvall TH-641 rotor (Thermo Fisher Scientific Inc., Waltham, MA) and pellets were resuspended in Tris-calcium (TNC) buffer (10 mM Tris-HCl [pH 7.4], 20 mM $CaCl_2$ (instead of the usual 10 mM $CaCl_2$ to ensure that the sample remains at 20 mM calcium) (Patient *et al.*, 2009)). Thereafter, the resuspended pellets were washed using TNC buffer. This was done by diluting the resuspended pellets in TNC buffer and ultra-centrifuging it for 2 hours at 134663.7 x g (31 500 rpm) using a Sorvall WX Ultra Series centrifuge and a Sorvall TH-660 rotor. The resulting pellets were resuspended in 200 µl TNC buffer.

The samples were sent to Dr. Anine Jordaan at the North-West University Laboratory for Electron Microscopy for TEM. In brief, a drop of the VLP suspension in Tris-calcium buffer was placed on a 300 mesh carbon-covered grid. The majority of the drop was removed with filter paper, leaving a thin watery film which was stained for 3 minutes in 1.5% ammonium aqueous molybdate (pH 7). The excess stain was blotted off with filter paper, and the grid was allowed to dry for 5 minutes. The grid was then inspected in a Tecnai G12 (FEI, Netherlands) transmission electron microscope at 120 kV. Electron micrographs were digitally recorded with a Gatan bottom mount camera and Digital Micrograph software.

2.3. Results and Discussion

2.3.1. Preparation of RVA/Human-wt/ZAF/GR10924/1999/G9P[6] DLPs

This investigation aimed to attempt to generate fully assembled RV-TLPs using the same RV GR10924 DLPs and African RV outer capsid proteins as Jere and co-workers (2012, 2014) in the presence of 20 mM calcium supplementation.

A pFBd_GR10924_VP2-VP6 donor plasmid (Fig. 2.2) was *in silico* designed to contain insect cell codon-optimized ORFs encoding RV GR10924 VP2 and VP6 which was purchased from GenScript (GenScript USA Inc., New Jersey, USA), as described in Section 2.2.3. After the arrival of pFBd_GR10924_VP2-VP6, it was transformed and propagated in *E. coli* JM109 cells. Thereafter, pFBd_GR10924_VP2-VP6 was purified.

To generate recombinant bacmid DNA encoding RV GR10924 VP2 and VP6, competent AcBACΔCC *E. coli* cells were transformed with purified pFBd_GR10924_VP2-VP6. Colonies that contained recombinant bacmid were white and colonies harbouring unaltered bacmid were blue (see Sections 2.2.1 and 2.2.7). Only about ~6 out of ~ 100 colonies were white, indicative of a low transposition and transformation efficiency. A possible explanation for the low transformation efficiency may be that archived competent AcBACΔCC *E. coli* cells were used instead of generating newly competent AcBACΔCC *E. coli* cells just before the transformation. However, enough white colonies were generated to continue the study.

To confirm successful transposition three white colonies of AcBACΔCC *E. coli* cells, transformed with pFBd_GR10924_VP2-VP6, were selected and streaked further onto LB-agar plates supplemented with X-Gal, IPTG, and antibiotics as per Section 2.2.7. This was to confirm that they were truly white colonies, and not colonies containing mixtures between recombinant and wild-type AcBACΔCC *E. coli* cells. Thereafter, 10 of the resulting white colonies from each streaked AcBACΔCC *E. coli* colony were selected for analysis. Also, three blue AcBACΔCC *E. coli* colonies harbouring empty bacmid DNA were selected for PCR analysis as a negative control. Bacmid DNA was extracted and analysed using PCR with M13 primers. Amplicons were visualised on agarose gels (Fig. 2.4, the amplicons containing RV ORFs are marked with an asterisk). The bacmid transposed with pFBd_GR10924_VP2-VP6 (referred to here as rBacmid_GR10924_VP2/6, followed by colony number) resulted in amplicons of approximately 6 300 bp. Amplicons of 300 bp were obtained from bacmid DNA from blue colonies (here referred to as wild-type (WT) bacmid).

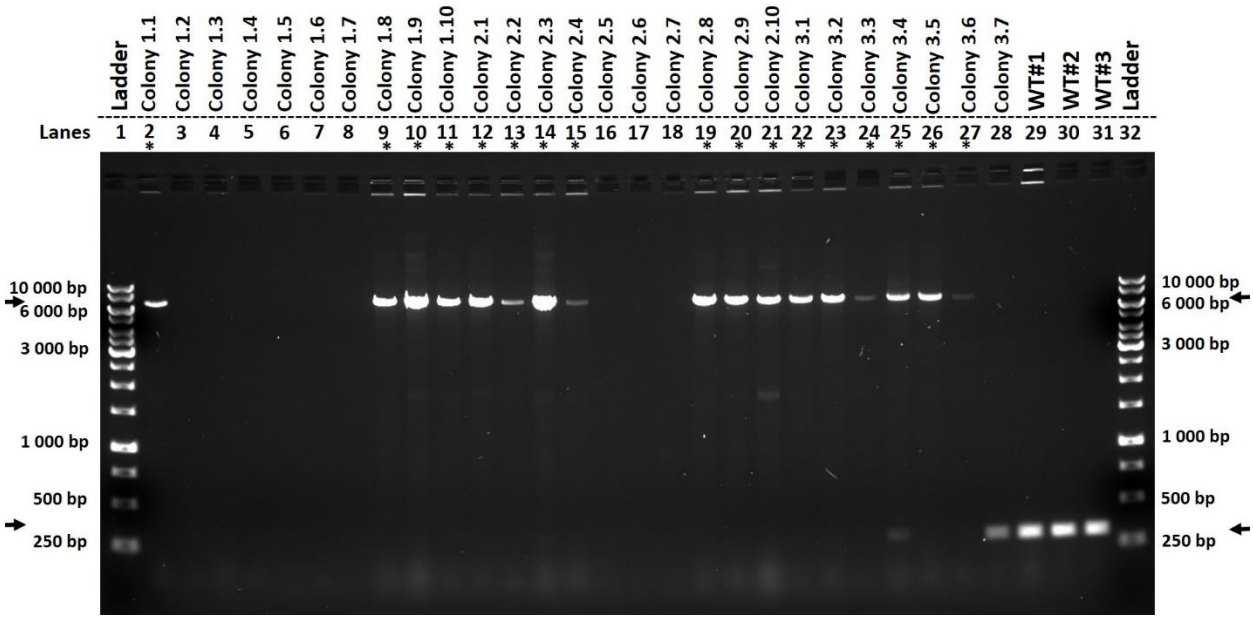

Figure 2.4: Agarose gel of PCR of bacmid DNA. The bacmid expression cassette was designed for preparing dualcistronic baculoviruses expressing RV GR10924 VP2 and VP6. The arrows indicate the expected bands. The asterisks indicate colonies containing recombinant bacmid DNA. Lanes 29-31 contained empty bacmid (wild-type). Lanes 1 and 32 contained GeneRuler 1 kb DNA Ladder (Thermofisher Scientific™, Catalogue number: SM0311).

Sixteen of the colonies (Fig. 2.4), colonies 1.1 (lane 2), 1.8-2.4 (lanes 9-15), 2.8-3.3 (lanes 19-24), and 3.5-3.6 (lanes 26-27), generated amplicons of approximately 6 300 bp during PCR analysis of the isolated bacmid DNA, indicative of pure recombinant bacmid DNA containing the transpositioned expression cassette encoding RV GR10924 VP2 and VP6 (Fig. 2.4). Three of the colonies (Fig. 2.4), colonies 2.4 (lane 15), 3.3 (lane 24), and 3.6 (lane 27) resulted in weak amplification, possibly due to low AcBACΔCC *E. coli* cell yield during overnight culturing, high salt content due to insufficient washing of the DNA pellet with 70% ethanol, or the loss of a large portion of the DNA during the DNA isolation. Purified bacmid DNA from nine colonies, colonies 1.2-1.7 (lanes 3-8) and 2.5-2.7 (lanes 16-18) did not generate amplicons during PCR analysis. This is possibly due to the loss of the pellets during the bacmid DNA isolation (see Section 2.2.8). Purified bacmid DNA from colony 3.4, in lane 25, resulted in two amplicons of 6 300 bp and 300 bp during PCR analysis. Although the 6 300 bp amplicon is correct, the presence of a 300 bp amplicon indicates wild-type bacmid contamination in this colony (bull's eye colonies). This is expected as some colonies appear predominantly white but are actually mixed colonies of recombinant and wild-type AcBACΔCC *E. coli* cells. Colony 3.7, in lane 28, also appeared white but, as indicated by the 300 bp amplicon (Fig. 2.3), was a wild-type AcBACΔCC *E. coli* colony. A possible explanation for this white appearance of a wild-type AcBACΔCC *E. coli*

colony may be that the colony was close to the edge of the LB-agar plate. Sometimes the X-Gal and IPTG do not completely cover the plate, especially near the edges. Therefore, in the absence of X-Gal a wild-type AcBACΔCC *E. coli* colony would appear white. The three blue colonies, selected as controls in lanes 29-31 resulted in the expected 300 bp amplicons (Fig. 2.3).

2.3.2. Generation of recombinant baculoviruses expressing RVA/Human-wt/ZAF/GR10924/1999/G9P[6] VP2 and VP6

Following the confirmation that recombinant bacmids (rBacmids) containing the RV GR10924 VP2 and VP6 expression cassette were generated (rBacmid_GR10924_ VP2/6), the next step was to generate recombinant baculoviruses (rBVs) expressing RV GR10924 VP2 and VP6 that assemble into DLPs.

Five white recombinant AcBACΔCC *E. coli* colonies (rBacmid_GR10924_VP2/6_#1.1; rBacmid_GR10924_VP2/6_#1.9; rBacmid_GR10924_VP2/6_#2.1; rBacmid_ GR10924_VP2/6_#2.3; rBacmid_GR10924_VP2/6_#2.8; rBacmid_GR10924_VP2/6 _#3.1; and rBacmid_GR10924_VP2/6_#3.5) and one wild-type blue colony (WT1, lane 29, Fig.2.4) were selected and used to inoculate LB media supplemented with the appropriate antibiotics as described in Section 2.2.8. Bacmid DNA was extracted and transfected into Sf9 insect cells to generate recombinant and wild-type baculoviruses. Sf9 cells were transfected with pmaxGFP to estimate transfection efficacy (see Section 2.2.12), which was estimated to be between 10-20%. This is lower than the 40% transfection efficacy of other studies (Roest *et al.*, 2016). However, higher transfection efficacy is not a critical component of baculovirus expression (Roest *et al.*, 2016), since the initial yield of recombinant baculoviruses can be increased by passaging.

Four of the recombinant baculovirus stocks (rBV_GR10924_VP2/6_#1.1; rBV_ GR10924_VP2/6_#1.9; rBV_GR10924_VP2/6_#2.1; rBV_GR10924_VP2/6_#3.1) were selected for plaque purification via agarose plaque assays. Plaque purification decreases the risk of wild-type baculovirus contamination and allows for the selection of individual recombinant baculoviruses since all recombinant baculoviruses do not express proteins equally well. Plaque purification allows the comparison of protein expression of the different baculoviruses and allows for the rough selection of those viruses that express the inserted ORFs best. Further, plaque purification via agarose

assay allowed for the estimation of the titer of the recombinant baculovirus P1 stock following transfection (Table 2.3).

Table 2.3: The titer of various rBV_GR10924_VP2/6 P1 stocks and the relevant white colony (from Fig 2.4) and recombinant bacmid.

White colony number (Fig 2.4)	Recombinant bacmid	Recombinant virus name	The titer of P1 stock
Colony 1.1	rBacmid_GR10924_VP2/6_#1.1	rBV_GR10924_VP2/6_#1.1	~1 X 10^7 pfu/ml
Colony 1.9	rBacmid_GR10924_VP2/6_#1.9	rBV_GR10924_VP2/6_#1.9	~2 X 10^7 pfu/ml
Colony 2.1	rBacmid_GR10924_VP2/6_#2.1	rBV_GR10924_VP2/6_#2.1	~1 X 10^7 pfu/ml
Colony 3.1	rBacmid_GR10924_VP2/6_#3.1	rBV_GR10924_VP2/6_#3.1	~1 X 10^7 pfu/ml

As per the Bac-to-Bac® Baculovirus Expression Systems manual (Life Technologies, Grand Island, NY), the titer following transfection should be in the range of 1 x 10^7 pfu/ml to 2 x 10^8 pfu/ml. Therefore, although the initial transfection efficacy was lower than expected, the titer following transfection was sufficient to continue with the study.

Five recombinant baculovirus plaques were picked during plaque purification. The picked recombinant plaque-purified baculovirus plaques were propagated three times on Sf9 cells to increase the titer. The resulting supernatants containing plaque-purified baculoviruses were stored as plaque-purified baculovirus stocks for further use.

To ensure that the picked plaques were not contaminated with wild-type baculoviruses, Sf9 cells were seeded in six-well plates (see Section 2.2.16). One well was not infected to be used as control, and another well was infected with wild-type baculovirus, also as control. Further, Sf9 cells were infected at a MOI of 5 with five plaques of rBV_GR10924_VP2/6_#1.1; rBV_GR10924_VP2/6_#1.9; rBV_GR10924_VP2/6_#2.1; rBV_GR10924_VP2/6_#3.1. The Sf9 cells were visualised using IFMA four days post-infection. This allowed for the first indication of RV GR10924 VP2 and VP6 expression (Fig. 2.5).

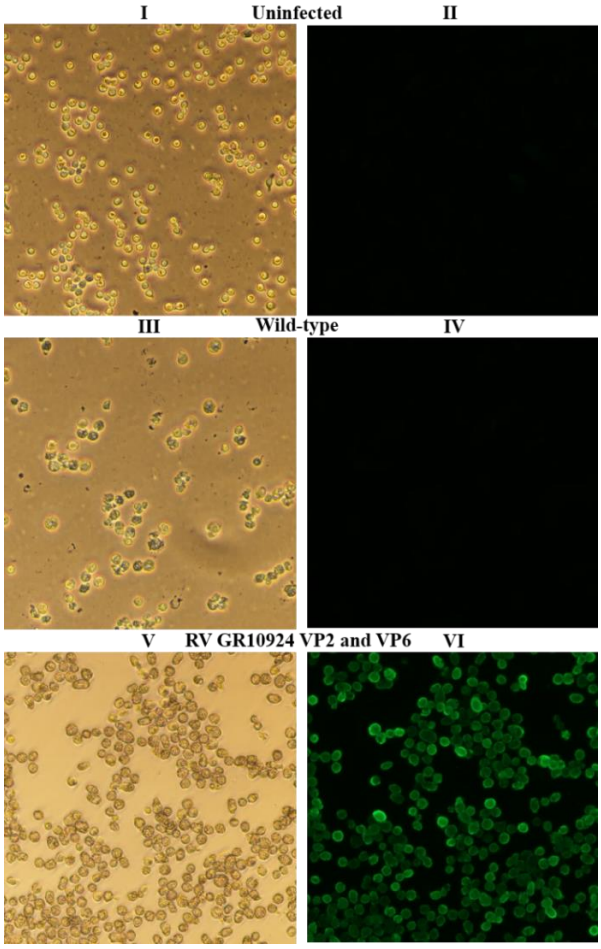

Figure 2.5: IFMA of Sf9 insect cells infected with rBV_GR10924_VP2/6_#3.1_#5. Uninfected Sf9 cells **(I)** bright field and **(II)** fluorescence. Sf9 cells infected with wild-type baculovirus **(III)** bright field and **(IV)** fluorescence. Sf9 cells infected with plaque-purified rBV_GR10924_VP2/6_#3.1_#5 **(V)** bright field and **(VI)** fluorescence. 400X magnification.

The uninfected Sf9 cells (Fig. 2.5: I) displayed no signs of CPE, however, the plate became over-confluent and during the removal of the supernatant, many of the uninfected Sf9 cells detached leading to the sparse appearance of the cells. As per Fig. 2.5: II, as expected the uninfected Sf9 cells displayed no fluorescence. As expected the polyclonal rabbit anti-RV VP2/6 DLP IgG raised against RV SA11 DLPs did not bind to Sf9 insect cell proteins. The Sf9 cells infected with wild-type baculovirus displayed visible signs of late-stage baculovirus infection on bright-field (Fig. 2.5: III) and as expected no fluorescence (Fig. 2.5: IV). Fig. 2.5: VI, indicates that the polyclonal rabbit anti-RV VP2/6 DLP IgG did not bind any of the native baculovirus proteins. The Sf9 cells infected with rBV_GR10924_VP2/6_#3.1_#5 (Fig. 2.5: V) displayed visible signs of late-stage baculovirus infection when viewed on bright-field 4 d.p.i. When the fluorescence was visualised for Fig. 2.5: VI, all the cells fluoresced. Fig. 2.5: V and VI were representative of all the wells (of the six-well plates) containing Sf9 cells infected with rBV_GR10924_VP2/6 (data not shown). This indicated the

expression of either RV group A VP2, VP6 or both VP2 and VP6, in the infected Sf9 cells following plaque purification. When a plaque is picked that is a mixture of recombinant and wild-type baculovirus, some of the infected Sf9 cells did not display fluorescence, those infected by wild-type baculovirus, while some small patches infected with the recombinant baculovirus do display fluorescence. The IFMA results confirmed the expression of RV GR10924 VP6 and VP2 by these plaque-purified recombinant baculoviruses.

Next, RV protein expression was visualised using SDS-PAGE analysis. Three plaques of rBV_GR10924_VP2/6_#1.1, rBV_GR10924_VP2/6_#2.1, and rBV_GR10924_VP2/6_#3.1 were selected, based on the IFMA data (data not shown, except for rBV_GR10924_VP2/6_#3.1_#5 in Fig. 2.5: V and VI as representative), and used to infect Sf9 cells seeded in six-well plates using a MOI of 5 (see Section 2.2.18). Each six-well plate contained a well infected with wild-type baculovirus and a well of uninfected Sf9 cells. The Sf9 cells were grown and infected in supplemented Gibco® TC-100 Insect Medium without additional calcium supplementation. The lysed cells were visualised using SDS-PAGE (Fig. 2.6).

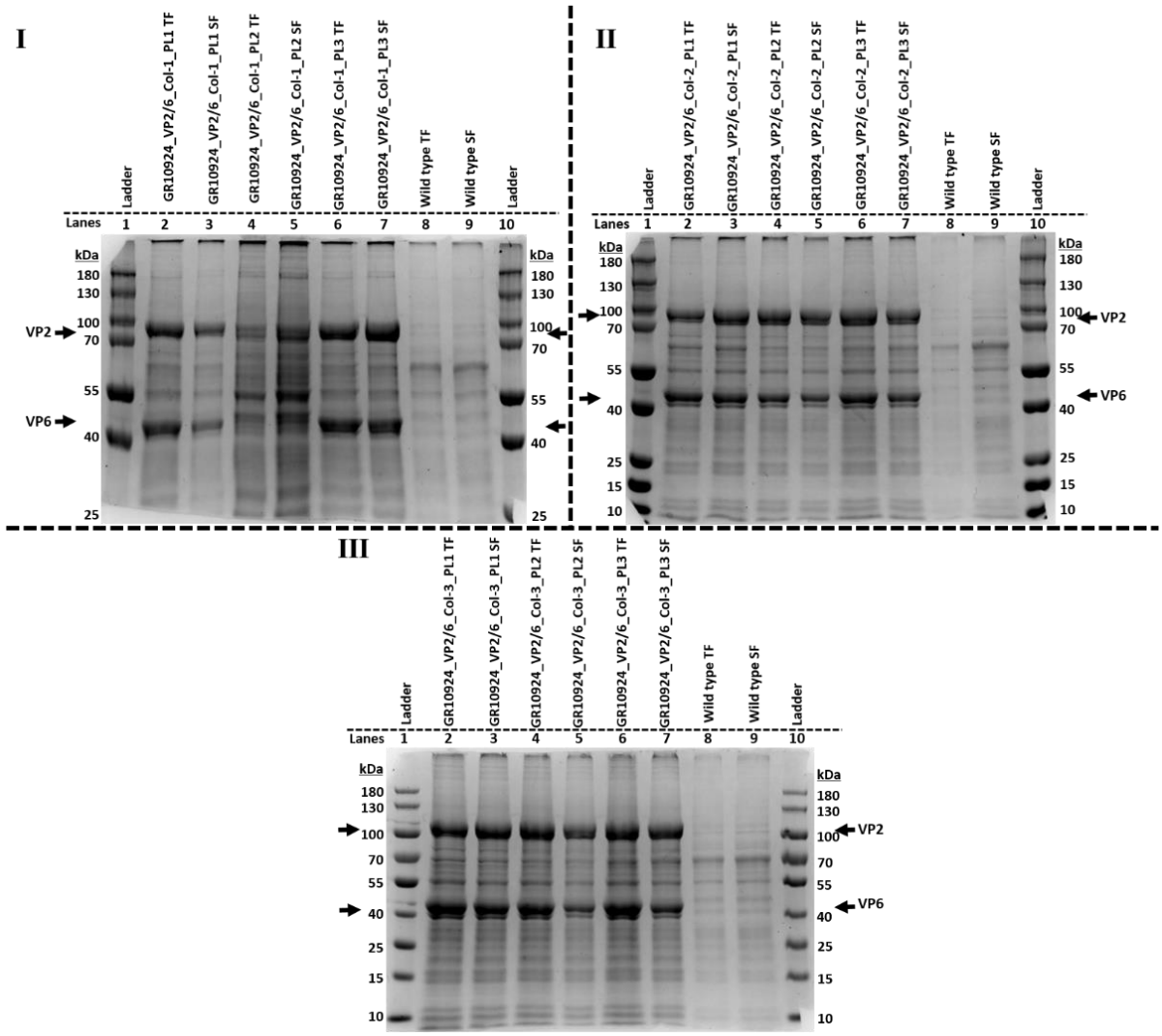

Figure 2.6: SDS-PAGE of RVA/Human-wt/ZAF/GR10924/1999/G9P[6] VP2 and VP6 expressed by plaque-purified rBV_GR10924_VP2/6. Rotavirus GR10924 VP2 and VP6 expressed by three plaques of dualcistronic rBV_GR10924_VP2/6, **(I)** rBV_GR10924_VP2/6_#1.1 **(II)** rBV_GR10924_VP2/6_#2.1 and **(III)** rBV_GR10924_VP2/6_#3.1. The total fraction and then the soluble fraction of each sample were loaded. Arrows indicate the expected sizes of the proteins. Lanes 8 and 9 of each gel contained wild-type (empty baculovirus) total and soluble fractions, respectively, as controls. Lanes 1 and 10 of each gel contained PageRuler™ Prestained Protein Ladder (Catalogue number: 26616, Thermofisher Scientific™).

Total and soluble fractions of the lysed Sf9 cells infected with the rBV, listed above each gel, were visualised on SDS-PAGE. Also, a total and soluble fraction of lysed Sf9 cells infected with wild-type baculovirus were run on each gel as a control. As per Fig. 2.6: I-III: lanes 2-7, proteins of approximately 100 kDa (corresponding to the expected size of VP2) and 45 kDa (corresponding to the expected size of VP6) were visualised on SDS-PAGE. The lanes containing wild-type infected Sf9 cell lysates do not display these overexpressed proteins, Fig. 2.6: I- III: lanes 8-9. The expression of VP2 (100 kDa) and VP6 (45 kDa) was comparable with that of Jere and co-workers (2012). However, Jere and co-workers (2012) expressed RV VP2/6/4/7 in both Sf9

and High Five cells, and reported that High Five cells generated three times more particles than Sf9 cells. Therefore, the overexpression of VP2 and VP6 in Sf9 cells compared with that of Jere and co-workers (2012) was unexpected (Jere *et al*., 2012). The approximately 100 kDa (VP2) and 45 kDa (VP6) bands were as expected in Fig. 2.6: I: lanes 2, 3, 6, 7; Fig. 2.6: II: lanes 2-7; and Fig. 2.6: III: lanes 2-7. However, the approximately 100 kDa (VP2) and 45 kDa (VP6) bands in Fig. 2.6: I: lanes 4 and 5, rBV_GR10924_VP2/6_ #1.1_PL2 ("PL" here refers to plaque) displayed double bands, instead of the expected single bands and no clear VP6 band.

Following confirmation of RV GR10924 VP2 and VP6 expression in six-well plates, the next step was to up-scale expression to 50 ml shaker cultures to increase the volume of the recombinant baculovirus stocks. Based on the expression visualised on SDS-PAGE, rBV_GR10924_VP2/6_#1.1_PL2 (Fig. 2.6: I: lanes 4 and 5), and rBV_ GR10924_VP2/6_#2.1_PL3 (Fig. 2.6: II: lanes 6 and 7), rBV_GR10924_VP2/6_#3.1_ PL2 (Fig. 2.6: III: lanes 4, 5), and rBV_GR10924_VP2/6_#3.1_PL3 (Fig. 2.6: III: 6 and 7) were selected for amplification in 50 ml shaker culture.

Following the generation of larger volumes of recombinant baculovirus stocks, the next step was to generate RV GR10924 DLPs, followed by an assessment of the DLP assembly via TEM analysis. Therefore, the titer of the amplified baculovirus stocks was quantified. Following quantification of the titre of the amplified baculovirus stocks, 50 ml shaker cultures were infected with recombinant plaque-purified baculoviruses confirmed to express RV GR10924 VP2 and VP6. The 50 ml shaker cultures were infected at a MOI of 5 with rBV_GR10924_VP2/6_#1.1_PL2, rBV_GR10924_VP2/6_ #2.1_PL3, rBV_ GR10924_VP2/6_#3.1_PL2, rBV_GR10924_ VP2/6_#3.1_PL3, and a wild-type baculovirus. Following the infection of the four 50 ml shaker cultures, the infected Sf9 cells were lysed. To ensure that sufficient RV GR10924 VP2 and VP6 to form RV-DLPs were expressed in shaker culture, the prepared proteins were first visualised on SDS-PAGE and western blot, before proceeding to TEM analysis, (Fig. 2.7).

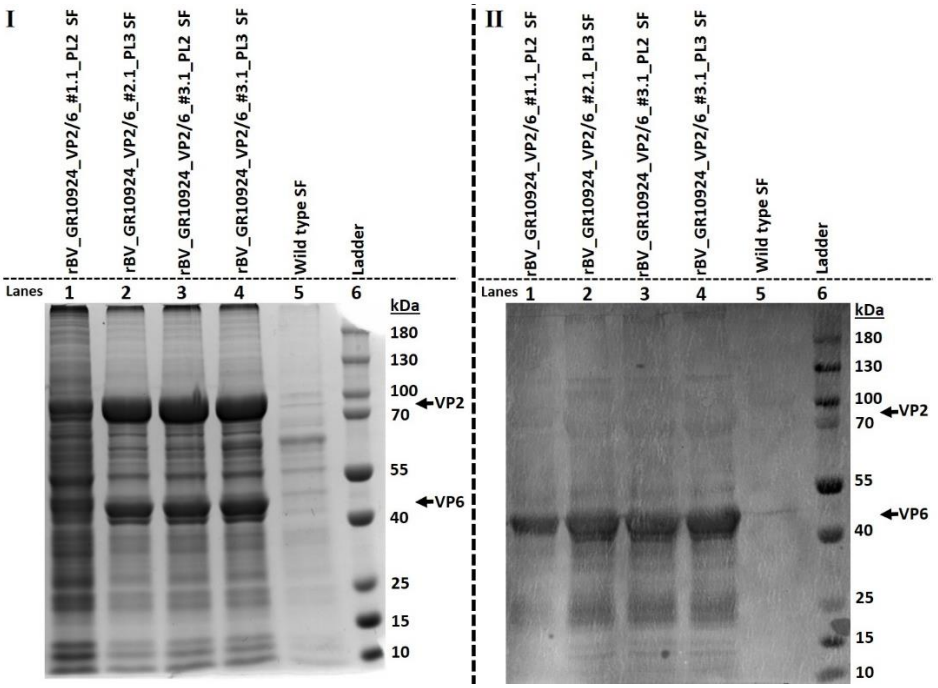

Figure 2.7: SDS-PAGE (I) and western blot analysis (II) of the expression of RVA/Human-wt/ZAF/GR10924/1999/G9P[6] VP2 and VP6 by plaque-purified rBV_GR10924_ VP2/6. Only the soluble fractions of each sample were loaded. Lanes 5 of each gel contained wild-type baculovirus as a control. Lane 6 of each gel contained PageRuler™ Prestained Protein Ladder (Catalogue number: 26616, Thermofisher Scientific™).

The expression of RV VP2 (100 kDa) and RV VP6 (45 kDa) was visualised on SDS-PAGE analysis following amplification of the plaque-purified recombinant baculovirus stocks, Fig. 2.7: I: lanes 1-4. The expression of VP2 (100kDa) and VP6 (45 kDa) by Sf9 cells infected with rBV_GR10924_ VP2/6_#2.1_PL3 (Fig. 2.7: I: lane 2), rBV_ GR10924_VP2/6_#3.1_PL2 (Fig. 2.7: I: lane 3), and rBV_GR10924_VP2/6_#3.1_PL3 (Fig. 2.7: I: lane 4) was comparable with that of Jere and co-workers (2012). The SDS-PAGE analysis was done in duplicate and western blot analysis was performed. The expression of RV VP6 (45 kDa) was visualised on western blot, Fig. 2.7: II: lanes 1-4. Rotavirus VP2 was not detected using western blot. The western blot analysis used polyclonal rabbit anti-RV VP2/6 DLP IgG raised against RV SA11 DLPs. Rotavirus VP6 is the dominant group antigen, and VP2 is located beneath VP6 within the RV-DLP, which may explain why VP2 is less immunogenic and thus not visualised using western blot analysis. It may also be that VP2 is less immunogenic in rabbits when compared to other animal models, such as e.g. mice. Based on the high levels of RV VP2 and VP6 expression, the next step was to assess RV-DLP assembly. As per Fig. 2.6: I: lanes 4 and 5, and Fig. 2.7: I: lane 1, rBV_GR10924_VP2/6_#1.1_PL2 displayed double bands on SDS-PAGE. When analysed with western blot the suspected VP6

band did bind polyclonal rabbit anti-RV VP2/6 DLP IgG, as per Fig. 2.7: I: lane 1. Likely the expression of VP2 and VP6 by this recombinant plaque-purified baculovirus was less than those of rBV_GR10924_ VP2/6_#2.1_PL3 (Fig. 2.7: I: lane 2, Fig. 2.7: II: lanes 2), rBV_ GR10924_VP2/6_ #3.1_PL2 (Fig. 2.7: I: lane 3, Fig. 2.7:II: lanes 3), and rBV_GR10924_VP2/6_#3.1_ PL3 (Fig. 2.7: I: lane 4, Fig. 2.7:II: lanes 4). Therefore, giving the appearance of double bands due to background Sf9 insect cell proteins or baculovirus proteins.

Following the confirmation of sufficient RV VP2 and VP6 expression in 50 ml shaker cultures, the next step was to assess the assembly of RV-DLPs using TEM. Therefore, plaque-purified rBV_GR10924_VP2/6_#3.1_PL3 (Fig. 2.7: I lane 4) was selected. A 50 ml shaker culture was infected at a MOI of 5 and the infected Sf9 cells lysed 5 d.p.i. The lysate was ultracentrifuged through a 40% sucrose cushion. Following ultracentrifugation, the assembly of RV-DLPs were analysed using TEM, Fig. 2.8.

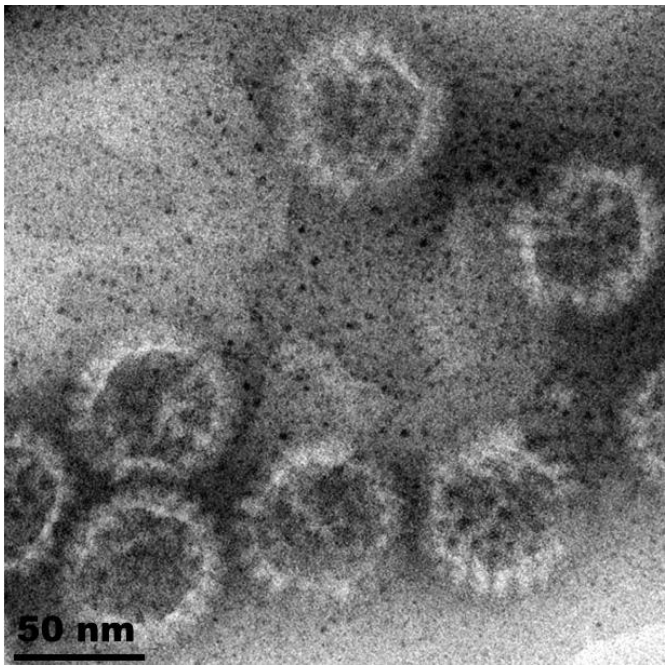

Figure 2.8: Electron micrograph of RVA/Human-wt/ZAF/GR10924/1999/G9P[6] VP2/6 DLPs. Rotavirus DLPs were produced by infecting Sf9 insect cells with dualcistronic plaque-purified rBV_GR10924_VP2/6_ #3.1_PL3 expressing RV GR10924 VP2 (C2) and VP6 (I2) proteins. Scale bar 50 nm.

As per Fig. 2.8, the assembly of RV GR10924 VP2/6 DLPs by rBV_GR10924_VP2/6_ #3.1_PL3 were comparable to those generated by Jere and co-workers (2012). The diameter (roughly 70 nm) and the morphology (brush-like appearance) were as expected for RV-DLPs. Therefore, the next step was to retrieve the archived

recombinant bacmids encoding African RV strain VP4 and VP7 outer capsids, generated by Jere and co-workers (2012).

2.3.3. Retrieval of three archived recombinant bacmids (rBacmid_G12P[4], rBacmid_G12P[6], and rBacmid_G12P[8])

To generate recombinant baculoviruses expressing VP4s and VP7s of African RV strains in co-infection of Sf9 cells in the presence of 20 mM calcium, three recombinant bacmids could be retrieved from the frozen -80°C archives. Three recombinant AcBACΔCC *E. coli* cell stocks containing dualcistronic recombinant bacmids (rBacmids) encoding RV VP7 (genotype G12) and RV VP4 (genotypes P[4], P[6], and P[8]) could be retrieved from frozen archives (strains listed in Table 2.1, see Section 2.2.2).

The three recombinant AcBACΔCC *E. coli* stocks were streaked on LB-agar plates (supplemented with X-Gal, IPTG, and antibiotics as per Section 2.2.7) and screened using blue-white selection (see Section 2.2.8). Following confirmation of their viability, the presence of the ORFs encoding African RV outer capsid proteins (genotypes G12P[4], G12P[6], and G12P[8]) was analysed by PCR. Thus, two white colonies of each of the recombinant AcBACΔCC *E. coli* cells, and two wild-type blue colonies (wild-type bacmid) were used to inoculate LB media supplemented with the appropriate antibiotics as described in Section 2.2.8. The wild-type bacmid was used as a control. Bacmid DNA was isolated following overnight culturing. PCR was performed using M13 primers (listed in Table 2.2, see Section 2.2.9), and amplicons were visualised on agarose gels (Fig. 2.9).

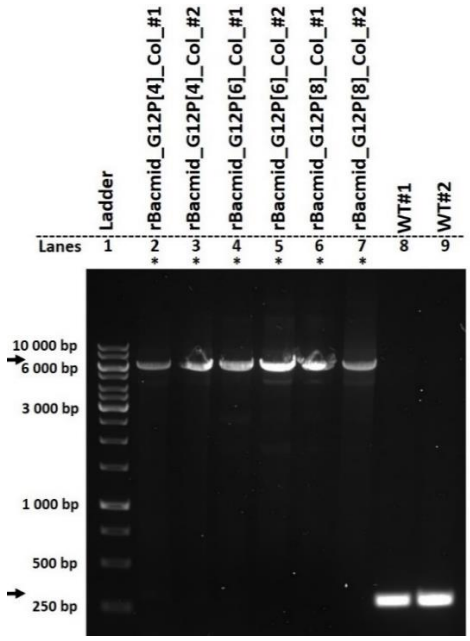

Figure 2.9: Agarose gel of PCR of isolated bacmid DNA encoding African RV strain VP4 and VP7 (genotypes G12P[4], G12P[6], and G12P[8]). The bacmid expression cassettes were designed for preparing dualcistronic baculoviruses expressing both VP4 and VP7 (Jere, 2012). Lanes 2-7 contained PCR amplicons from various recombinant bacmids listed above each lane. Asterisks indicate colonies that contained recombinant bacmid DNA. Lanes 8 and 9 contained wild-type bacmid. Lane 1 contained GeneRuler 1 kb DNA Ladder (Thermofisher Scientific™, Catalogue number: SM0311).

PCR of recombinant bacmid DNA isolated from all six white colonies resulted in amplicons of approximately 6300 bp for rBacmid_G12P[4]_Col_#1 (Fig. 2.10: lane 2), rBacmid_G12P[4]_Col_#2 (Fig. 2.9: lane 3), rBacmid_G12P[6]_Col_#1 (Fig. 2.9: lane 4), rBacmid_G12P[6]_Col_#2 (Fig. 2.9: lane 5), rBacmid_G12P[8]_Col_#1 (Fig. 2.9: lane 6), and rBacmid_G12P[8]_Col_#2 (Fig. 2.9: lane 7) as expected and no 300 bp bands were present, indicating that the recombinant bacmid DNA was not contaminated with wild-type bacmid. Lanes 2 and 7 had relatively fewer amplicons than lanes 3-6, possibly due to less recombinant bacmid DNA isolated. The density of the AcBACΔCC *E. coli* cells following overnight culturing of these AcBACΔCC *E. coli* cells, before bacmid DNA isolation (see Section 2.2.8), may have been lower than the other revived AcBACΔCC *E. coli* cell stocks. Thus, resulting in less DNA isolation. Therefore, fewer amplicons were generated following PCR relative to the other PCR reactions. This may be expected due to the long-term storage of these AcBACΔCC *E. coli* cells. The PCR of wild-type (empty) bacmid DNA resulted in amplicons of 300 bp (lanes 8 and 9), as expected (Fig. 2.3). Lanes 4-7 contained small amounts of non-specific amplicons of roughly 5000 bp, 2500 bp and 2000 bp.

2.3.4. Generation of rBV_G12P[4], rBV_G12P[6], and rBV_G12P[8]

To generate recombinant baculoviruses, firstly, the six recombinant AcBACΔCC *E. coli* colonies and one wild-type blue colony, analysed using PCR, were used to inoculate LB media (supplemented as per Section 2.2.8). The bacmid DNA of rBacmid_G12P[4]_Col_#1 (Fig. 2.9: lane 2), rBacmid_G12P[4]_Col_#2 (Fig. 2.9: lane 3), rBacmid_G12P[6]_Col_#1 (Fig. 2.9: lane 4), rBacmid_G12P[6]_Col_#2 (Fig. 2.9: lane 5), rBacmid_G12P[8]_Col_#1 (Fig. 2.9: lane 6), rBacmid_G12P[8]_Col_#2 (Fig. 2.9: lane 7), and wild-type bacmid was isolated. The isolated bacmid DNA was used to transfect Sf9 cells. Following transfection, when complete CPE was observed (~6 d.p.i.) the supernatant was removed and stored as a P1 stock.

Three of the generated recombinant baculoviruses were selected: rBV_G12P[4]_Col#1, rBV_G12P[6]_Col#1, and rBV_G12P[8]_Col#1, further referred to as rBV_G12P[4], rBV_G12P[6], and rBV_G12P[8], respectively. These recombinant baculoviruses were blindly passaged three times on Sf9 cells to increase the titer. Thereafter, Sf9 cells were infected with P3 rBV stocks of rBV_G12P[4], rBV_G12P[6] and rBV_G12P[8] at a MOI of 5 and lysed four days post-infection. The lysates were analysed using SDS-PAGE, Fig. 2.10.

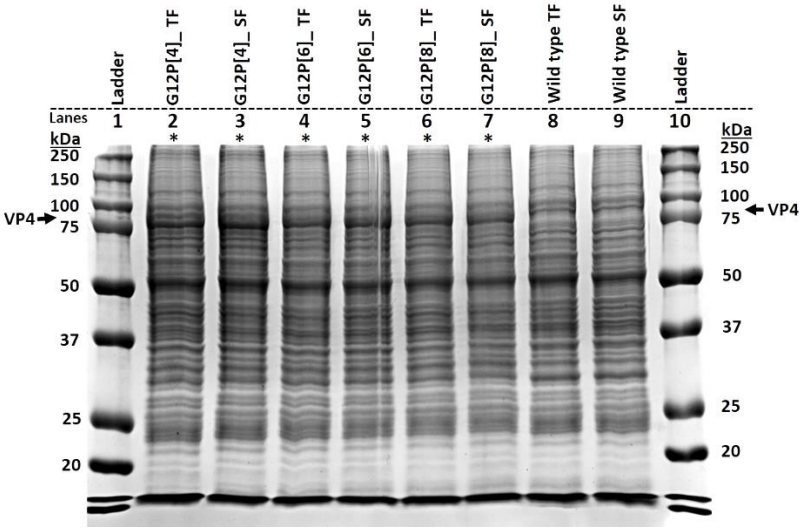

Figure 2. 10: SDS-PAGE of prepared proteins from rBV_G12P[4], rBV_G12P[6], and rBV_G12P[8] before plaque purification. Lanes 8 and 9 contained wild-type (empty baculovirus) total and soluble fractions, respectively, as controls. The asterisks indicate lanes that likely contain expressed RV VP4. Lanes 1 and 10 contained Precision Plus Protein™ Dual Color Standards (Catalogue number: #1610374, Bio-Rad, California, USA).

Rotavirus VP4 (85 kDa) could be visualised in Fig. 2.10 from rBV_G12P[4] (Fig. 2.10: lanes 2 and 3), rBV_G12P[6] (Fig. 2.10: lanes 4 and 5), and rBV_G12P[8] (Fig. 2.10:

lanes 6 and 7) before plaque purification. The expression of RV VP4 was lower than that obtained by Jere and co-workers (2012, 2014). No expression of RV VP7 was seen on SDS-PAGE. This was not unexpected, since the expression of RV VP7 (35 kDa) is usually difficult to visualise on SDS-PAGE using Coomassie staining.

Parallel to the blind passaging of the recombinant baculoviruses, the corresponding P1 baculovirus stocks of rBV_G12P[4], rBV_G12P[6], and rBV_G12P[8] were plaque purified. The titre of the P1 recombinant baculovirus stocks were determined to be: 1 x 10^7 pfu/ml for rBV_G12P[4], 1 x 10^6 pfu/ml for rBV_G12P[6], and 1 x 10^7 pfu/ml for rBV_G12P[8]. The baculovirus titer of rBV_G12P[4] P1 stock and rBV_G12P[8] P1 stock were as expected from the Bac-to-Bac® Baculovirus Expression Systems manual (Life Technologies, Grand Island, NY, USA). However, the titer of rBV_G12P[6] was 10 times lower than expected.

Following the confirmation of RV VP4 expression on SDS-PAGE analysis of the blindly passaged recombinant baculovirus, the purified baculovirus plaques were propagated (see Section 2.2.13). The resulting supernatant containing plaque-purified baculoviruses was stored as plaque-purified baculovirus stocks for further use (see Sections 2.2.13 and 2.2.14).

To confirm the expression of RV VP4 and VP7 by the plaque-purified rBV_G12P[4], rBV_G12P[6] and rBV_G12P[8], three plaques of rBV_G12P[4], rBV_G12P[6] and rBV_G12P[8] were picked and passaged three times. Thereafter, Sf9 cells were infected in six-well plates at a MOI of 5. Also, one well was infected with wild-type baculovirus to serve as a control. The infected Sf9 cells were lysed five days post-infection (d.p.i.), and the proteins were analysed using SDS-PAGE, Fig. 2.11.

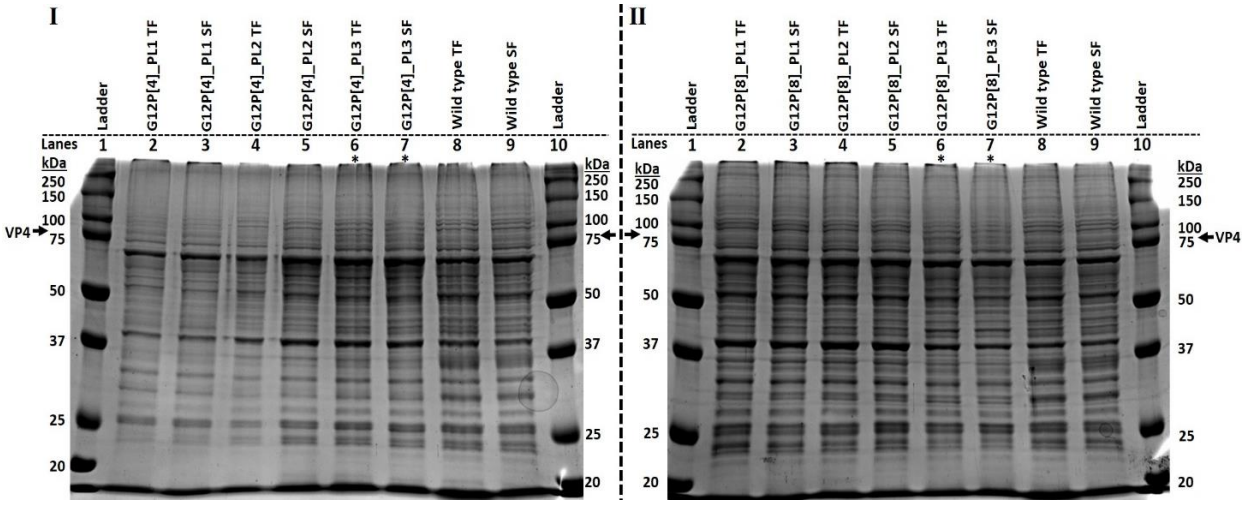

Figure 2.11: SDS-PAGE of lysed Sf9 insect cells infected with plaque-purified (I) rBV_G12P[4] and (II) rBV_G12P[8]. Lanes 8 and 9 of each gel contained wild-type (empty baculovirus) total and soluble fractions as control. The asterisks indicate lanes that contained expressed RV VP4. Lanes 1 and 10 of each gel contained Precision Plus Protein™ Dual Color Standards (Catalogue number: #1610374, Bio-Rad, California, USA).

No protein expression could be visualised in lysates from Sf9 cells infected with three plaques of rBV_G12P[6] (gel not shown). Therefore, rBV_G12P[6] plaques 1-3 were excluded from further attempts. Faint bands of VP4 of 85 kDa expressed by plaque-purified rBV_G12P[4]_PL3 (Fig. 2.11: I: lane 6 and 7) and rBV_G12P[8]_PL3 (Fig. 2.11: II: lane 6 and 7) were visualised on SDS-PAGE. Thus, after plaque-purification of the recombinant baculoviruses, and three passages of the plaque-purified rBVs, overall less protein expression was observed. Due to the unavailability of antibodies against RV VP4 and VP7 at this point in the study, western blot analysis could not be performed. In contrast to the recombinant dualcistronic baculoviruses expressing RV VP2/6 DLPs, further passaging of the recombinant dualcistronic baculoviruses expressing RV outer capsid VP4 and VP7 did not increase viral titer (results not shown). Transfection and purification were repeated multiple times without resulting in better expression.

Near the end of the study polyclonal rabbit anti-RV, SA11 TLP IgG (serum kindly provided by Professor A.C. Potgieter, Deltamune, RSA) became available. Unexpectedly, this made it possible to confirm the expression of African RV outer capsid proteins using IFMA. Sf9 cells were infected with rBV_G12P[4]_PL3 (plaque 3), rBV_G12P[6]_PL3 and rBV_G12P[8]_PL3 at a MOI of 10 visualised four days post-infection, Fig. 2.12.

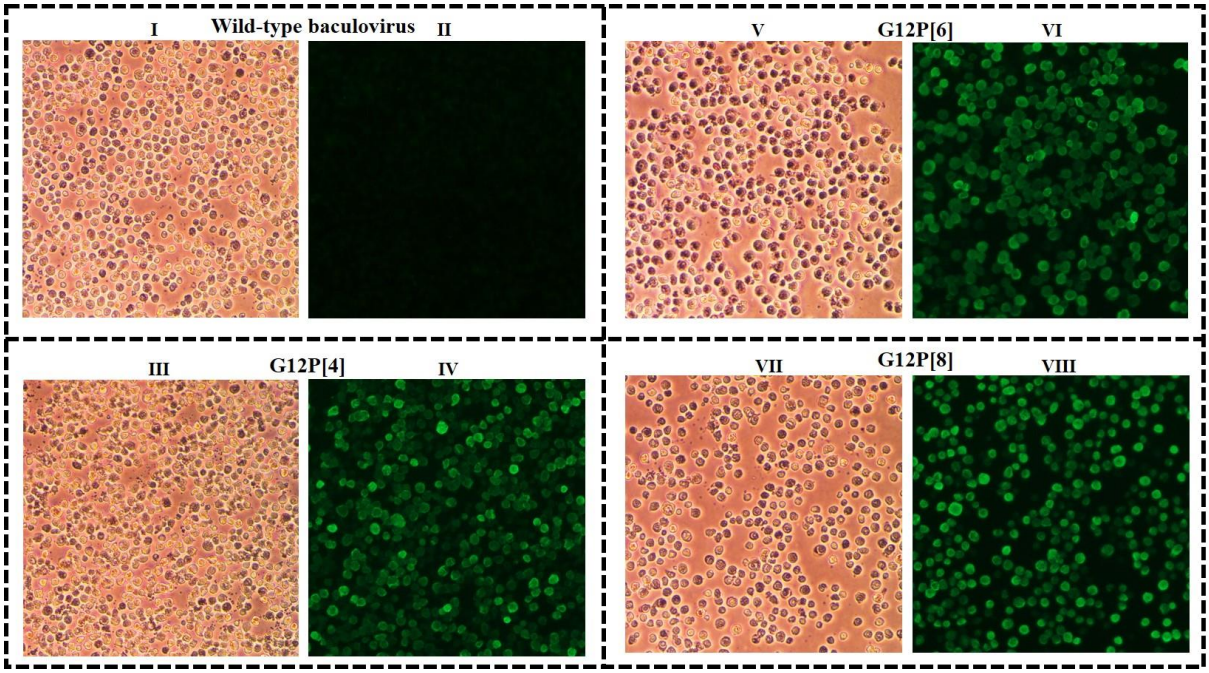

Figure 2.12: IFMA of Sf9 insect cells infected with rBV_G12P[4]_PL3, rBV_G12P[6]_PL3, and rBV_G12P[8]_PL3. Sf9 cells infected with wild-type baculovirus **(I)** bright field and **(II)** fluorescence. Sf9 cells infected with rBV_G12P[4]_PL3 **(III)** bright field and **(IV)** fluorescence. Sf9 cells infected with rBV_G12P[4]_PL3 **(V)** bright field and **(VI)** fluorescence. Sf9 cells infected with rBV_G12P[4]_PL3 **(VII)** bright field and **(VIII)** fluorescence. 400X magnification.

As expected, the Sf9 cells infected with wild-type baculovirus (Fig. 2.12: **I**), rBV_G12P[4]_PL3 (Fig. 2.12: **III**), rBV_G12P[6]_PL3 (Fig. 2.12: **V**), and rBV_G12P[8]_PL3 (Fig. 2.12: **VII**) all displayed visible signs of infection when visualised under bright field. The Sf9 cells infected with wild-type baculovirus did not display visible signs of fluorescence (Fig. 2.12: **II**), as expected, and almost no background fluorescence. Interestingly, the VP7 (G12) and VP4 (P[4], P[6] and P[8]) cross-reacted with polyclonal rabbit anti-RV SA11 TLP IgG. Fluorescence could be visualised in the wells containing Sf9 cells infected with rBV_G12P[4]_PL3 (Fig. 2.12: **IV**), rBV_G12P[6]_PL3 (Fig. 2.12: **VI**), and rBV_G12P[8]_PL3 (Fig. 2.12: **VIII**), indicative of RV outer capsid protein expression. However, IFMA analysis using polyclonal rabbit anti-RV SA11 TLP IgG did not allow differentiation between RV VP4 and VP7 expression. Rotavirus SA11 (genotype G3P[2]) and the African rotaviruses (genotypes G12P[4], G12P[6] and G12P[8]) used are group A RVs, which likely display conserved regions on VP4 and VP7 that lead to heterotypic antibody binding (Clarke & Desselberger, 2015). It is interesting to note that heterotopic immunity is thought to be due to repeated RV infections. To our knowledge, apart from serology, this is the first time cross-reactivity between polyclonal rabbit anti-RV SA11 TLP IgG and VP7 (G12) and VP4 (P[4], P[6] and P[8]) is reported.

2.3.5. Evaluation of the assembly of baculovirus-expressed RV proteins into chimaeric RV-VLPs

To generate chimeric RV-TLPs, dualcistronic plaque-purified rBV_GR10924_VP2/6_#3.1_PL3 and dualcistronic recombinant plaque-purified rBV_G12P[4]_PL3 were used for co-infection. The media and all buffers were supplemented to a final concentration of 20 mM calcium chloride.

To evaluate the expression and assembly of RV VP2, VP6, VP4 and VP7 during co-infection in 50 ml Sf9 insect cell shaker cultures using SDS-PAGE, Sf9 cells were co-infected with rBV_GR10924_VP2/6_#3.1_PL3 and rBV_G12P[4]_PL3 both at a MOI of 5 and the cells were lysed five days post-infection. The lysate was ultracentrifuged through a 40% sucrose cushion, the pellets were resuspended in TNC buffer and a fraction was visualised on SDS-PAGE, Fig. 2.13.

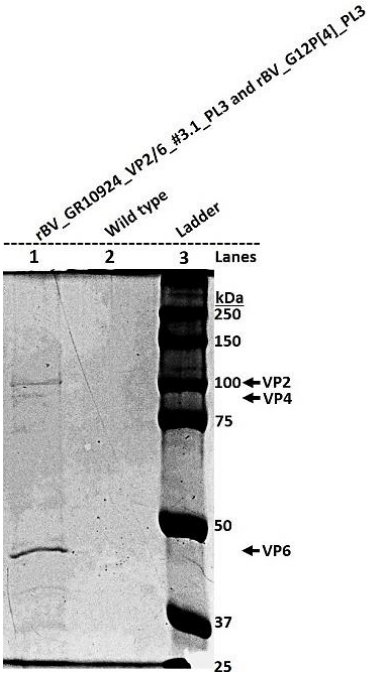

Figure 2.13: SDS-PAGE of RV-VLPs from lysates ultracentrifuged through a 40% sucrose cushion. Lane 1 contained ultracentrifuged lysate from Sf9 cells co-infected with dualcistronic rBV_GR10924_ VP2/6_#3.1_PL3, and rBV_G12P[4]_PL3. Lane 2 contained ultracentrifuged lysate from Sf9 insect cells infected with empty baculovirus (wild-type) as a control. Lane 3 contained Precision Plus Protein™ Dual Color Standards (Catalogue number: #1610374, Bio-Rad, California, USA).

The yield following ultracentrifugation through a 40% sucrose cushion was very low. Therefore, the bands on the SDS-PAGE gel were very faint. However, bands of approximate sizes 100kDa (VP2), 85kDa (VP4) and 45kDa (VP6) could be detected: Fig. 2.13: lane 1. The band around 39 kDa may be the low-level expression of RV VP7, however, this was uncertain. Antibodies against VP7 of RVA were unavailable

at this point in the study, therefore, VP7 expression could not be assessed using western blot analysis.

To assess the assembly of African RV VP7 and VP4 (G12P[4]) onto GR10924 VP2/6 DLPs, during co-infection experiments, the ultracentrifuged lysates, from which a fraction was previously analysed by SDS-PAGE, were analysed using TEM. Ultracentrifuged lysates from Sf9 cells infected with dualcistronic plaque-purified rBV_GR10924_VP2/6_#3.1_PL3 at a MOI of 5, and lysed 4 d.p.i., was sent as a control for TEM (Fig. 2.11: **I**), Fig. 2.14.

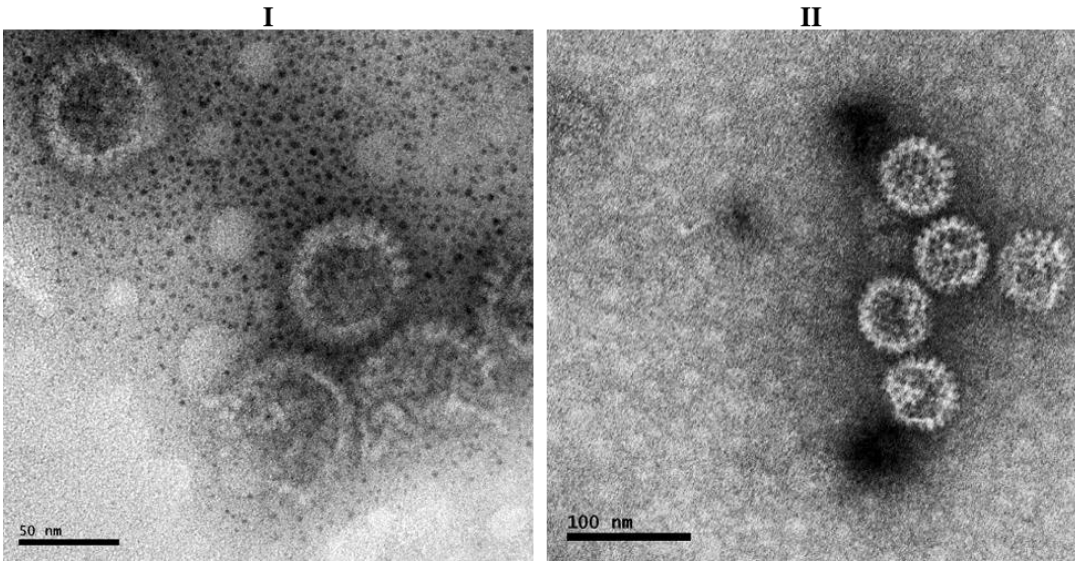

Figure 2.14: Electron micrograph of co-infected Sf9 insect cells. (I) RV-DLPs of RV GR10924 VP2 and VP6 were produced by infecting Sf9 cells with rBV_GR10924_ VP2/6_#3.1_PL3 expressing VP2 (C2) and VP6 (I2). Scale bar 50 nm. **(II)** Rotavirus DLPs of RV GR10924 that were produced by co-infecting Sf9 cells with rBV_GR10924_VP2/6_#3.1_PL3 expressing VP2 (C2) and VP6 (I2), and plaque-purified rBV_G12P[4]_PL3 expressing VP4 (P[4]) and VP7 (G12). Scale bar 100 nm.

As expected assembled RV-DLPs composed of RV GR10924 VP2 and VP6 expressed by Sf9 cells infected with rBV_GR10924_VP2/6_#3.1_PL3 were observed (Fig. 2.11: **I**). The diameter of the RV-DLPs was approximately 64-70 nm, as expected. RV-DLPs have a brush appearance on the edges, in contrast to the smooth edge of RV-TLPs (Fig. 1.9). Only RV-DLPs were observed when Sf9 cells were co-infected with plaque-purified rBV_GR10924_VP2/6_#3.1_PL3 and plaque-purified rBV_ G12P[4]_PL3 (Fig. 2.11: **II**). The RV-DLPs were approximately 64-70 nm. Different strategies for RV-VLP generation via co-infection were attempted, such as varying the MOI of the dualcistronic recombinant baculoviruses, varying the time of infection and using various recombinant baculovirus plaques, without resulting in any RV-TLP assembly.

2.4. Summary

Of the RV-VLPs generated by Jere and co-workers (2012, 2014) less than 30% of the RV GR10924 DLPs were covered with VP4 and VP7 outer capsid proteins. It was hypothesised that the TC-100 medium, used by Jere and co-workers (2012, 2014), contained insufficient calcium of 8,83 mM and that supplementation to a final concentration of 20 mM calcium may improve RV-TLP assembly (personal communication of M.K. Estes, S.E. Crawford and B.V. Prasad to A.A. Van Dijk, 2018).

Thus, to test this hypothesis the co-infection experiments done by Jere and co-workers (2012) were reattempted using the Bac-to-Bac BVES to repeat some of the heterologous co-infections.

Firstly, recombinant baculoviruses expressing RV GR10924 VP2 and VP6 DLPs were generated. The recombinant baculoviruses expressing RV GR10924 VP2 and VP6 were plaque-purified, amplified, and used to generate RV-DLPs. Assembly of the RV-DLPs was evaluated using TEM and based on protein expression and RV-DLP assembly rBV_GR10924_VP2/6_#3.1_PL3 was selected for co-infections.

Secondly, recombinant baculoviruses expressing African RV strain outer capsids (G12P[4], G12P[6] and G12P[8]) were generated. The recombinant baculoviruses were plaque-purified and amplified. Of the three recombinant baculoviruses expressing African RV VP4 and VP7 (genotypes G12P[4], G12P[6], and G12P[8]) rBV_G12P[4]_PL3 was selected for co-infections based on protein expression. Interestingly, the heterotypic antibody response was observed during IFMA. Polyclonal rabbit anti-RV SA11 TLP IgG cross-reacted with insect cell-expressed African RV VP4 (genotypes [4], [6], and [8]) and VP7 (genotype G12). However, IFMA did not allow for differentiation between polyclonal rabbit anti-RV SA11 TLP IgG binding to VP4 or binding to VP7. To our knowledge, apart from serology, this is the first time that cross-reactivity between polyclonal rabbit anti-RV SA11 (genotype G3P[2]) TLP IgG and VP7 (G12) and VP4 (P[4], P[6] and P[8]) is reported.

Co-infections of Sf9 cells in TC-100 medium supplemented with 20 mM calcium were done using rBV_GR10924_VP2/6_#3.1_PL3 and rBV_G12P[4]_PL3 at a MOI of 5 each. The resulting RV-VLPs were isolated using ultracentrifugation through a 40% sucrose cushion and analysed using TEM. However, only RV-DLPs were formed as

was determined by diameter (70 nm) and morphology (particles had rough brush-like structures instead of the smooth outer edge characteristic of VP7 assembly).

The co-infection with two dualcistronic baculoviruses in the presence of 20 mM calcium supplementation was not successful in generating RV-TLPs. Therefore, the generation of quadcistronic recombinant baculoviruses simultaneously expressing VP2/6/4/7 was attempted, see Chapter 3.

Addendum: Transcapsidating RVA SA11 VP2/6 DLPs with RVG 03V0567 VP4/7

The possibility of generating chimeric intergroup RV-VLPs composed of RVA SA11 VP2/6 DLPs and RVG 03V0567 VP4/7 outer capsids was investigated in parallel to the work on generating chimeric RV-TLPs composed of RV GR10924 VP2/6 DLPs transcapsidated with African RV VP4/7 (genotypes G12P[4/6/8]) (see Section 2.3).

Except for different donor plasmids, the same methods and materials previously described in the text (see Section 2.2) were used. The pFBd_Luan_SA11_VP2-VP6 (Theart, 2022) donor plasmid (kindly provided by Mr. L.J.C. Theart) was transformed into competent AcBACΔCC *E. coli* cells, generating rBacmid_SA11_VP2/6. Purified rBacmid_SA11_VP2/6 was transfected into Sf9 cells and resulted in dualcistronic rBV_SA11_VP2/6 that expressed RVA SA11 VP2 and VP6 (Clade A RV). A 50 ml Sf9 insect cell shaker culture was infected with rBV_SA11_VP2/6_#3_PL1, as per Section 2.2.20, with 20 mM calcium supplementation and as expected resulted in the formation of RV SA11 DLPs (results not shown). Further, a pFBd_RVG_VP4-VP7 donor plasmid was *in silico* designed and purchased from GenScript. Purified pFBd_RVG_VP4-VP7 was transformed into competent AcBACΔCC *E. coli* cells generating rBacmid_ RVG _VP4/7 which was purified and used to transfect Sf9 cells. Transfection resulted in the generation of dualcistronic rBV_RVG_VP4/7 that expressed RVG 03V0567 VP4 and VP7 outer capsid proteins (Clade B RV). A 50 ml Sf9 insect cell shaker culture was co-infected with rBV_SA11_VP2/6_#3_PL1 and rBV_RVG_VP4/7_#1 _PL2, with 20 mM calcium supplementation, to generate RV-VLPs. However, as with the RV GR10924 VP2/6 transcapsidation with African RV VP4/7 (genotypes G12P[4/6/8]) (see Section 2.3.5), only RV-DLPs were detected by TEM analysis based on diameter and morphology (results not shown). Co-infection with two dualcistronic baculoviruses rBV_SA11_VP2/6_#3_PL1 and rBV_RVG_VP4/7_#1_PL2), with 20 mM calcium supplementation, was also not successful in generating RV-TLPs. Therefore, as stated

above, the generation of quadcistronic recombinant baculoviruses simultaneously expressing VP2/6/4/7 was attempted, see Chapter 3.

The results of the transcapsidation of RVA SA11 VP2/6 DLPs with RVG VP4/7 are not shown here, since they are essentially the same as the chimeric RV GR10924 VP2/6 transcapsidation with African RV VP4/7 (genotypes G12P[4/6/8]) approach (see Section 2.3), therefore, the inclusion thereof would only serve to lengthen this MSc without contributing any scientific progress or insight.

Chapter 3: Investigating the possibility of generating RV-TLPs using recombinant quadcistronic VP2/6/4/7 recombinant baculoviruses.

3.1. Introduction

The co-infection approach using two dualcistronic recombinant baculoviruses (rBVs) did not yield any RV-TLPs (Chapter 2). Therefore, the approach of the experiments reported in this chapter was to generate quadcistronic recombinant baculoviruses for simultaneous expression of RV VP2, VP6, VP4 and VP7 in each infected insect cell.

The population of cells optimally expressing recombinant proteins that need to assemble as functional units decrease drastically the more recombinant baculoviruses, expressing different proteins, are used during co-infection (Belyaev *et al.*, 1995). Thus, using multicistronic baculovirus expression strategies may be advantageous over monocistronic baculovirus expression strategies when a single cell must express multiple proteins at specific ratios (Belyaev *et al.*, 1995; Vieira *et al.*, 2005). The theoretical percentage of individual cells receiving equal ratios of the recombinant baculoviruses is 12.78% when infected with 2 different recombinant baculoviruses each at a MOI of 5 (Belyaev *et al.*, 1995). This may result in an unbalanced synthesis of the expressed proteins in these cells.

Here, three quadcistronic pFBq donor plasmids encoding all four TLP proteins (VP2/6/4/7) were designed and ordered from GenScript. A pFBq encoding RVA/Simian-tc/ZAF/SA11-N5/1958/G3P5B[2] VP2/6/4/7; a pFBq encoding RVA/Human-wt/GR10924/ 1999/G9P[6] VP2/6 and RV African strain VP4/7 (G12P[4]); and a pFBq encoding RVA/Simian-tc/ZAF/SA11-N5/1958/G3P5B[2] VP2/6 and RVG/chicken/03V0567/DEU/ 2003 VP4/7. These donor plasmids were used to generate quadcistronic recombinant baculoviruses. The quadcistronic recombinant baculoviruses were to be used to generate fully assembled homologous SA11 TLPs by infecting Sf9 cells at a high MOI in medium supplemented to 20 mM calcium.

3.2. Materials and Methods

The same Bac-to-Bac BEVS described in Section 2.2 was used here, but with some modifications. These changes were using different donor plasmids, a different method of generating competent *E. coli* bacterial cells, Grace's Insect Medium (Gibco™, Thermofisher Scientific™, Catalogue number: 11605045) instead of TC-100 Insect Medium, using caesium chloride (CsCl) isopycnic separation of RV-VLPs, and quantification of RV-VLP yield.

3.2.1. Design of pFastBACquad donor plasmids containing insect cell codon-optimised ORFs encoding RV VP2/6/4/7

To attempt to generate fully assembled RV-TLPs composed of RV GR10924 VP2/6 DLPs with RV African strain VP4 and VP7 (genotype G12P[4]), and to evaluate the structural compatibility of RVA SA11 VP2/6 DLPs and RVG 03V0567 VP4 and VP7 outer capsid proteins, the pFBq donor plasmid was selected (Fig. 3.1). In Chapter 2 the pFBq donor plasmids generated by Jere and co-workers (2012) contained 2 ORFs encoding African RV outer capsid proteins VP4 and VP7. Here, the pFBq donor plasmids contained four ORFs encoding all four RV VLP proteins VP2, VP6, VP4 and VP7. Three pFBqs were *in silico* designed to contain the insect cell codon-optimised sequences of various RV VP2, VP6, VP4 and VP7 are listed in Table 3.1, see Fig 3.1 for plasmid maps. Since pFBq was not an open-source plasmid at GenScript, empty pFBq was retrieved from the -20°C archives and sent to GenScript to be used for the generation of the three pFBqs.

Table 3.1: Rotavirus strains and genome segments used in the pFBq donor plasmids.

Strain	Genome segment	Encoded protein	Genbank accession number	Donor plasmid	Restriction enzyme sites for inserts
RVA/Simian-tc/ZAF/SA11-N5/1958/G3P5B[2]	GS2	VP2	JQ688674	pFBq_SA11_VP2/6/4/7 pFBq_SA11_VP2/6_RVG_VP4/7	SmaI & SpeI
RVA/Simian-tc/ZAF/SA11-N5/1958/G3P5B[2]	GS6	VP6	JQ688678	pFBq_SA11_VP2/6/4/7 pFBq_SA11_VP2/6_RVG_VP4/7	NotI & KpnI
RVA/Simian-tc/ZAF/SA11-N5/1958/G3P5B[2]	GS4	VP4	JQ688676	pFBq_SA11_VP2/6/4/7	Bsu36I & SnaBI
RVA/Simian-tc/ZAF/SA11-N5/1958/G3P5B[2]	GS9	VP7	JQ688681	pFBq_SA11_VP2/6/4/7	StuI & MluI
RVG/chicken/03V0567/DEU/2003	GS4	VP4	NC_021589	pFBq_SA11_VP2/6_RVG_VP4/7	Bsu36I & SnaBI
RVG/chicken/03V0567/DEU/2003	GS9	VP7	NC_021582	pFBq_SA11_VP2/6_RVG_VP4/7	StuI & MluI
RVA/Human-wt/ZAF/GR10924/1999/G9P[6]	GS2	VP2	FJ183354	pFBq_GR10924_VP2/6_G12P[4]	SmaI & SpeI
RVA/Human-wt/ZAF/GR10924/1999/G9P[6]	GS6	VP6	FJ183358	pFBq_GR10924_VP2/6_G12P[4]	NotI & KpnI
RVA/Human-wt/ZAF/3176WC/2009/G12P[6]	GS9	VP7	HQ657165	pFBq_GR10924_VP2/6_G12P[4]	StuI & MluI
RVA/Human-wt/ZAF/3133WC/2009/G12P[4]	GS4	VP4	HQ657174	pFBq_GR10924_VP2/6_G12P[4]	Bsu36I & SnaBI

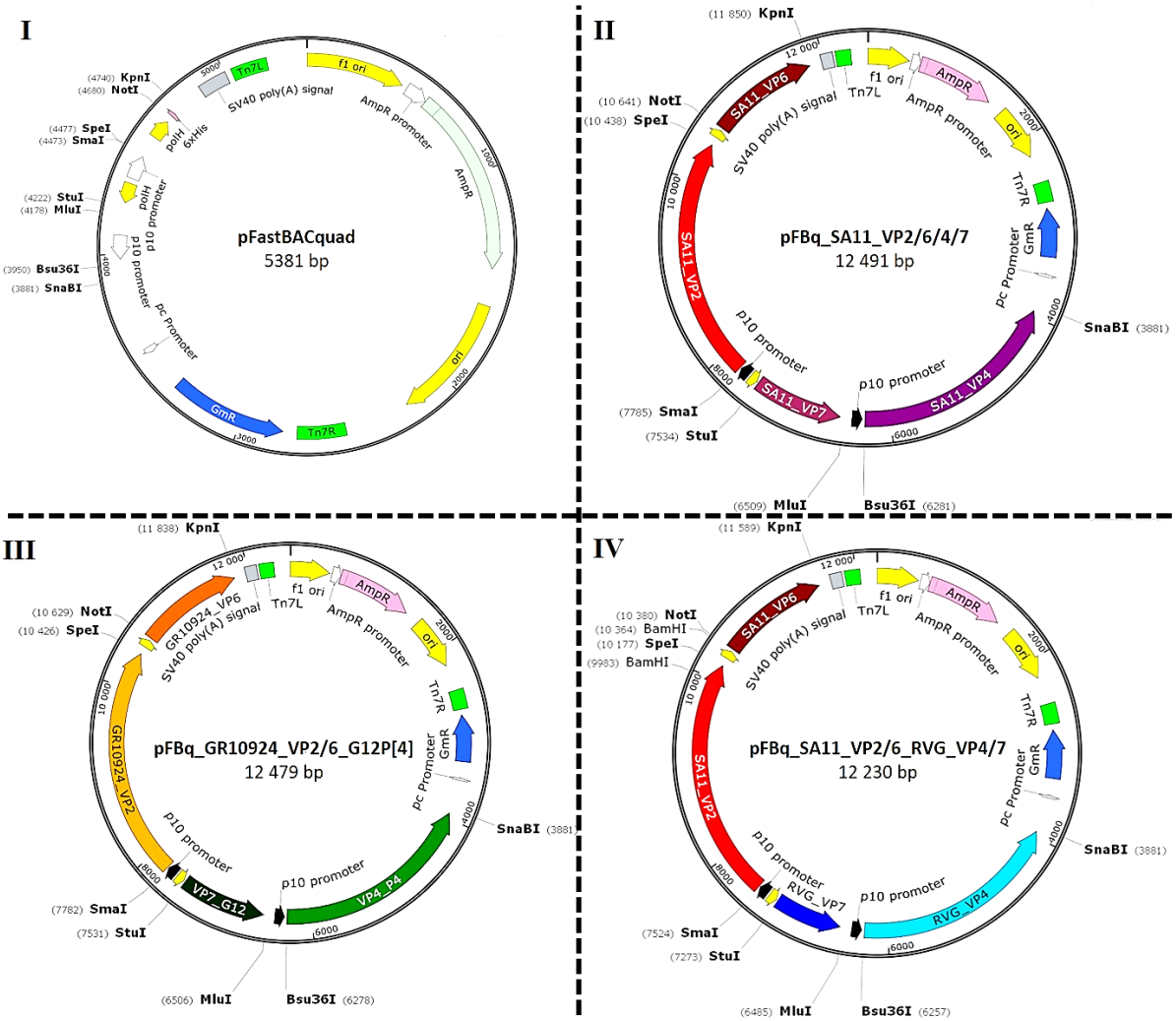

Figure 3.1: Plasmid maps of pFBq donor plasmids. The various ORFs were insect cell codon-optimised. **(I)** pFBq (5381 bp) generated by Prof. A.C. Potgieter. **(II)** pFBq_SA11_VP2/6/4/7 (12491 bp) containing the ORFs encoding SA11 VP2, VP6, VP4 and VP7. **(III)** pFBq_GR10924_VP2/6_ G12P[4] (12479 bp) containing the ORFs encoding GR10924 VP2 and VP6, and African RV strain VP4 and VP7 (genotype G12P[4]). **(IV)** pFBq_SA11_VP2/6_RVG_4/7 (12 230 bp) containing the ORFs encoding RVA SA11 VP2 and VP6, and RVG 03V0567 VP4 and VP7. *E. coli* JM109 bacterial cells that acquired pFBq plasmid DNA were selected through resistance to ampicillin.

The insect cell codon-optimized ORFs were inserted into the pFBq using restriction enzymes listed in Table 3.1. The usage of identical insertion sites in the pFBqs for the various ORFs encoding RV proteins allows for the easier and cost-effective future generation of new pFBq donor plasmids.

All three pFBq donor plasmids were *in silico* designed on the same principle. The pFBq contains two pairs of a p10 and a polh promoter in opposite orientations. In the one orientation, the VP4 ORFs were inserted under the control of the p10 promoter and the VP7 ORFs were inserted under the control of the polh promoter. In the opposite orientation, the VP2 ORFs were inserted under the control of the second p10 promoter and the VP6 ORFs were inserted under the control of the second polh promoter. Thus,

the pFBq_SA11_VP2/6/4/7 donor plasmid contained the ORFs (Table 3.1) encoding RV SA11 VP2, VP6, VP4 and VP7. The pFBq_GR10924_VP2/6_G12P[4] donor plasmid contained the ORFs (Table 3.1) encoding RV GR10924 VP2 and VP6, and African RV strain VP4 and VP7 (G12P[4]). The pFBq_SA11_VP2/6_RVG_4/7 donor plasmid contained the ORFs (Table 3.1) encoding RVA SA11 VP2 and VP6, and RVG 03V0567 VP4 and VP7. The pFBq donor plasmids were ordered from GenScript (GenScript USA Inc. New Jersey, NJ).

3.2.2. Preparation of competent bacterial cells

Competent *E. coli* JM109 cells and AcBACΔCC *E. coli* cells were generated using the Rubidium Chloride-based method for generating competent *E. coli* cells (Hanahan, 1983; Sambrook & Russell, 2001), instead of the one-step preparation method (Chung *et al.*, 1989) (see Section 2.2.4) due to low transformation and transpositioning efficiency of the latter.

In short, the archived cells were retrieved from glycerol stocks, streaked out on Luria Bertani (LB) agar plates and incubated overnight at 37°C. LB agar plates and LB broth used to generate competent *E. coli* JM109 cells contained no antibiotics, and those used to generate competent AcBACΔCC *E. coli* cells were supplemented with 50 µg/ml kanamycin and 10 µg/ml tetracycline. Single colonies were picked and cultured overnight in 5 ml LB broth at 37°C and shaking at 225 rpm. Thereafter, 1.2 ml of overnight cell culture was added to 50 ml LB. The cells were grown at 37°C and shaken at 225 rpm to early log phase (OD_{600} = 0.5, Biochrom Libra S12 UV/Vis Spectrophotometer, Harvard Bioscience, UK), roughly 3 hours, followed by centrifugation at 5000 x g, at 4°C for 10 minutes and the supernatant was removed. The cells were resuspended in 20 ml TFB 1 (100 mM RbCl, 50 mM $MnCl_2$, 30 mM potassium acetate, 10 mM $CaCl_2$ and 15% glycerol, pH 5,8) pre-chilled to 4°C and incubated on wet ice for 5 min. Thereafter, cells were centrifuged at 5000 x g and 4°C for 10 minutes before being resuspended in 2 ml of TFB 2 (10 mM MOPS, 10 mM RbCl, 75 mM $CaCl_2$ and 15% glycerol, pH 6,5) pre-chilled to 4°C and incubated on wet ice for 45 min. 100 µl aliquots of the cells were added into ice-cold microcentrifuge tubes and snap-frozen in liquid nitrogen. The newly competent *E. coli* JM109 cells and competent AcBACΔCC *E. coli* cells were archived at -80°C.

3.2.3. Production of chimaeric RV-TLPs

To generate RV-TLPs, plaque-purified quadcistronic rBV_SA11_VP2/6/4/7 were used to infect Sf9 cells at a MOI of 20. Infected cultures were incubated at 28°C and 125 rpm in Gibco® Grace's Insect Medium (Gibco™, Thermofisher Scientific™, Catalogue number: 11605045) supplemented with 20 mM calcium and 1 tablet of Pierce™ Protease Inhibitor Mini Tablets, EDTA-free (Thermofisher Scientific™ Inc., Waltham, MA, Cat no. A32955) until CPE was reached in approximately 95% of the infected cell culture (roughly five days post-infection).

3.2.4. Isolation of RV SA11 TLPs and verification assembly by TEM

To isolate RV-VLPs from lysates, the lysates were ultracentrifuged for 2 hours at 135121.5 x g (28 100 rpm) through a 40% sucrose cushion using a Sorvall WX Ultra Series centrifuge and a Sorvall TH-641 rotor. The pellets were resuspended in Tris-calcium (TNC) buffer (10 mM Tris-HCl [pH 7.4], 20 mM $CaCl_2$). Thereafter, the resuspended pellets were washed by diluting the resuspended pellets in TNC buffer and ultra-centrifuging them for 2 hours at 134663.7 x g (31 500 rpm) using a Sorvall WX Ultra Series centrifuge and a Sorvall TH-660 rotor. The resulting pellets were resuspended in 300 µl TNC buffer.

To separate the RV-TLPs and RV-DLPs the particles were ultracentrifuged through a caesium chloride (CsCl) gradient. A refractive index (RI) of 1.3680 (Jere, 2012) was used. The CsCl gradient was ultracentrifuged for 20 hours at 166251.5 x g (35 000 rpm) using a Sorvall WX Ultra Series centrifuge and a Sorvall TH-660 rotor. For RV virions, two major bands of triple-layered particles (TLPs) (density 1.36 g/cm^3) and double-layered particles (DLPs) (density 1.38 g/cm^3) were expected (Gray & Desselberger, 2000). The bands were collected and washed by diluting them with TNC buffer, followed by ultra-centrifuging them for 2 hours at 134663.7 x g (31 500 rpm) using a Sorvall WX Ultra Series centrifuge and a Sorvall TH-660 rotor. The resulting pellets were resuspended in 100 µl TNC buffer and sent for TEM analysis by Mr. Mohamed Jaffer at the Electron Microscope Unit of the University of Cape Town.

3.2.5. Quantification of Rotavirus virus-like particle yield

To quantify the RV-VLP yield, following ultracentrifugation the RV-VLPs were resuspended in TNC buffer. The OD_{260} was determined using a NanoDrop One spectrophotometer (Thermo Scientific, Waltham, MA, USA). And the approximate yield of RV-VLPs was determined as described in Rotaviruses: Methods and Protocols (Gray & Desselberger, 2000):

$$\text{Virus Concentration (µg/ml)} = OD_{260} \times \text{Dilution Factor} \times 185 \text{ µg/ml}$$

3.3. Results and Discussion

3.3.1. Preparation of recombinant bacmids encoding RV SA11 VP2, VP6, VP4, and VP7

The assembly of RV-TLPs using quadcistronic recombinant baculoviruses expressing homologous RV SA11 VP2, VP6, VP4 and VP7 with 20 mM calcium supplementation was attempted before attempting to generate transcapsidated chimeric RV-TLPs.

The pFBq_SA11_VP2/6/4/7 donor plasmid was transformed, propagated and archived in *E. coli* JM109 cells. Thereafter, pFBq_SA11_VP2/6/4/7 was purified (see Sections 2.2.5, 2.2.6, and 3.2.4).

To generate recombinant bacmid DNA encoding RV SA11 VP2, VP6, VP4 and VP7 competent AcBACΔCC *E. coli* cells were transformed with purified pFBq_SA11_ VP2/6/4/7. The transformation mixture was plated on LB-agar plates (see Section 2.2.7). About 27 out of 100 colonies were white.

To confirm that the transposition of the expression cassette was successful, nine white colonies were selected for analysis. Also, one blue AcBACΔCC *E. coli* colony harbouring unaltered bacmid DNA was selected as a control for PCR analysis. The bacmid DNA was extracted and analysed using PCR with M13 primers. Amplicons were visualised on an agarose gel (Fig. 3.2). The amplicons containing RV ORFs are marked with an asterisk. The bacmid transposed with pFBq_SA11_VP2/6/4/7 (referred to here as rBacmid_SA11_ VP2/6/4/7, followed by colony number) resulted in amplicons of approximately 10 500 bp, while amplicons of 300 bp were obtained from bacmid DNA from blue WT colonies.

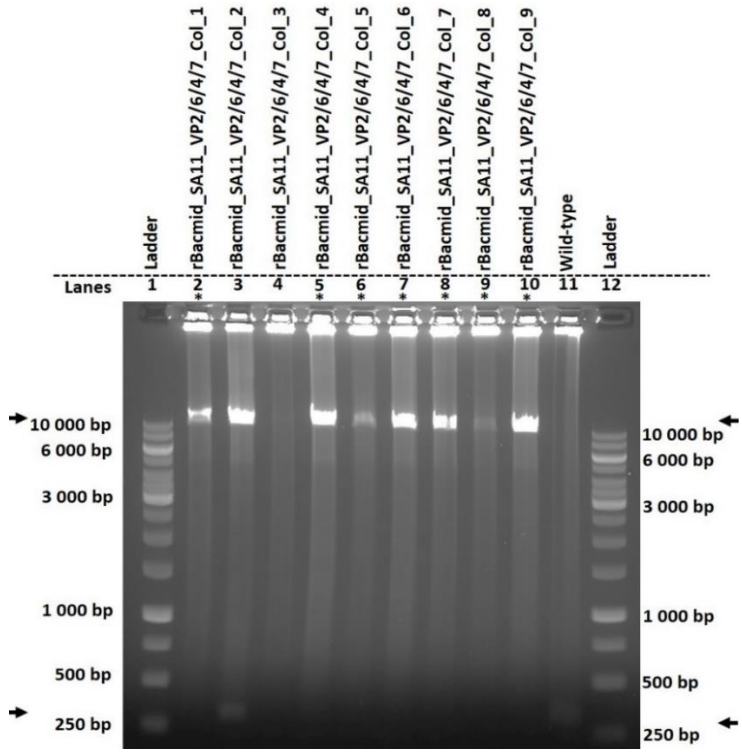

Figure 3.2: Agarose gel of PCR of bacmid DNA encoding RV SA11 VP2, VP6, VP4 and VP7. Expected bands are indicated with arrows. Asterisks indicate colonies containing recombinant bacmid DNA. Lane 11 contained empty WT bacmid. Lanes 1 and 12 contained GeneRuler 1 kb DNA Ladder (Thermofisher Scientific™, Catalogue number: SM0311).

Bacmid DNA from seven of the nine white colonies (Fig. 3.2), colonies 1 (lane 2), and 4-9 (lanes 5-10), generated amplicons of approximately 10 500 bp and did not have amplicons of approximately 300 bp. This was indicative of pure recombinant bacmid DNA containing the transpositioned expression cassette encoding RV SA11 VP2, VP6, VP4 and VP7. PCR analysis of bacmid DNA from colony 2 (lane 3) resulted in two bands, one of rBacmid DNA of 10 500 bp and one of 300 bp, indicative of a mixed colony of recombinant and wild-type bacmid DNA. This was expected since some AcBACΔCC *E. coli* colonies appear predominantly white but are actually mixed colonies of recombinant and wild-type AcBACΔCC *E. coli* cells. Therefore, this colony was excluded from the study. PCR of purified bacmid DNA from colony 3 (lane 4) did not generate any amplicons. This was possibly due to the loss of the pellets during the bacmid DNA isolation (see Section 2.2.8). Colonies 5 (lane 6) and 8 (lane 9) resulted in weak amplification, this may be due to a low AcBACΔCC *E. coli* cell yield during overnight culturing, high salt content due to insufficient washing of the DNA pellet with 70% ethanol, or the loss of a large portion of the DNA during the DNA isolation. As expected, PCR of the blue AcBACΔCC *E. coli* colony, selected as a control in lane 11 resulted in an amplicon of 300 bp, although faint, indicated empty bacmid DNA.

3.3.2. Generation of a quadcistronic rBV_SA11_VP2/6/4/7

After confirming that recombinant bacmids (rBacmids) containing the RVA/Simian-tc/ZAF/SA11-N5/1958/G3P5B[2] VP2, VP6, VP4 and VP7 expression cassette were generated (rBacmid_SA11_VP2/6/4/7), the next step was to generate recombinant baculoviruses expressing RV SA11 VP2, VP6, VP4 and VP7 (rBV_SA11_VP2/6/4/7).

Six white recombinant AcBACΔCC *E. coli* colonies (rBacmid_SA11_VP2/6/4/7_Col_1, rBacmid_SA11_VP2/6/4/7_Col_4, rBacmid_SA11_VP2/6/4/7_Col_5, rBacmid_SA11_VP2/6/4/7_Col_6, rBacmid_SA11_VP2/6/4/7_Col_7, and rBacmid_SA11_VP2/6/4/7_Col_9) and one wild-type blue colony (Fig. 3.2: lane 10) were selected and used to inoculate LB media supplemented with the appropriate antibiotics, as described in Section 2.2.8. Their bacmid DNA was purified and transfected into Sf9 cells, seeded in six-well plates (Section 2.2.12), to generate recombinant and wild-type baculoviruses. Sf9 cells were transfected with pmaxGFP to estimate the transfection efficacy (see Section 2.2.12). The transfection efficacy was estimated to be between 10-20%. The Sf9 cells were grown, transfected and infected in Gibco® TC-100 Insect Medium with calcium chloride supplementation to a final concentration of 20 mM calcium.

Following the observation of CPE, the supernatant was removed six days post-infection and stored as the P1 rBV stock. Three of the P1 rBV stocks (rBacmid_SA11_VP2/6/4/7_Col_1, rBacmid_SA11_VP2/6/4/7_Col_4, rBacmid_SA11_VP2/6/4/7_Col_5) were selected for plaque purification via agarose plaque assays (see Section 2.2.13). The titer of the recombinant baculovirus P1 stock following transfection was 1 X 10^7 pfu/ml (Table 3.2), which was in line with the Bac-to-Bac® Baculovirus Expression Systems manual (Life Technologies, Grand Island, NY).

Table 3.2: The titer of various rBV_SA11_VP2/6/4/7 P1 stocks and the relevant white colony (from Fig. 3.2) and corresponding recombinant bacmids.

White colony number (Fig. 3.2)	Recombinant bacmid	Recombinant virus name	The titer of P1 stock
Colony 1	rBacmid_SA11_VP2/6/4/7_Col_1	rBV_SA11_VP2/6/4/7_Col_1	~1 X 10^7 pfu/ml
Colony 4	rBacmid_SA11_VP2/6/4/7_Col_4	rBV_SA11_VP2/6/4/7_Col_4	~1 X 10^7 pfu/ml
Colony 5	rBacmid_SA11_VP2/6/4/7_Col_5	rBV_SA11_VP2/6/4/7_Col_5	~1 X 10^7 pfu/ml

Five plaques of each of the three recombinant baculoviruses were picked and passaged four times on Sf9 cells to increase their titer. The resulting supernatants were stored as plaque-purified rBV_SA11_VP2/6/4/7 stocks for further use.

As the first indication of RV protein expression by the various rBV_SA11_VP2/6/4/7 plaques, and to determine if there were contaminating wild-type baculoviruses, six-well plates were seeded with Sf9 cells (see Section 2.2.16). One well was not infected, as a control, and one well was infected with wild-type baculovirus, also as a control. Sf9 cells were infected with passage four of the plaques of rBV_SA11_VP2/6/4/7_ Col_1, rBV_SA11_VP2/6/4/7_Col_4, rBV_SA11_VP2/6/4/7_ Col_5 at a MOI of 5 and analysed by IFMA four days post-infection. Only the results of rBV_SA11_VP2/6/4/7_Col_4_ PL2 are shown, (Fig. 3.3).

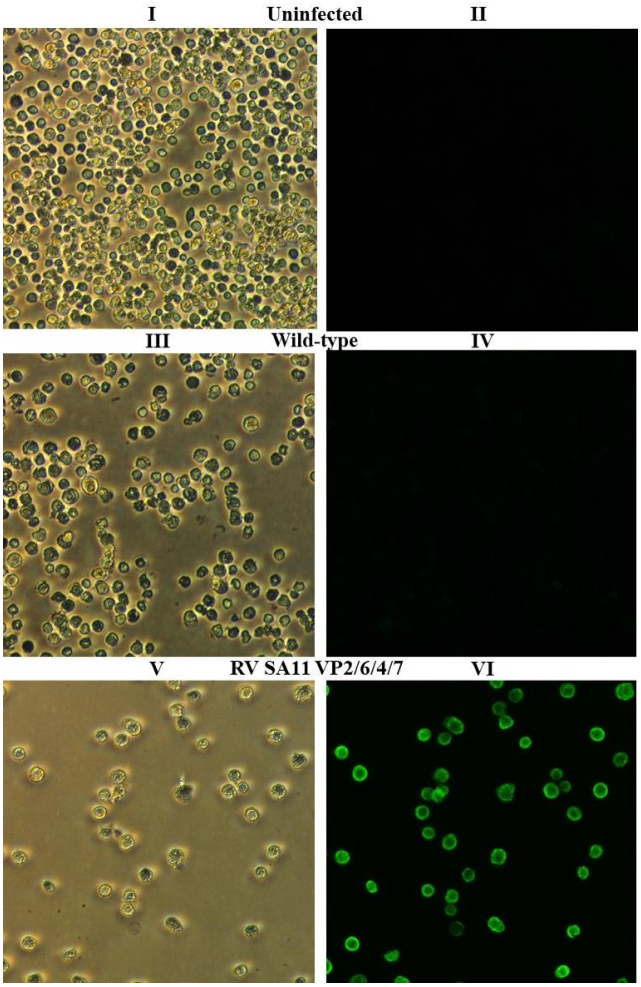

Figure 3.3: IFMA of Sf9 insect cells infected with rBV_SA11_VP2/6/4/7_Col_4_PL2. Uninfected Sf9 cells **(I)** bright field and **(II)** fluorescence. Sf9 cells infected with wild-type (empty) baculoviruses **(III)** bright field and **(IV)** fluorescence. Sf9 cells infected with rBV_SA11_VP2/6/4/7_Col_4_PL2, four days post-infection, **(V)** bright field and **(VI)** fluorescence. 400X magnification.

No signs of CPE in the uninfected Sf9 cells were detected (Fig. 3.3: I). As expected the uninfected Sf9 cells did not fluoresce (Fig. 3.3: II), and very little background fluorescence was visualised. Sf9 cells infected with a wild-type baculovirus displayed visible signs of late-stage baculovirus infection on bright-field (Fig. 3.3: III). As expected, no fluorescence was visualised in the well infected with wild-type baculovirus (Fig. 3.3: IV). Very little background fluorescence was visualised in Fig. 3.3: VI. This indicated that the polyclonal rabbit anti-RV VP2/6 TLP IgG did not bind any of the native Sf9 cell proteins, or to any native baculovirus proteins. When viewed on bright-field 4 d.p.i., the Sf9 cells infected with rBV_SA11_VP2/6/4/7_Col_4_PL2 (Fig. 3.3: V) displayed visible signs of late-stage baculovirus infection. Fluorescence could be visualised in all the infected Sf9 cells (Fig. 3.3: VI). All 15 recombinant baculovirus plaques displayed fluorescence comparative with Fig. 3.3: V and Fig. 3.3: VI (data not shown), therefore the IFMA of rBV_SA11_VP2/6/4/7_Col_4_PL2 was selected as representative. The fluorescence of Sf9 cells infected with plaques of rBV_SA11_VP2/6/4/7_Col_1, rBV_SA11_VP2/6/4/7_ Col_4, rBV_SA11_VP2/6/4/7_ Col_5 indicated RV group A VP6 expression.

Next, SDS-PAGE analysis was done to determine the expression of RV VP2, VP6, VP4 and VP7. Sf9 cells were seeded in six-well plates (see Section 2.2.18). Three plaques of rBV_SA11_VP2/6/4/7_Col_1, rBV_SA11_VP2/6/4/7_Col_4, rBV_SA11_ VP2/6/4/7_Col_5 were selected based on IFMA data and used to infect Sf9 cells at a MOI of 5. Each six-well plate contained a well of Sf9 cells infected with wild-type baculovirus, to serve as a control during SDS-PAGE, (Fig. 3.4).

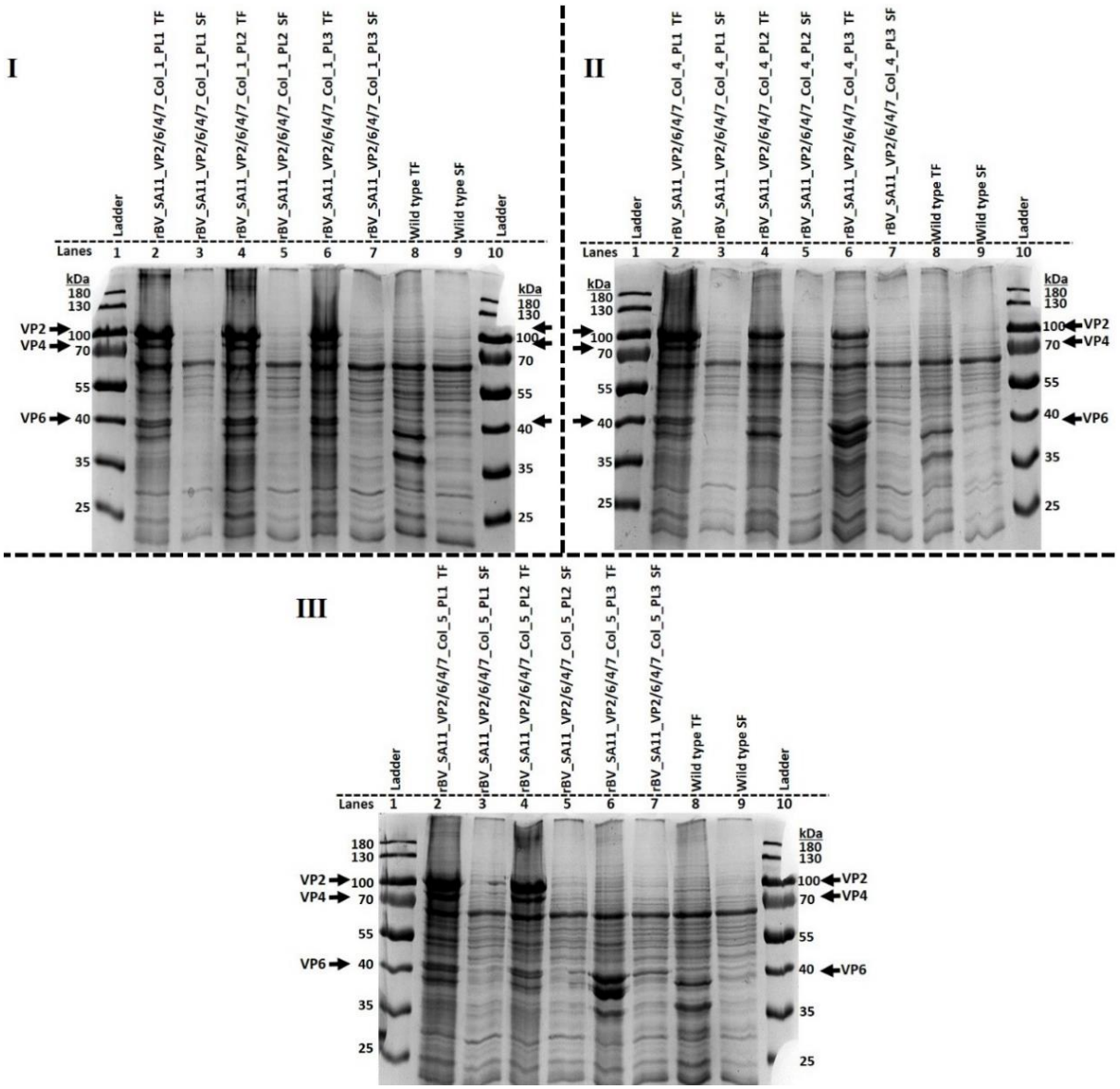

Figure 3.4: SDS-PAGE of baculovirus expressed RV proteins of plaque-purified rBV_SA11_VP2/6/4/7. Rotavirus SA11 VP2, VP6, and VP4 expressed by three plaques of quadcistronic rBV_SA11_VP2/6/4/7, **(I)** rBV_SA11_VP2/6/4/7_Col_1 **(II)** rBV_SA11_VP2/6/4/7_Col_4 and **(III)** rBV_ SA11_VP2/6/4/7_Col_5. The total fraction and soluble fraction of each sample were loaded. Arrows indicate the expected sizes of the proteins. Lanes 8 and 9 of each gel contained wild-type (empty baculovirus) total and soluble fractions, respectively, as controls. Lanes 1 and 10 of each gel contained PageRuler™ Prestained Protein Ladder (Catalogue number: 26616, Thermofisher Scientific™).

The total and soluble fractions of lysed Sf9 cells were analysed, Fig 3.4. Proteins of approximately 100 kDa (corresponding to the expected size of VP2), approximately 88 kDa (corresponding to the expected size of VP4) and approximately 45 kDa (corresponding to the expected size of VP6) were visualised (Fig. 3.4: I-III: lanes 2, 4 and 6). As expected wild-type infected Sf9 cell lysates (Fig. 3.4: I-III: lanes 8-9) did not display these proteins. The expressed RV proteins were only observed in the total fraction and not in the soluble fraction. In addition to being insoluble, the expression

of RV SA11 VP2 and VP6 by quadcistronic rBV_SA11_VP2/6/4/7 was less than that of RV GR10924 VP2 and VP6, which was soluble, achieved when using dualcistronic rBV_GR10924_VP2/6 (Fig. 2.6 and Fig. 2.7). Interestingly, although expression of VP4 by quadcistronic rBV_SA11_VP2/6/4/7 was insoluble, a higher yield of RV VP4 was achieved compared to the expression by the dualcistronic rBV_G12P[4], rBV_G12P[6], or rBV_G12P[8] (Fig. 2.10 and Fig. 2.11). For rBV_SA11_VP2/6/4/7_ Col_5_PL3 the approximately 100 kDa band of VP2 was absent (Fig. 3.4: III: lanes 6 and 7). Therefore, rBV_SA11_ VP2/6/4/7_Col_5_PL3 was excluded from the rest of the study. The level of RV protein by quadcistronic rBV_SA11_VP2/6/4/7 expression in Sf9 cells was less than that achieved by Jere and co-workers (2012) in High Five cells. However, this was not surprising as Jere and co-workers (2012) reported that expression of RV GR10924 VP2 and RV VP6 in High Five cells yielded three times more particles than Sf9 cells.

To increase the solubility of RV proteins expressed using quadcistronic rBV_SA11_VP2/6/4/7, Sf9 cells were infected with varying MOIs of 1, 5 and 10, and at room temperature. Also, the medium was changed from TC-100 Insect Medium to Grace's Insect Medium, since Grace's Insect Medium is richer in nutrients (personal communication Prof. A.C. Potgieter). However, the solubility did not increase.

The next step was to scale up expression to 50 ml Sf9 insect cell shaker cultures. Therefore, to increase the volume of the recombinant baculovirus stocks, of rBV_SA11_VP2/6/4/7_Col_1_PL1, rBV_SA11_VP2/6/4/7_Col_4_PL1, and rBV_ SA11_VP2/6/4/7_Col_5_PL2, 50 ml Sf9 insect cell shaker cultures were infected at a MOI of 0,1. These baculoviruses were selected based on the expression visualised on SDS-PAGE, (Fig. 3.4). The titers of these recombinant baculovirus stocks were quantified using agarose plaque assays (see Section 2.2.13). The titer of the recombinant baculovirus P5 stocks was ~1 X 10^8 pfu/ml to ~5 X 10^8 pfu/ml which was in line with the Bac-to-Bac® Baculovirus Expression Systems manual (Life Technologies, Grand Island, NY), Table 3.3.

Table 3.3: The titer of rBV_SA11_VP2/6/4/7 plaque stocks at passage 4.

White colony number (Fig. 3.2)	Recombinant virus name	The titer of rBV stock at passage 4
Colony 1	rBV_SA11_VP2/6/4/7_Col_1_PL1	~2 X 10^8 pfu/ml
Colony 4	rBV_SA11_VP2/6/4/7_Col_4_PL1	~5 X 10^8 pfu/ml
Colony 5	rBV_SA11_VP2/6/4/7_Col_5_PL5	~1 X 10^8 pfu/ml

To test whether RV-VLPs were generated, two 50 ml Sf9 insect cell shaker cultures were infected at a MOI of 5 with rBV_SA11_VP2/6/4/7_Col_1_PL1, and rBV_SA11_VP2/6/4/7_Col_4_PL1, respectively. Five days post-infection the cells were lysed, the lysate was centrifuged at 13 000 x g, and the supernatant was ultracentrifuged through a 40% sucrose cushion. The pellets were run in duplicate on SDS-PAGE and blotted onto a nitrocellulose membrane (Whatman® GmbH. Dassel, Germany) (see Section 2.2.19). The membrane was cut in half for western blot with two different primary antibodies. One membrane was incubated with a polyclonal rabbit anti-RV VP2/6 DLP IgG serum (raised against RV SA11 DLPs), and the other membrane was incubated with a polyclonal rabbit anti-RV SA11 TLP IgG serum (raised against caesium chloride purified SA11 virions) as primary antibody, Fig. 3.5. The sera were kindly provided by Professor A.C. Potgieter, Deltamune, RSA.

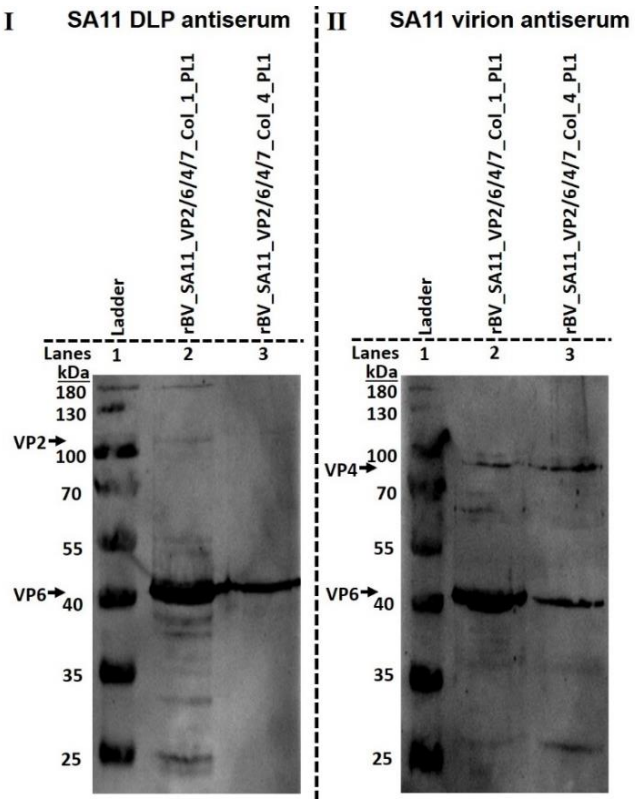

Figure 3.5: Western blot of lysates of Sf9 cells infected with rBV_SA11_VP2/6/4/7 following ultracentrifugation through a 40% sucrose cushion. Western blot using **(I)** polyclonal rabbit anti-RV VP2/6 DLP antiserum, and **(II)** polyclonal rabbit anti-RV SA11 virion antiserum, as primary antibodies. Lane 2 of each membrane contained ultracentrifuged lysate from Sf9 cells infected with rBV_SA11_VP2/6/4/7_Col_1_PL1, and lane 3 of each membrane contained ultracentrifuged lysate from Sf9 cells infected with rBV_SA11_VP2/6/4/7_Col_4_PL1. Lane 1 of both blots contained PageRuler™ Prestained Protein Ladder (Catalogue number: 26616, Thermofisher Scientific™).

Bands of approximately 45 kDa corresponding with RV SA11 VP6 were visualised (Fig. 3.5: I and II: lanes 2 and 3). A very faint band of approximately 100 kDa corresponding with RV SA11 VP2 was seen in Fig. 3.5: I: lane 2. This is in contrast to

the absence of VP2 visualised on a western blot of RV GR10924 VP2 and VP6 (Fig. 2.7). Rotavirus VP2 is located within the DLPs and may have had very little exposure to the immune response when generating DLP antiserum. Faint bands of approximately 88 kDa corresponding with RV SA11 VP4 could be visualised in Fig. 3.5: II: lanes 2 and 3. Clear bands of RV VP7 could not be identified using polyclonal rabbit anti-RV SA11 virion antiserum. Since VP6 is the dominant group antigen, it was not surprising that both primary antibodies bound VP6 best.

The visualisation of RV VP2, VP6 and VP4 on western blot seemed to indicate that a small portion of the expressed RV proteins formed soluble RV-VLPs.

3.3.3. TEM evaluation of the assembly of RV-VLPs from quadcistronic rBVs expressing RV SA11 VP2, VP6, VP4 and VP7

To assess the assembly of RV-TLPs via TEM analysis, three 50 ml shaker cultures were infected at a MOI of 5 each with rBV_SA11_VP2/6/4/7_Col_1_PL1, rBV_SA11_VP2/6/4/7_Col_4_PL1, and rBV_SA11_VP2/6/4/7_Col_5_PL2. Five days post-infection the infected Sf9 cells were lysed. Particles present in the soluble fractions of the lysates were purified, as described in Section 2.2.22. The samples were subjected to SDS-PAGE (Fig. 3.6), before proceeding to TEM analysis.

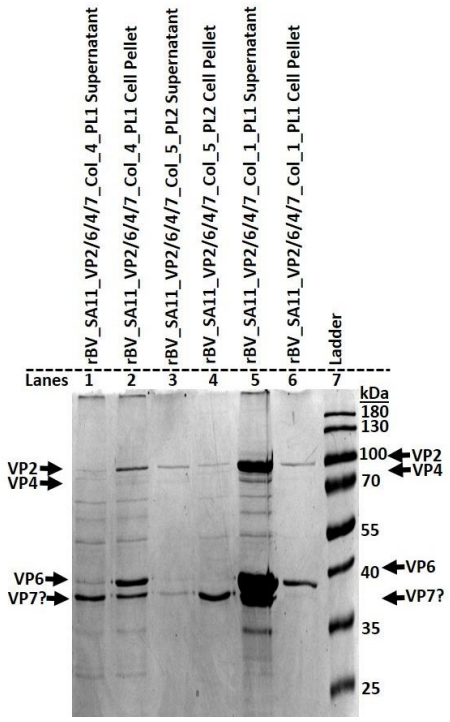

Figure 3.6: SDS-PAGE of three cell lysates of Sf9 cell infected with rBV_SA11_VP2/6/4/7. The supernatant and cell pellet of each lysate of Sf9 cells infected with rBV_SA11_VP2/6/4/7_Col_1_PL1 (lanes 1 and 2), rBV_SA11_VP2/6/4/7_Col_5_PL2 (lanes 3 and 4), and rBV_SA11_VP2/6/4/7_Col_4_ PL1 (lanes 5 and 6) were ultracentrifuged through a 40% sucrose cushion. Lane 7 contained PageRuler™ Prestained Protein Ladder (Catalogue number: 26616, Thermofisher Scientific™).

Bands of approximately 100 kDa (VP2), 88 kDa (VP4), 45 kDa (VP6) and 37 kDa (VP7) were seen in the supernatant of rBV_SA11_VP2/6/4/7_Col_1_PL1 (Fig. 3.6: lane 5), and the cell pellet of rBV_SA11_VP2/6/4/7_Col_4_PL1 (Fig. 3.6: lane 2). The cell pellet of rBV_SA11_VP2/6/4/7_Col_4_PL1 (Fig. 3.6: lane 2) only displayed a very faint band of 88 kDa (VP4). The supernatant of rBV_SA11_VP2/6/4/7_Col_1_PL1 (Fig. 3.6: lane 5) and the cell pellet of rBV_SA11_VP2/6/4/7_Col_4_PL1 (Fig. 3.6: lane 2) correspond to the expected band pattern of TLPs. Only the supernatant of rBV_SA11_VP2/6/4/7_ Col_1_PL1 (Fig. 3.6: lane 5) displayed the expected soluble fraction of TLPs. Whereas, the supernatant of rBV_SA11_VP2/6/4/7_Col_4_PL1 (Fig. 3.6: lane 1) and the cell pellet of rBV_SA11_VP2/6/4/7_Col_5_PL2 (Fig. 3.6: lane 4) displayed bands of 37 kDa (VP7), the bands of 100 kDa (VP2), 88 kDa (VP4), and 45 kDa (VP6) were very faint. Although TLP assembly may still have occurred, these lanes did not display the expected RV protein ratio for TLPs. The supernatant of rBV_SA11_VP2/6/4/7_ Col_5_PL2 (Fig. 3.6: lane 3) only displayed very faint bands indicative of a very low RV-VLP yield, and the cell pellet of rBV_SA11_VP2/6/4/7_Col_ 1_PL1 (Fig. 3.6: lane 6) displayed predominantly bands of 100 kDa (VP2) and 45 kDa (VP6) indicative of predominant DLP formation. Some unidentified bands of 35 kDa,

70 kDa, 60 kDa and 55 kDa were observed in Fig. 3.6 lanes 1, 2 and 5. However, the presence of faint bands representing cellular proteins or baculovirus proteins following ultracentrifugation was not unexpected.

The bands of 37 kDa corresponding with the approximate size of VP7 (37 kDa) were unexpected following the absence of VP7 confirmation by western blot. However, previous studies have visualised RV VP7 on SDS-PAGE using Coomassie staining following the isolation of RV-VLPs using ultracentrifugation of lysates through a cushion (Patton *et al.*, 2000; Yao *et al.*, 2012).

Following the SDS-PAGE, the OD_{260} of rBV_SA11_VP2/6/4/7_Col_1_PL1 (Fig. 3.6: lane 5) was determined using a NanoDrop One spectrophotometer (Thermo Scientific, Waltham, MA, USA). The RV-VLP concentration and yield were determined as listed in Table 3.4.

Table 3.4: RV-VLP concentration and yield following ultracentrifugation (see Section 3.3.4).

Ultracentrifugation type	RV-VLP concentration	RV-VLP yield
40% sucrose cushion	~600 µg/ml	~33 µg

The sample was sent to Mr. Mohamed Jaffer at the Electron Microscope Unit of the University of Cape Town to be analysed using TEM, Fig. 3.7.

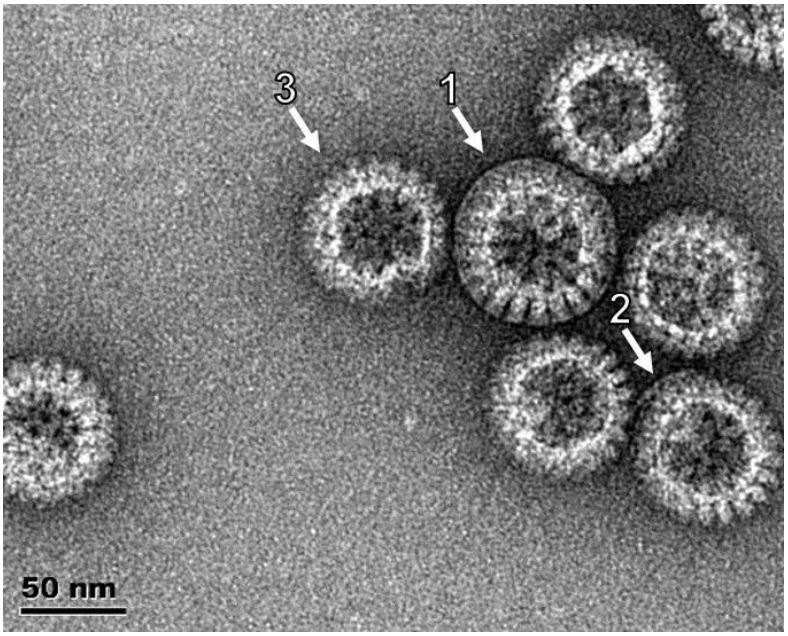

Figure 3.7: Electron micrograph of RVA/Simian-tc/ZAF/SA11-N5/1958/G3P5B[2] RV-VLPs. Rotavirus TLPs were produced by infecting Sf9 cells with a quadcistronic rBV_SA11_VP2/6/4/7_Col_1_PL1 encoding VP2 (C5), VP6 (I2), VP4 (P[2]) and VP7 (G3). Scale bar 50 nm. (Arrow 1) Fully assembled RV-TLP, (arrow 2) partially assembled RV-TLP and (arrow 3) RV-DLP.

A few completely assembled TLPs were seen in the sample of Sf9 cells infected with quadcistronic rBV_SA11_VP2/6/4/7_Col_1_PL1. As indicated by the size (about 75 nm in diameter) and morphology (the smooth appearance of the outer layer of the TLP). However, the TLPs (Fig. 3.7: arrow 1) constituted the smallest portion of the RV-VLPs, thereafter were partially assembled TLPs (Fig. 3.7: arrow 2), and most of the RV-VLPs generated were DLPs (Fig. 3.7: arrow 3) as indicated by their smaller size and brush-like appearance.

3.3.4. Caesium chloride isopycnic separation of RV-VLPs

Following the first indication of the full assembly of TLPs in this study, rBV_SA11_ VP2/6/4/7_Col_ 1_PL1 was selected for further up-scaling of RV-VLP production.

Three 50 ml Sf9 cell shaker cultures were infected with rBV_SA11_VP2/6/4/7_Col_ 1_PL1 at an MOI of 20 (see Section 3.3.3). The higher MOI was to increase RV protein expression. The cells were lysed four days post-infection and the supernatants were ultracentrifuged through a 40% sucrose cushion (see Section 3.3.3). The pellet was resuspended in TNC buffer, a fraction was analysed on SDS-PAGE (Fig. 3.8: I), and another fraction was kept for TEM. To separate TLPs, CsCl isopycnic centrifugation was used (see Section 3.3.3). Following CsCl isopycnic centrifugation, the two bands were collected and analysed using SDS-PAGE, Fig. 3.8: III, before proceeding to TEM.

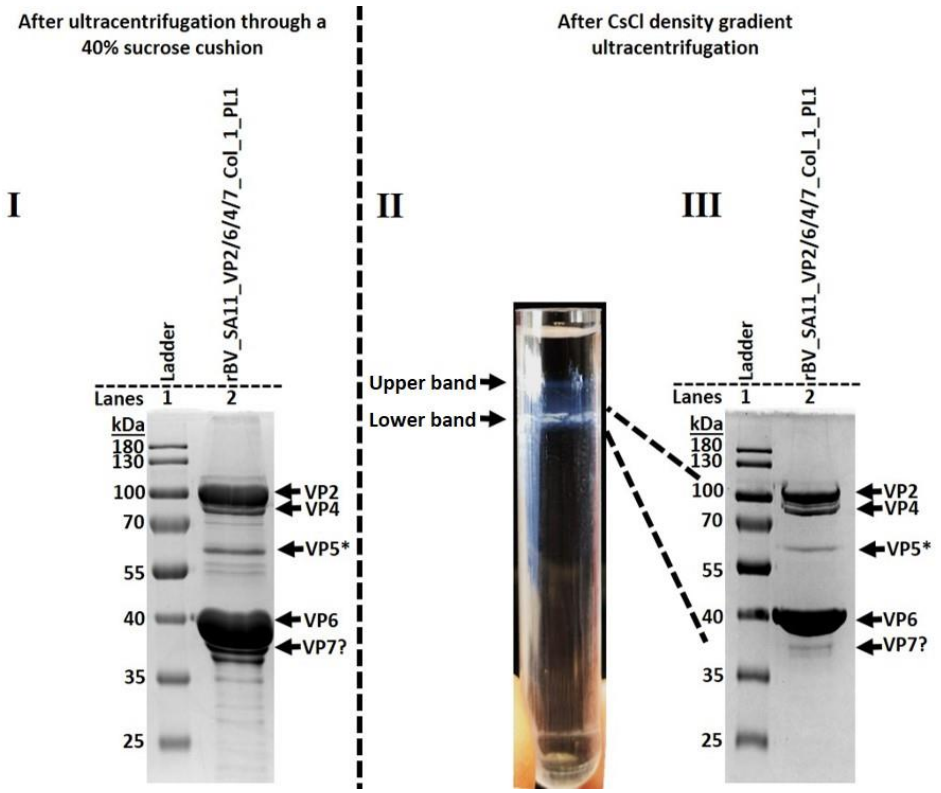

Figure 3.8: Ultracentrifuged lysates of Sf9 cells infected with rBV_SA11_VP2/6/4/7_Col_1_PL1. **(I)** The supernatant was ultracentrifuged through a 40% sucrose cushion and resuspended in TNC buffer, and loaded on SDS-PAGE (lane 2). **(II)** CsCl isopycnic centrifugation of the resuspended RV-VLPs, at a refractive index of 1,3680, and two bands were displayed. **(III)** The bands were collected and the lower band ran on SDS-PAGE (Lane 2). Lanes 1 contained PageRuler™ Prestained Protein Ladder (Catalogue number: 26616, Thermofisher Scientific™).

Bands of approximately 100 kDa (VP2), 88 kDa (VP4), 45 kDa (VP6) and 37 kDa (VP7) were seen in the supernatant of rBV_SA11_VP2/6/4/7_Col_1_PL1 (Fig. 3.8: I and II: lane 2). The bands of 100 kDa (VP2) and 45 kDa (VP6) composed the largest fraction of the proteins seen in Fig. 3.8: I: lane 2, which may be indicative of the presence of DLP along with the TLPs and/or the isolation of VP6 aggregates. A band of 60 kDa was observed which may correspond to VP5* of cleaved VP4, even though protease inhibitors were added (Fig. 3.8: I: lane 2). Some unidentified bands of 35 kDa, 55 kDa, 60 kDa and 70 kDa were observed in Fig. 3.8: I: lane 2. However, the presence of faint bands representing cellular proteins or baculovirus proteins following ultracentrifugation was not unexpected.

The CsCl isopycnic separation resulted in two main bands with a faint smear between them (Fig. 3.8: II). The lower band and faint dispersed middle section were pooled and analysed on SDS-PAGE. Bands of 100 kDa (VP2), 88 kDa (VP4), and 45 kDa (VP6) that corresponded to the normal TLP protein ratio were visualised (Fig. 3.8: III: lane 2). The intensity of the 88 kDa (VP4) band became slightly stronger following CsCl

isopycnic centrifugation (Fig. 3.8: I-III: lane 2), and the intensity of the VP6 band deduced. A dispersed band of 37 kDa (VP7) was seen (Fig. 3.8: III: lane 2). The dispersed appearance of baculovirus expressed RV VP7 on SDS-PAGE has previously been reported and was likely due to glycosylation of VP7 by insect cells (Trask & Dormitzer, 2006). A band of 60 kDa was also observed which may correspond to RV VP5* of cleaved RV VP4 (Fig. 3.8: I-III: lane 2). The RV protein ratios following CsCl isopycnic separation corresponded to fully, or partially, assembled TLPs. The reduction in VP6 band intensity may indicate that VP6 aggregates were removed. The large band of VP4, and presence of VP7, were surprising given that native DLPs usually compose the lower density band following CsCl isopycnic separation. However, due to the small quantity of the upper band following purification, it was not analysed on SDS-PAGE. Therefore, a comparison of protein composition between the upper and lower bands was not possible.

Following SDS-PAGE the virus-like particle concentration of the three samples was estimated (see Section 3.3.4), Table 3.5. Roughly ten times more RV-VLPs were obtained from lysates, from the three 50 ml insect cell shaker cultures infected at an MOI of 20, following ultracentrifugation through a 40% sucrose gradient. The samples were sent for TEM analysis by Mr. Mohamed Jaffer at the Electron Microscope Unit of the University of Cape Town, Fig. 3.9.

Table 3.5: RV-VLP concentration and yield following ultracentrifugation (see Section 3.3.4).

Ultracentrifugation type	**RV-VLP concentration**	**RV-VLP yield**
40% sucrose cushion	~1 140 µg/ml	~340 µg
CsCl isopycnic separation	~1170 µg/ml	~24 µg
	~880 µg/ml	~80 µg

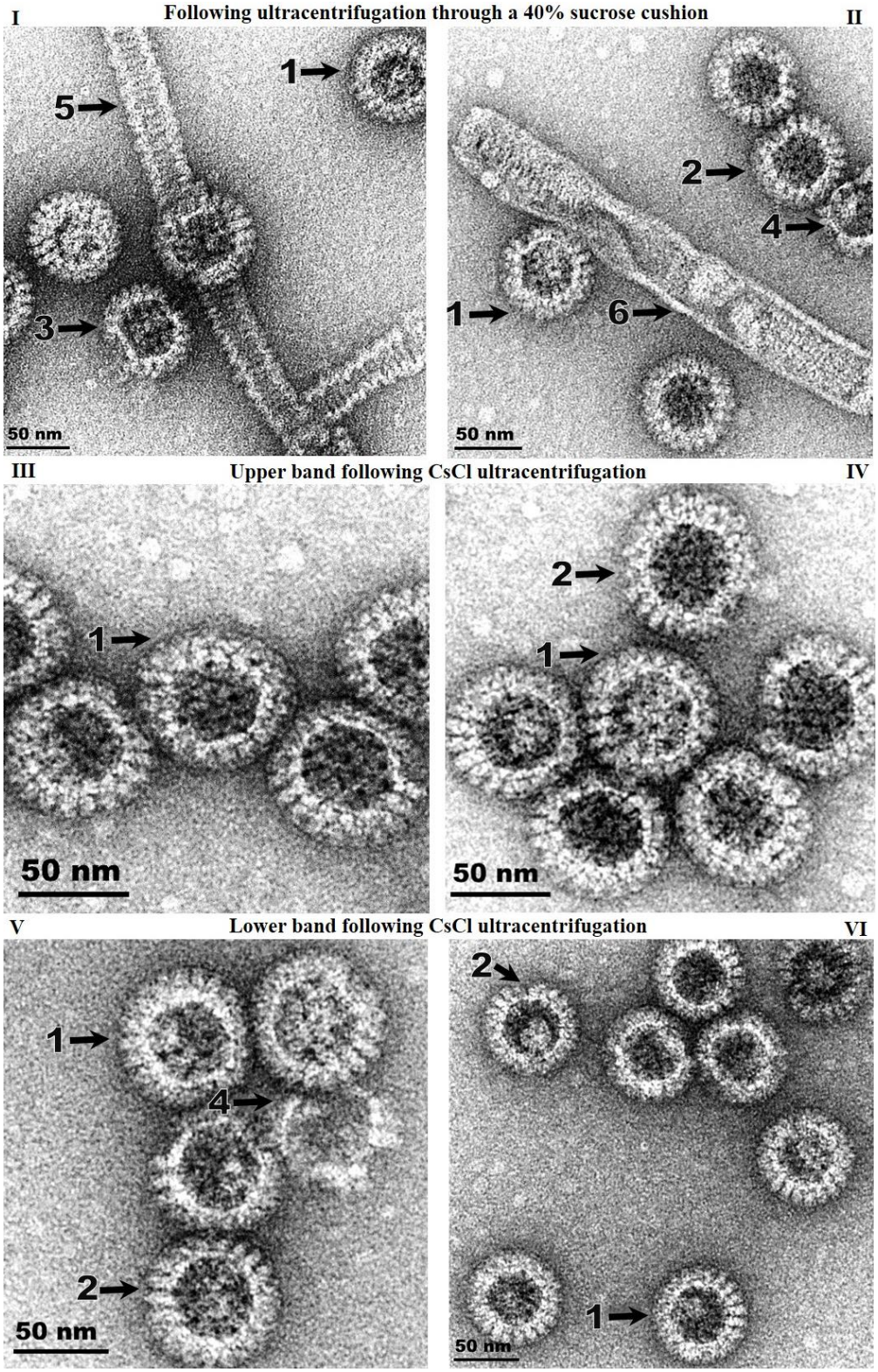

Figure 3.9: Electron micrographs of RVA/Simian-tc/ZAF/SA11-N5/1958/G3P5B[2] VP2/6/4/7 TLPs. The TLPs were produced by infecting Sf9 cells with quadcistronic rBV_SA11_VP2/6/4/7_ Col_1_PL1 encoding VP2 (C5), VP6 (I2), VP4 (P[2]) and VP7 (G3). A fraction of the pellet following ultracentrifugation through a 40% sucrose gradient was visualised **(I-II)**. The pellet was then CsCl isopycnic separated and the upper band **(III-IV)** and lower band **(V & VI)** were visualised. (Arrows 1) Fully assembled RV-TLP, (arrows 2) putative partially assembled RV-TLP, (arrows 3) possible RV-DLP, (arrows 4) partially disassembled RV-DLP, (arrow 5) putative ‘‘relaxed” form of AcMNPV baculovirus nucleocapsid and (arrow 6) putative budded AcMNPV baculovirus. Scale bar 50 nm.

Predominantly fully assembled TLPs were seen in all three of the samples (Fig. 3.9: I-VI: arrows 1) as indicated by the size (about 75 nm in diameter) and morphology (the smooth appearance of the outer layer of the TLP). The resuspended pellet following ultracentrifugation through a 40% sucrose cushion displayed a mixture of fully assembled TLPs (Fig. 3.9: I and II: arrows 1), putative partially assembled TLPs (Fig. 3.9: I: arrow 2), DLPs (Fig. 3.9: I: arrows 3), possible partially disassembled DLPs (Fig. 3.9: II: arrow 4), putative ‘‘relaxed” form of AcMNPV baculovirus nucleocapsid (Fig. 3.9: I: arrow 5) and putative budded AcMNPV baculoviruses (Fig. 3.9: II: arrow 6). Such a mixture was expected. The presence of both the ‘‘relaxed” form of AcMNPV baculovirus nucleocapsid and the budded AcMNPV baculoviruses, following ultracentrifugation through a 40% sucrose cushion, was not unexpected and were removed by CsCl isopycnic centrifugation. Although the exact identity of the tubular structures was uncertain, the shape of the tubular structures closely resembles that of AcMNPV baculovirus nucleocapsid (Wang *et al.*, 2016) and does not display the quasi-hexagonal surface lattice characteristic of RV VP6 tubes or aggregates (Lepault *et al.*, 2001).

As expected, the upper band following CsCl isopycnic centrifugation (Fig. 3.8: II) displayed predominantly fully assembled TLPs (Fig. 3.9: III-IV: arrows 1), no DLPs (Fig. 3.9: III-IV), and very few partially coated TLPs. The particles that were not complete TLPs only had very small patches of the VP7 outer capsid missing (Fig. 3.9: IV: arrows 2). However, it was not possible to ascertain whether these particles were partially coated before handling and analysis or whether they were subsequently broken during handling, transport and analysis. The collected lower band following CsCl isopycnic separation (Fig. 3.8: II) predominantly displayed fully assembled TLPs (Fig. 3.9: V-VI: arrows 1). A small portion of partially assembled TLPs (Fig. 3.9: VI: arrow 2), and an instance of a disassembled DLP (Fig. 3.9: V: arrow 4), were seen. Partially disassembled DLPs may have lost their integrity due to storage, transportation, or mechanical forces during sample preparation. The predominant TLP composition of both of the bands following CsCl isopycnic centrifugation was unexpected since native RV DLPs usually occupy the lower band. However, the absence of the contents of the native viral core in RV-VLPs, compared to native DLPs, may have affected the density ratio of DLPs and TLPs. Further, very few DLPs were visualised before CsCl isopycnic centrifugation, and in both of the bands, fully

assembled RV TLPs were seen. Therefore, the exact cause for the appearance of the two bands and the faint smear between them was uncertain, and since the upper band was not run on SDS-PAGE further analysis and comparison of protein composition could not be done. No putative AcMNPV baculovirus, AcMNPV nucleocapsid, or cell debris was seen on TEM following CsCl isopycnic centrifugation (Fig. 3.9: III-VI).

Due to an oversight, the diameter of the particles was not indicated on the TEM images of the TLPs, however, future analysis will include images displaying the measured diameter. Further, due to time constraints and the unavailability of antibodies specific to only VP4 and VP7 during this study, immunogold labelling could not be performed. This would allow for the definitive visualization of VP4 and VP7 during TEM analysis, however, this is planned for future work.

The quadcistronic Bac-to-Bac BVES resulted in the generation of fully assembled TLPs, whereas co-infection experiments using two dualcistronic recombinant baculoviruses did not (see Chapter 2, section 2.3.5). Following infection of three 50 ml Sf9 cell shaker cultures, supplemented with 20 mM calcium, with an MOI of 20 and lysing the cells four days post-infection, the yield of fully assembled homologous SA11 TLPs significantly increased. Most of the generated RV-VLPs were fully assembled TLPs. Very few of the RV-VLPs were DLPs, although, some partially assembled TLPs were seen. The ratio of fully assembled homologous TLPs greatly increased when comparing the fully assembled homologous SA11 TLPs generated in this study to the fully assembled homologous GR10924 TLPs generated by Jere and co-workers (2012). Even in the case of the particles that were not complete TLPs, the amount of VP7 assembly onto the DLPs greatly increased.

TEM analysis did not allow differentiation between RV-VLPs which were partially assembled before analysis and those that might have lost their outer capsids following handling, treatment and storage. It has previously been reported that TLPs can spontaneously disassemble into DLPs during storage without the addition of chelating agents (Mellado *et al.*, 2009; Peixoto *et al.*, 2007). The largely TLP composition of the samples following CsCl isopycnic centrifugation suggests that the isolated VLPs may have been predominantly fully assembled TLPs at the point of collection and that subsequent handling had damaged some of the TLPs. The dominantly TLP composition of the sample following pelleting through a 40% sucrose cushion also

suggests that the sample may likely have been predominantly fully, or partially, assembled TLPs.

The use of quadcistronic recombinant baculoviruses at a high MOI in the medium supplemented to 20 mM calcium presents a cost-effective platform to study the formation of chimeric RV-VLPs.

The next steps were to evaluate the assembly of the SA11 TLPs insect cell medium with and without calcium supplementation, and also to use the pFBq_GR10924_VP2/6_G12P[4] donor plasmid in the Bac-to-Bac BVES to attempt to generate fully assembled heterologous chimeric RV-VLP in the presence of 20 mM calcium. However, due to time constraints, the study was halted at this point. Therefore, the necessity of calcium supplementation when using quadcistronic rBVs for the assembly of TLPs could not be evaluated. Therefore, it could only be concluded that fully assembled TLPs were successfully generated when using quadcistronic rBVs with calcium supplementation and that assembly could not be achieved when co-infecting dualcistronic rBVs in insect medium supplemented to 20 mM calcium. Further studies may elucidate the necessity of calcium supplementation when using quadcistronic rBVs and evaluate the assembly of heterologous TLPs when using quadcistronic rBVs.

3.4. Summary

Towards the aim of generating chimaeric TLPs, three pFBq donor plasmids encoding all four TLP proteins (VP2/6/4/7) were *in silico* designed. pFBq_SA11_VP2/6/4/7, pFBq_GR10924_VP2/6_G12P[4] and pFBq_SA11_VP2/6_RVG_VP4/7 were obtained from GenScript and were propagated and archived in *E. coli* JM109 cells.

Before assessing the generation of heterologous chimeric TLPs using quadcistronic recombinant baculoviruses, the assembly of homologous SA11 VP2/6/4/7 TLPs were assessed. Purified pFBq_SA11_VP2/6/4/7 was used to generate recombinant rBacmid_ SA11_VP2/6/4/7 which was used to generate quadcistronic recombinant baculoviruses (rBV_SA11_VP2/6/4/7). The rBV_SA11_VP2/6/4/7 were plaque-purified, propagated, and used to express SA11 VP2, VP6, VP4 and VP7 (Fig. 3.4). Most of the expressed SA11 VP2, VP6, VP4 and VP7 was insoluble. However, a fraction of the RV proteins correctly assembled into soluble RV-VLPs which were detectible using western blot, but not visible on SDS-PAGE before ultracentrifugation through a 40% sucrose cushion.

Infection of Sf9 cells with rBV_SA11_VP2/6/4/7_Col_4_PL1_#1, at a MOI of 20 and with 20 mM calcium supplementation, resulted in the formation of fully assembled TLPs (Fig. 3.9). The majority of the RV-VLPs were fully assembled TLPs following CsCl isopycnic separation. The formation of RV-VLPs is restricted to a narrow range of physicochemical parameters (Mellado *et al.*, 2009) and RV protein expression levels (Roldão *et al.*, 2012). Hence, further optimization of this expression system may further increase the yield of the RV-VLPs.

Here we report that fully assembled TLPs could be generated using quadcistronic recombinant baculoviruses expressing SA11 VP2, VP6, VP4 and VP7 when using a high MOI and Grace's Insect Medium supplemented to 20 mM calcium. This quadcistronic BVES system presents a cost-effective platform to investigate the formation of chimaeric RV-VLPs. However, due to time constraints, the effect of supplementation of the insect medium to 20 mM calcium on the assembly of TLPs could not be definitively evaluated, nor could further optimization and evaluation of the assembly of heterologous RV-VLPs be investigated.

Chapter 4: Concluding Discussion

Rotavirus (RV) is the primary cause of diarrhoea-related deaths worldwide among children younger than 5 years old (Tate *et al.*, 2016). The estimated mortality in 2016 in sub-Saharan Africa was 104 733 (Troeger, Khalil*, et al.*, 2018). The two main commercially available RV vaccines, RotaTeq and Rotarix, are live attenuated vaccines. They have lower efficacy in developing countries compared to developed countries (Burnett *et al.*, 2020; Henschke *et al.*, 2022; Jonesteller *et al.*, 2017; Tate *et al.*, 2012). This may in part be explained by differences in circulating strains in developing countries (Isanaka *et al.*, 2021; Jason *et al.*, 2010; Jere *et al.*, 2014; Nelson *et al.*, 2009; Varghese *et al.*, 2022). Using another live RV vaccine to cover this gap in efficacy would be hampered by the existing partial immunity. Rotavirus VLPs are promising candidate dead-subunit vaccines (Crawford *et al.*, 1994; Istrate *et al.*, 2008; Jere *et al.*, 2014), since RV-VLPs have been shown to protect against RV infections in animal models (Bertolotti-Ciarlet *et al.*, 2003; Ciarlet *et al.*, 1998; Redmond *et al.*, 1993; Saif & Fernandez, 1996). Thus, regional specific transcapsidated VLP-based dead subunit vaccines present safe alternatives to live attenuated vaccines (Fuenmayor *et al.*, 2017; Kurokawa *et al.*, 2021; Mohsen *et al.*, 2017).

Jere and co-workers (2014) applied a novel approach that may be instrumental in speeding up vaccine research and development. Whole genome rotavirus consensus sequences were obtained directly from human stool samples and insect cell codon-optimized to be used for baculovirus expression of homologous and heterologous RV-VLPs. This bypassed the need for the time-consuming intermediate step of adapting RVs to cell culture (Jere *et al.*, 2014). However, during the co-infection of dualcistronic recombinant baculoviruses (rBVs) rBV_GR10924_VP2/6 and dualcistronic rBVs encoding African strain VP4/7s only about 30% of homologous RV-VLPs (RV GR10924 VP2/6/4/7), and 10-20% of the heterologous RV-VLPs generated, were TLPs (Jere *et al.*, 2014).

Partial assembly of VP7 onto DLPs was hypothesised to be due to an insufficient concentration of 8,83 mM calcium in the TC-100 Insect Medium (Sigma-Aldrich, St. Louis, MO) used by Jere and co-workers (2012, 2014). Therefore, supplementing the media to 20 mM calcium may improve the assembly of VP7 onto DLPs (personal communication of M.K. Estes, S.E. Crawford and B.V. Prasad to A.A. Van Dijk, 2018).

To test this hypothesis, the Bac-to-Bac BVES was used to repeat some of the heterologous co-infections done by Jere and co-workers (2012, 2014) with 20 mM calcium supplementation.

Due to the loss of the original pFBd_GR10924_VP2-VP6 donor plasmid, it was again *in silico* designed, ordered, and used to generate dualcistronic rBV_GR10924_VP2/6. Rotavirus VP2 and VP6 expression by Sf9 insect cells infected with dualcistronic rBV_GR10924_VP2/6 was comparable with that of Jere and co-workers (2012). This was surprising given that Jere and co-workers (2012) used High Five insect cells reported to express RV VP2, VP6, VP4 and VP7 three times more than Sf9 cells. Rotavirus DLPs were generated by the expressed RV GR10924 VP2/6 and visualised using TEM (Fig 2.14).

Recombinant bacmids generated by Jere and co-workers (2012, 2014) were used to generate dualcistronic VP4/7 rBV_G12P[4], rBV_G12P[6], and rBV_G12P[8]. The yield of VP4 and VP7 was lower than expected and repeated attempts at optimization failed to increase the protein yield. Interestingly, during IFMA of Sf9 cells infected with rBV_G12P[4], rBV_G12P[6], and rBV_G12P[8], the expressed VP7 (G12) and VP4 (P[4], P[6] and P[8]) cross-reacted with polyclonal rabbit anti-SA11 virion IgG serum raised against CsCl purified SA11 (genotype G3P[2]) virions (Fig. 2.12). To our knowledge, this is the first report of heterotypic binding of polyclonal rabbit anti-SA11 virion IgG to VP7 (G12) and VP4 (P[4], P[6] and P[8]) during IFMA. The heterotypic antibody binding was likely due to conserved regions on VP4 and/or VP7 since both SA11 and the African rotaviruses are group A RVs (Clarke & Desselberger, 2015).

Co-infection of Sf9 cells using dualcistronic rBV_GR10924_VP2/6 and dualcistronic rBV_G12P[4] was done in TC-100 Insect Medium supplemented to a final concentration of 20 mM calcium. However, only DLPs were generated as visualised on TEM. The logistics of maintaining various plaques of rBV_GR10924_VP2/6, rBV_G12P[4], rBV_G12P[6], and rBV_G12P[8] at relatively comparable titers was taxing. It was also not possible to express VP4 and VP7 using dualcistronic rBV_G12P[4], rBV_G12P[6], and rBV_G12P[8] (Fig. 2.10 and Fig. 2.11) to a yield comparable with either Jere and co-workers (2012) or VP2 and VP6 expression using dualcistronic rBV_GR10924_VP2/6 (Fig. 2.6 and 2.7). This was despite repeated

attempts at transfection, plaque purification and plaque selection, passaging and infections at various MOIs.

The possibility of generating chimeric intergroup RV-VLPs as discussed in the addendum to Chapter 2 (see Section 2.4) was evaluated using co-infections of rBV_SA11_VP2/6 (RVA) and rBV_RVG_VP4/7, with 20 mM calcium supplementation. However, only RVA SA11 DLPs were visualised by TEM (data not shown).

The addition of 20 mM calcium during co-infection of dualcistronic rBVs encoding VP2/6 and dualcistronic rBVs encoding VP4/7 did not yield fully or partially assembled TLPs. Therefore, it was hypothesised that co-infection with dualcistronic rBVs was contributing to sub-optimal RV protein expression ratios and hampering TLP assembly. The protein yield of VP4/7 was considerably lower than that of VP2/6 when using dualcistronic rBVs. Further, the likelihood of a cell receiving an equal ratio of rBVs encoding VP2/6 and rBVs encoding VP4/7 was estimated to be only 12,78%, when infecting cells with a MOI of 5 (Belyaev *et al.*, 1995). Thus, protein expression of RV proteins resembling the normal TLP protein composition ratio by co-infection was very unlikely and likely shifted the reaction equilibrium to favour DLP formation (Roldão *et al.*, 2012; Roldão *et al.*, 2007).

Therefore, a quadcistronic recombinant baculovirus expression strategy to simultaneously express RV VP2, VP6, VP4 and VP7 was applied. This approach had the benefit of expressing all four RV structural proteins in each infected cell. Towards this aim, three pFBq donor plasmids encoding all four TLP proteins (VP2/6/4/7) were *in silico* designed. The pFBq_SA11_VP2/6/4/7, pFBq_GR10924_ VP2/6_G12P[4] and pFBq_ SA11_VP2/6_RVG_VP4/7 were purchased from GenScript.

First, attempts were made to generate homologous SA11 TLPs. Quadcistronic rBV_SA11_VP2/6/4/7 were indeed generated using the pFBq_SA11_VP2/6/4/7 donor plasmid in the Bac-to-Bac Baculovirus expression system. Expression of SA11 VP2, VP6, VP6 and VP7 were confirmed on SDS-PAGE. However, the expressed proteins were predominantly insoluble (Fig. 3.4). Various attempts at increasing solubility failed (see Section 3.3.2). Although the majority of the proteins were insoluble, soluble SA11 VLPs could be isolated using ultracentrifugation through a 40% sucrose gradient and analysed using western blotting (Fig. 3.5).

Infections of Sf9 cells in Grace's Insect Medium supplemented to 20 mM calcium with rBV_SA11_VP2/6/4/7 at a MOI of 20 were successful in generating fully assembled homologous SA11 TLPs. When the SA11 VLPs were analysed on TEM, the majority of RV-VLPs were fully assembled homologous SA11 VP2/6/4/7 TLPs (Fig. 3.9). In principle, this shows that the quadcistronic Bac-to-Bac BVES presents a cost-effective platform to generate fully assembled TLPs, without the logistical load of maintaining various recombinant baculoviruses that express proteins at comparable yields and comparable titers. Here, quadcistronic recombinant baculoviruses, and 20 mM calcium supplementation, allowed for the complete assembly of VP7 onto the DLPs when compared to the dualcistronic approach of Jere and co-workers (2014).

Due to time constraints, the problem of protein insolubility could not be investigated. Also, there was not enough time to use the quadcistronic Bac-to-Bac BVES to generate fully assembled chimeric RV-VLPs composed of GR10924 DLPs and an African strain outer capsid, nor could the possibility of generating chimeric RV-VLPs composed of RVA SA11 DLPs and RVG 03V0567 VP4/7 be investigated.

Two main problems still face the quadcistronic Bac-to-Bac BVES. The first is to determine the exact cause of the insolubility of the expressed RV SA11 VP2/6/4/7, and the second is to optimise the storage conditions of TLPs.

The usage of quadcistronic rBVs allowed for more optimal RV protein expression ratios per cell that approach the normal RV-VLP protein mass ratio optimal for TLP formation. Increasing the solubility of the RV proteins may improve TLP yield even further. Stoichiometric ratios, thermodynamic aggregation conditions, and spatial and temporal protein conditions influence RV-VLP yield (Mellado *et al.*, 2009; Roldão *et al.*, 2012). These conditions are usually sub-optimal *in vivo* resulting in very little of the expressed RV proteins forming RV-VLPs (Jiang *et al.*, 1999; Mellado *et al.*, 2009; Palomares *et al.*, 2002; Vieira *et al.*, 2005). Here, the insolubility of the expressed RV proteins (Fig. 3.4) likely compounded the already sub-optimal conditions for RV-VLP formation. It has also been reported that aggregation of kinetically trapped stable intermediates of expressed rotavirus proteins occur at very high protein concentrations (Zeng *et al.*, 1994). This leads to an insufficient concentration of free monomers for VLP assembly, possibly leading to decreased RV-VLP formation and yield (Roldão *et al.*, 2012). Therefore, it was postulated that a decrease in temperature, decreasing the

MOI, or changing the medium from TC-100 Insect medium to Graces Insect medium may increase solubility (see Section 3.3.2). However, varying these factors, during this study, did not improve the rotavirus protein solubility (data not shown).

Therefore, further attempts to increase protein solubility, such as an approach similar to the recent work on increasing the solubility of baculovirus-expressed African horsesickness virus (AHSV) VP7 (comparable to RV VP6) via site-directed mutagenesis (Bekker *et al.*, 2022) may prove beneficial to increase the solubility of RV proteins in the current study. Bekker *et al*. (2022) used site-directed mutagenesis to target specific regions of AHSV VP7 that are involved in self-assembly to disrupt the self-assembly of AHSV VP7. This resulted in fully soluble AHSV VP7 which could interact with AHSV VP3 to form core-like particles (Bekker *et al.*, 2022). Another approach may be the addition of chaperone-expressing plasmids transfected into Sf9 cells before infection with recombinant baculoviruses which may aid in increasing the solubility of quadcistronic baculovirus-expressed RV proteins. Lastly, the usage of insect cell codon optimization may have negatively impacted rotavirus protein conformation and expression. Codon optimization selects codons based on the codon optimality but does not take into account the optimal codons for best protein folding (Hia & Takeuchi, 2021). Classical codon optimization increases the overall translation rate of a protein without considering the time necessary for correct protein folding. This may inadvertently decrease the time available for protein folding (Hia & Takeuchi, 2021). Which, in the case of this study, may have resulted in misfolded RV structural proteins causing insoluble aggregates. Another possible drawback of codon optimisation is the possibility of ribosomal collisions (Hia & Takeuchi, 2021). Normally stretches of the mRNA transcript use sub-optimal codons to decrease translation time for optimal ribosomal progression on the transcript. However, codon optimization increases the translation rate of the entire transcript without regard for its effect on elongation speed during translation. This may also inadvertently cause ribosome collisions on the transcript. Since newly codon-optimised transcripts may have increased translation rates of one section of the transcript without increasing that of a subsequent section. Thus, when ribosomes move from the optimised to the less-optimised sections the difference in elongation time may cause a second ribosome on the optimised section to collide with a ribosome that has reached the less optimal

stretch (Hia & Takeuchi, 2021). Such a collision may result in sub-optimal protein expression in some codon-optimized ORFs.

Another problem may be the possible disassembly of the TLPs during storage and handling. At a constant pH, an increase in temperature and ionic strength induces the transition of TLPs to DLPs (Martin *et al.*, 2002). It has also been reported that rotavirus TLPs can spontaneously disassemble into DLPs without the addition of chelating agents reducing the free calcium concentration *in vitro* (Mellado *et al.*, 2009; Peixoto *et al.*, 2007). TLPs that disassemble *in vitro* may reassemble. The critical physicochemical parameters of *in vitro* assembly kinetics of RV-VLPs, and the reassembly efficiency of TLPs, are pH, temperature, and calcium concentration (Mellado *et al.*, 2009). The minimum *in vitro* calcium concentration is 1 mM (Mellado *et al.*, 2009), and calcium concentrations of up to 50 mM calcium have been shown to favour TLP formation (Mellado *et al.*, 2009; Ready *et al.*, 1988). *In vitro* assembly studies of VP2/6/7 could only achieve a RV-VLP constitution of 80% TLPs (Mellado *et al.*, 2009). Therefore, the spontaneous disassembly of TLPs may occur in the presence of DLPs that fail to reassemble into TLPs during storage or transport. The addition of 10% glycerol to the TNC buffer, used to resuspend RV-VLPs following ultracentrifugation, may prevent the disassembly of TLPs *in vitro* (Mellado *et al.*, 2009). Therefore, the few DLPs that were observed following CsCl isopycnic separation of the SA11 VLPs (Fig. 3.9) may have been the result of the spontaneous disassembly of TLPs.

In future studies expression systems other than insect cells may also be beneficial for the generation of rotavirus TLPs. Rotavirus VP7 is a glycoprotein, and using mammalian or avian cells may be advantageous since their glycosylation pathways are identical to the native glycosylation pathways normally used by RVs. Transfecting mammalian cells with expression plasmids, encoding all four RV-VLP proteins, to generate RV-VLPs may allow for optimisation of RV protein expression. For example, a tricistronic HSV-1 amplicon vector construct containing ORFs encoding RV VP2/6/7 has been used to generate RV VP2/6/7 TLPs in mammalian cells and to vaccinate mice which resulted in partial protection of the mice against RV challenges (Laimbacher *et al.*, 2012). Another approach may be to use an inducible *piggyBac* transposon-based expression system (Li *et al.*, 2013) in mammalian or avian cell lines

to inducibly express RV-VLP proteins. This may improve RV VP7 expression and glycosylation.

The use of RV-VLPs in native RV host cells may also be instrumental in understanding RV assembly and entry by using nanoluciferase (Nluc) fragment complementation to track viral assembly and viral entry in host cells. This approach would be similar to that of a recent study which used Severe Acute Respiratory Syndrome Coronavirus 2 (SARS-CoV2) VLPs and a nanoluciferase (Nluc) fragment complementation to track viral assembly and viral entry of SARS-CoV2 (Kumar *et al.*, 2021). This approach may help shed light on questions concerning RV assembly and entry.

In conclusion, here a quadcistronic Bac-to-Bac BVES approach presented a better and more cost-effective platform to investigate the formation of chimeric RV-VLPs, than using a co-infection approach using dualcistronic rBVs, and was successful in generating fully assembled SA11 VP2/6/4/7 TLPs.

Appendix A: Conference outputs

- L.J.C. Theart, **P. Le Roux**, A.A. van Dijk. Developing a SA11 DLP as a universal backbone for chimeric TLPs. 12th African Rotavirus Symposium in Johannesburg, South Africa, 30 July – 1 August 2019.
- **P. le Roux**, A.C. Potgieter, and A.A. van Dijk. Generating a recombinant baculovirus expressing four rotavirus SA11 proteins VP2/6/7/4 simultaneously. 14th Internasional dsRNA Symposium in Banff, Canada, 10-14 October 2022.

  Award: Poster award received at the 14th International dsRNA Symposium 2022 for Combatting and Exploiting dsRNA Viruses.

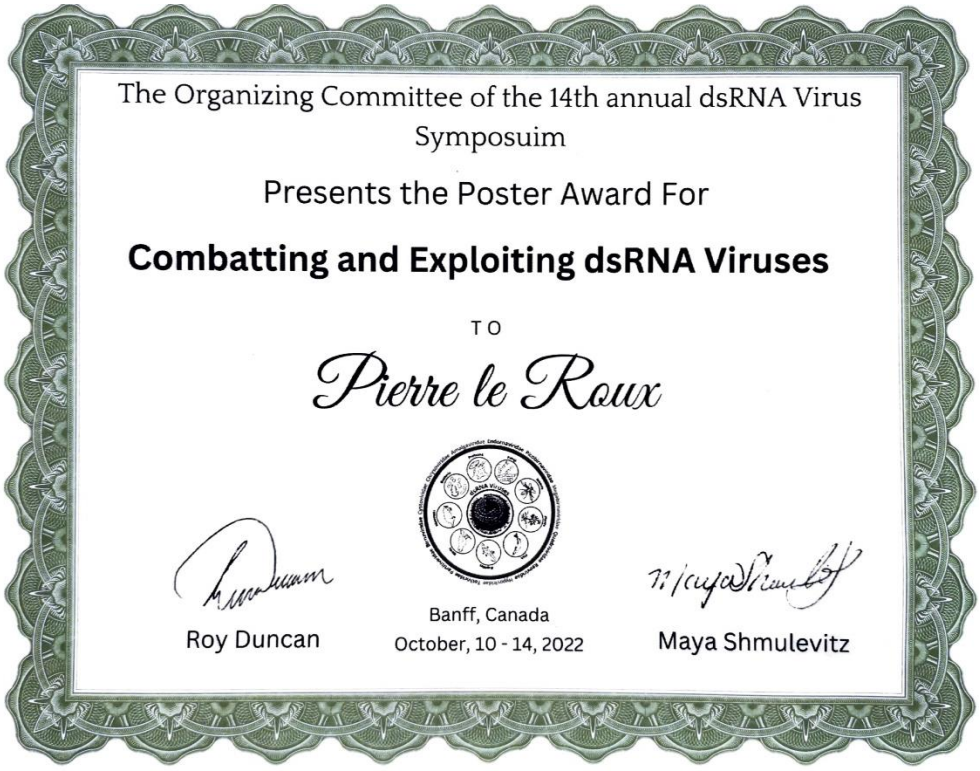

Appendix B: Abbreviations

AcMNPV	Autographa californica multi-capsid nucleopolyhedrosis virus
AGE	acute gastroenteritis
ATP	adenosine triphosphate
APS	ammoniumperoxodisulphate
A_{230}	absorbance at 230 nm
A_{260}	absorbance at 260 nm
A_{280}	absorbance at 280 nm
bp	base pair
BRV	bovine rotavirus
BV	baculovirus
BVs	baculoviruses
BVES	baculovirus vector expression system
Ca^{2+}	calcium
$CaCl_2$	calcium chloride
Cat no.	catalogue number
ccc-DNA	covalently closed circular deoxyribonucleic acid
CPE	cytopathic effect
H_20	water
dH_20	distilled water
ddH_20	double distilled water
DLP	double-layered particle
DLPs	double-layered particles
DNA	deoxyribonucleic acid
dNTPs	deoxynucleoside triphosphate
d.p.i.	days post-infection
Dr.	doctor
ds	double-stranded
dsRNA	double-stranded ribonucleic acid
E. coli	*Escherichia coli*
EDTA	ethylene diamine tetra acetic acid
EM	electron microscopy
ER	endoplasmic reticulum
EtBr	ethidium bromide
Ex	excitation range
FB	FastBac
FBS	foetal bovine serum
Fig.	figure
g	gram
GFP	green fluorescent protein
GS	genome segment
GTE	glucose tris-chloride edta
G-type	glycosylated structure
IFMA	immunofluorescent monolayer assay
IgG	immunoglobulin G
IgA	immunoglobulin A
IPTG	isopropyl β-d-1-thiogalactopyranoside
KAc	potassium acetate
kb	kilobase pairs
kDa	kilo Dalton
LB	Luria broth

MA	Massachusetts
MAbs	monoclonal antibodies
MCS	multiple cloning site
mg	milligram
Mg^{2+}	magnesium
$MgCl_2$	magnesium chloride
ml	millilitre
mM	millimolar
min	minutes
Mr.	mister
MOI	multiplicity of infection
mRNA	messenger RNA
NaOH	sodium hydroxide
NaCl	sodium chloride
NCDV	Nebraska calf diarrhoea virus
ng	nanogram
NGS	next generation sequencing
NJ	new jersey
nm	nanometre
NP40	nonyl phenoxyl-polyethoxyl-ethanol
NSP	non-structural viral protein
NWU	north-west university
NY	new york
ORF	open reading frame
Ori	origin of replication
P1/2/3/4	passage 1/2/3/4
PAGE	polyacrylamide gel electrophoresis
PBS	phosphate-buffered saline
PCR	polymerase chain reaction
pFB	pFastBac
pFBq	pFastBacquad
pFBd	pFastBacdual
Pfu	plaque-forming units
PL	plaque
polh	polyhedron
Prof.	professor
P-type	protease sensitivity
rBacmid	recombinant bacmid
rBV	recombinant baculovirus
rBVs	recombinant baculoviruses
RdRP	RNA-dependent RNA polymerase
RE	restriction enzymes
RNA	ribonucleic acid
Rpm	revolutions per minute
RRV	Rhesus rotavirus
RV	rotavirus
RVs	rotaviruses
RVA	group A rotavirus
RVG	group G rotavirus
RV-DLP	rotavirus double-layered particle
RV-DLPs	rotavirus double-layered particles

RV-TLP	rotavirus triple-layered particle
RV-TLPs	rotavirus triple-layered particles
RV-VLP	rotavirus virus-like particle
RV-VLPs	rotavirus virus-like particles
SA11	Simian agent 11
SDS	sodium-dodecyl-sulphate
SDS-PAGE	sodium-dodecyl-sulphate polyacrylamide gel electrophoresis
Sf9	*Spodoptera frugiperda* 9
SF	soluble fraction
SLP	single-layered particle
SLPs	single-layered particles
SOC	super optimal broth with catabolite repression
ss	single-stranded
TAE	tris-acetate EDTA (ethylenediaminetetraacetic acid)
TE	tris EDTA
TEM	transmission electron microscopy
TEMED	tetramethylethylenediamine
TF	total fraction
TGS	tris, glycine, sds
Tn7L	tn7 site left
Tn7R	tn7 site right
Tris	tris(hydroxymethyl)aminomethane
Tris-Cl	tris chloride
TEM	transmission electron microscopy
TLP	triple-layered particle
TLPs	triple-layered particles
USA	United States of America
UV	ultraviolet
v/v	volume/volume
V	volt
VLPs	virus-like particles
VP	virus protein
VPD	viroporin domain
VP2/6	virus protein 2 and virus protein 6
VP2/6/4/7	virus protein 2, virus protein 6, virus protein 4 and virus protein 7
VP4/7	virus protein 4 and virus protein 7
WHO	world health organization
WT	wild-type
w/v	weight/volume
X-gal	5-bromo-4-chloro-3-indolyl-beta-d-galacto-pyranoside
µg	microgram
µl	microliter
°C	degrees celsius
(+)ssRNAs	positive sense single-stranded ribonucleic acid
× g	g-force

Appendix C: Permissions

ELSEVIER LICENSE

TERMS AND CONDITIONS

This Agreement between Mr. Pierre Le Roux ("You") and Elsevier ("Elsevier") consists of your license details and the terms and conditions provided by Elsevier and Copyright Clearance Center.

License Number	5345830583231
License date	Jul 11, 2022
Licensed Content Publisher	Elsevier
Licensed Content Publication	Elsevier Books
Licensed Content Title	Virus Taxonomy
Licensed Content Author	Andrew M.Q. King
Licensed Content Date	Jan 1, 2012
Licensed Content Pages	97
Start Page	541
End Page	637
Type of Use	reuse in a thesis/dissertation
Portion	figures/tables/illustrations
Number of figures/tables/illustrations	1
Format	both print and electronic
Are you the author of this Elsevier chapter?	No
Will you be translating?	No
Title	Investigating the feasibility of generating chimeric intergroup rotavirus triple-layered virus-like particles on SA11 double-layered particles
Institution name	North-West University
Expected presentation date	Dec 2022
Portions	"Table 24: Genome segments and protein products of Simian rotavirus A/SA11". The table on page 609.
Requestor Location	Mr. Pierre Le Roux Building F3, Room 211 North-West University 11 Hoffman St Potchefstroom North-West Province 2531 South Africa Attn: Mr. Pierre Le Roux
Publisher Tax ID	ZA 4110266048
Total	0.00 USD

ELSEVIER LICENSE

TERMS AND CONDITIONS

This Agreement between Mr. Pierre Le Roux ("You") and Elsevier ("Elsevier") consists of your license details and the terms and conditions provided by Elsevier and Copyright Clearance Center.

License Number	5345880972340
License date	Jul 11, 2022
Licensed Content Publisher	Elsevier
Licensed Content Publication	Virus Research
Licensed Content Title	Rotaviruses
Licensed Content Author	Ulrich Desselberger
Licensed Content Date	Sep 22, 2014
Licensed Content Volume	190
Licensed Content Issue	n/a
Licensed Content Pages	22
Start Page	75
End Page	96
Type of Use	reuse in a thesis/dissertation
Portion	figures/tables/illustrations
Number of figures/tables/illustrations	2
Format	both print and electronic
Are you the author of this Elsevier article?	No
Will you be translating?	No
Title	Investigating the feasibility of generating chimeric intergroup rotavirus triple-layered virus-like particles on SA11 double-layered particles
Institution name	North-West University
Expected presentation date	Dec 2022
Portions	"Fig. 1. Aspects of rotavirus structure" on page 77, and "Fig. 4. The rotavirus replication cycle" on page 80.
Requestor Location	Mr. Pierre Le Roux Building F3, Room 211 North-West University 11 Hoffman St Potchefstroom North-West Province 2531 South Africa Attn: Mr. Pierre Le Roux
Publisher Tax ID	ZA 4110266048
Total	0.00 USD

JOHN WILEY AND SONS LICENSE

TERMS AND CONDITIONS

This Agreement between Mr. Pierre Le Roux ("You") and John Wiley and Sons ("John Wiley and Sons") consists of your license details and the terms and conditions provided by John Wiley and Sons and Copyright Clearance Center.

License Number	5345910220212
License date	Jul 11, 2022
Licensed Content Publisher	John Wiley and Sons
Licensed Content Publication	Immunology and Cell Biology
Licensed Content Title	Fields Virology, 4th Edition
Licensed Content Author	Gunasegaran Karupiah
Licensed Content Date	Jun 1, 2002
Licensed Content Volume	80
Licensed Content Issue	3
Licensed Content Pages	2
Type of use	Dissertation/Thesis
Requestor type	University/Academic
Format	Print and electronic
Portion	Figure/table
Number of figures/tables	1
Will you be translating?	No
Title	Investigating the feasibility of generating chimeric intergroup rotavirus triple-layered virus-like particles on SA11 double-layered particles
Institution name	North-West University
Expected presentation date	Dec 2022
Portions	"Fig 2: Gene coding assignments and..." in Chapter 54: Rotaviruses and Their Replication.
Requestor Location	Mr. Pierre Le Roux Building F3, Room 211 North-West University 11 Hoffman St Potchefstroom North-West Province 2531 South Africa Attn: Mr. Pierre Le Roux
Publisher Tax ID	EU826007151
Total	0.00 USD

ELSEVIER LICENSE

TERMS AND CONDITIONS

This Agreement between Mr. Pierre Le Roux ("You") and Elsevier ("Elsevier") consists of your license details and the terms and conditions provided by Elsevier and Copyright Clearance Center.

License Number	5345940668067
License date	Jul 11, 2022
Licensed Content Publisher	Elsevier
Licensed Content Publication	Virology
Licensed Content Title	Rotavirus RNA polymerases resolve into two phylogenetically distinct classes that differ in their mechanism of template recognition
Licensed Content Author	Kristen M. Ogden,Reimar Johne,John T. Patton
Licensed Content Date	15–30 September 2012
Licensed Content Volume	431
Licensed Content Issue	1-2
Licensed Content Pages	8
Start Page	50
End Page	57
Type of Use	reuse in a thesis/dissertation
Portion	figures/tables/illustrations
Number of figures/tables/illustrations	3
Format	both print and electronic
Are you the author of this Elsevier article?	No
Will you be translating?	No
Title	Investigating the feasibility of generating chimeric intergroup rotavirus triple-layered virus-like particles on SA11 double-layered particles
Institution name	North-West University
Expected presentation date	Dec 2022
Portions	“Table 2: Terminal sequences of RV (+)RNA encoding VP1" on page 51, "Fig. 1. Maximum likelihood phylogenetic trees comparing..." on page 52, and "Fig. 3. Viral (+)RNA recognition by clade A and clade B VP1" on page 55.
Requestor Location	Mr. Pierre Le Roux Building F3, Room 211 North-West University 11 Hoffman St Potchefstroom North-West Province, 2531 South Africa Attn: Mr. Pierre Le Roux
Publisher Tax ID	ZA 4110266048
Total	0.00 USD

ELSEVIER LICENSE

TERMS AND CONDITIONS

This Agreement between Mr. Pierre Le Roux ("You") and Elsevier ("Elsevier") consists of your license details and the terms and conditions provided by Elsevier and Copyright Clearance Center.

License Number	5345950140545
License date	Jul 11, 2022
Licensed Content Publisher	Elsevier
Licensed Content Publication	Structure
Licensed Content Title	Mechanism for Coordinated RNA Packaging and Genome Replication by Rotavirus Polymerase VP1
Licensed Content Author	Xiaohui Lu, Sarah M. McDonald, M. Alejandra Tortorici, Yizhi Jane Tao, Rodrigo Vasquez-Del Carpio, Max L. Nibert, John T. Patton, Stephen C. Harrison
Licensed Content Date	Nov 12, 2008
Licensed Content Volume	16
Licensed Content Issue	11
Licensed Content Pages	11
Start Page	1678
End Page	1688
Type of Use	reuse in a thesis/dissertation
Portion	figures/tables/illustrations
Number of figures/tables/illustrations	1
Format	both print and electronic
Are you the author of this Elsevier article?	No
Will you be translating?	No
Title	Investigating the feasibility of generating chimeric intergroup rotavirus triple-layered virus-like particles on SA11 double-layered particles
Institution name	North-West University
Expected presentation date	Dec 2022
Portions	"Figure 1. Structure of the VP1 Apoenzyme" on page 1681.
Requestor Location	Mr. Pierre Le Roux Building F3, Room 211 North-West University 11 Hoffman St Potchefstroom, North-West Province, 2531, South Africa Attn: Mr. Pierre Le Roux
Publisher Tax ID	ZA 4110266048
Total	0.00 USD

AMERICAN SOCIETY FOR MICROBIOLOGY – JOURNALS LICENSE TERMS AND CONDITIONS

Order Date	13-Jul-2022
Order License ID	1246845-1
ISSN	0022-538X
Type of Use	Republish in a thesis/dissertation
Publisher	AMERICAN SOCIETY FOR MICROBIOLOGY
Portion	Image/photo/illustration
Licensed Content	
Publication Title	Journal of virology
Article Title	Characterization of virus-like particles produced by the expression of rotavirus capsid proteins in insect cells.
Author/Editor	AMERICAN SOCIETY FOR MICROBIOLOGY
Date	01/01/1967
Language	English
Country	United States of America
Rightsholder	American Society for Microbiology - Journals
Publication Type	Journal
Start Page	5945
End Page	5952
Issue	9
Volume	68
URL	https://journals.asm.org/journal/jvi
Request Details	
Portion Type	Image/photo/illustration
Number of images / photos / illustrations	1
Format (select all that apply)	Print, Electronic
Who will republish the content?	Academic institution
Duration of Use	Life of current edition
Lifetime Unit Quantity	Up to 499
Rights Requested	Main product
Distribution	Worldwide
Translation	Original language of publication
Copies for the disabled?	No
Minor editing privileges?	No
Incidental promotional use?	No
Currency	USD
New Work Details	
Title	Investigating the feasibility of generating chimeric intergroup rotavirus triple-layered virus-like particles on SA11 double-layered particles

Instructor name	Prof. A.A. van Djik
Institution name	North-West University
Expected presentation date	2022-11-01
Additional Details	
Order reference number	N/A
The requesting person / organization to appear on the license	Pierre le Roux
Reuse Content Details	
Title, description or numeric reference of the portion(s)	"FIG. 1. Electron micrographs of different formulations of VLPs produced by coexpression of baculovirus recombinants containing rotavirus genes" on page 5948.
Editor of portion(s)	Crawford, S E; LabbÃ©, M; Cohen, J; Burroughs, M H; Zhou, Y J; Estes, M K
Volume of serial or monograph	68
Page or page range of portion	5945-5952
Title of the article/chapter the portion is from	Characterization of virus-like particles produced by the expression of rotavirus capsid proteins in insect cells.
Author of portion(s)	Crawford, S E; LabbÃ©, M; Cohen, J; Burroughs, M H; Zhou, Y J; Estes, M K
Issue, if republishing an article from a serial	9
Publication date of portion	1994-09-01

AMERICAN SOCIETY FOR MICROBIOLOGY – JOURNALS LICENSE TERMS AND CONDITIONS

Order Date	14-Jul-2022
Order License ID	1247371-1
ISSN	1098-5514
Type of Use	Republish in a thesis/dissertation
Publisher	AMERICAN SOCIETY FOR MICROBIOLOGY
Portion	Image/photo/illustration
Licensed Content	
Publication Title	Journal of virology: JVI
Article Title	Expression of rotavirus VP2 produces empty corelike particles.
Author/Editor	American Society for Microbiology
Date	01/01/1971
Language	English
Country	United States of America
Rights holder	American Society for Microbiology - Journals
Publication Type	e-Journal
Start Page	2946
End Page	2952
Issue	6
Volume	65
URL	https://journals.asm.org/journal/jvi
Request Details	
Portion Type	Image/photo/illustration
Number of images / photos / illustrations	1
Format (select all that apply)	Print, Electronic
Who will republish the content?	Academic institution
Duration of Use	Life of current edition
Lifetime Unit Quantity	Up to 499
Rights Requested	Main product
Distribution	Worldwide
Translation	Original language of publication
Copies for the disabled?	No
Minor editing privileges?	No
Incidental promotional use?	No
Currency	USD
New Work Details	
Title	Investigating the feasibility of generating chimeric intergroup rotavirus triple-layered virus-like particles on SA11 double-layered particles
Instructor name	Prof. A.A. van Dijk
Institution name	North-West University
Expected presentation date	2022-11-01

Additional Details	
Order reference number	N/A
The requesting person / organization to appear on the license	Pierre le Roux
Reuse Content Details	
Title, description or numeric reference of the portion(s)	FIG. 8. Empty single-shelled particles formed by coexpression of heterologous VP2 and VP6.
Editor of portion(s)	LabbÃ©, M; Charpilienne, A; Crawford, S E; Estes, M K; Cohen, J
Volume of serial or monograph	65
Page or page range of portion	2946-2952
Title of the article/chapter the portion is from	Expression of rotavirus VP2 produces empty corelike particles.
Author of portion(s)	LabbÃ©, M; Charpilienne, A; Crawford, S E; Estes, M K; Cohen, J
Issue, if republishing an article from a serial	6
Publication date of portion	1991-06-01

AMERICAN SOCIETY FOR MICROBIOLOGY – JOURNALS LICENSE TERMS AND CONDITIONS

Order Date	20-Jul-2022
Order License ID	1249316-1
ISSN	0022-538X
Type of Use	Republish in a thesis/dissertation
Publisher	AMERICAN SOCIETY FOR MICROBIOLOGY
Portion	Chart/graph/table/figure
Licensed Content	
Publication Title	Journal of virology
Article Title	Full genome-based classification of rotaviruses reveals a common origin between human Wa-Like and porcine rotavirus strains and human DS-1-like and bovine rotavirus strains.
Author/Editor	AMERICAN SOCIETY FOR MICROBIOLOGY
Date	01/01/1967
Language	English
Country	United States of America
Rightsholder	American Society for Microbiology - Journals
Publication Type	Journal
Start Page	3204
End Page	3219
Issue	7
Volume	82
URL	https://journals.asm.org/journal/jvi
Request Details	
Portion Type	Chart/graph/table/figure
Number of charts / graphs / tables / figures requested	1
Format (select all that apply)	Print, Electronic
Who will republish the content?	Academic institution
Duration of Use	Life of current edition
Lifetime Unit Quantity	Up to 499
Rights Requested	Main product
Distribution	Worldwide
Translation	Original language of publication
Copies for the disabled?	No
Minor editing privileges?	No
Incidental promotional use?	No
Currency	USD
New Work Details	
Title	Investigating the feasibility of generating chimeric intergroup rotavirus triple-layered virus-like particles on SA11 double-layered particles
Instructor name	Prof. Albie van Djik
Institution name	North-West University

Expected presentation date	2022-11-01
Additional Details	
Order reference number	N/A
The requesting person / organization to appear on the license	Pierre le Roux
Reuse Content Details	
Title, description or numeric reference of the portion(s)	"TABLE 2: Application of the proposed classification and nomenclature to the structural and nonstructural" on page 3215.
Editor of portion(s)	Matthijnssens, Jelle; Ciarlet, Max; Heiman, Erica; Arijs, Ingrid; Delbeke, Thomas; McDonald, Sarah M.; Palombo, Enzo A.; Iturriza-Gómara, Miren; Maes, Piet; Patton, John T.; Rahman, Mustafizur; Van Ranst, Marc
Volume of serial or monograph	82
Page or page range of portion	3204-3219
Title of the article/chapter the portion is from	Full genome-based classification of rotaviruses reveals a common origin between human Wa-Like and porcine rotavirus strains and human DS-1-like and bovine rotavirus strains.
Author of portion(s)	Matthijnssens, Jelle; Ciarlet, Max; Heiman, Erica; Arijs, Ingrid; Delbeke, Thomas; McDonald, Sarah M.; Palombo, Enzo A.; Iturriza-Gómara, Miren; Maes, Piet; Patton, John T.; Rahman, Mustafizur; Van Ranst, Marc
Issue, if republishing an article from a serial	7
Publication date of portion	2008-04-01

AMERICAN SOCIETY FOR MICROBIOLOGY – JOURNALS LICENSE TERMS AND CONDITIONS

Order Date	26-Jul-2022
Order License ID	1251312-1
ISSN	0022-538X
Type of Use	Republish in a thesis/dissertation
Publisher	AMERICAN SOCIETY FOR MICROBIOLOGY
Portion	Image/photo/illustration
Licensed Content	
Publication Title	Journal of virology
Article Title	Cross-linking of rotavirus outer capsid protein VP7 by antibodies or disulfides inhibits viral entry.
Author/Editor	AMERICAN SOCIETY FOR MICROBIOLOGY
Date	01/01/1967
Language	English
Country	United States of America
Rightsholder	American Society for Microbiology - Journals
Publication Type	Journal
Start Page	10509
End Page	10517
Issue	20
Volume	85
URL	https://journals.asm.org/journal/jvi
Request Details	
Portion Type	Image/photo/illustration
Number of images / photos / illustrations	2
Format (select all that apply)	Print, Electronic
Who will republish the content?	Academic institution
Duration of Use	Life of current edition
Lifetime Unit Quantity	Up to 499
Rights Requested	Main product
Distribution	Worldwide
Translation	Original language of publication
Copies for the disabled?	No
Minor editing privileges?	No
Incidental promotional use?	No
Currency	USD
New Work Details	
Title	Investigating the feasibility of generating chimeric intergroup rotavirus triple-layered virus-like

	particles on SA11 double-layered particles
Instructor name	Prof. A.A. van Djik
Institution name	North-West University
Expected presentation date	2022-11-01
Additional Details	
Order reference number	N/A
The requesting person / organization to appear on the license	Pierre le Roux
Reuse Content Details	
Title, description or numeric reference of the portion(s)	Fig. 1. Structure of rhesus rotavirus VP7" on page 6 and "Fig. 4. Positions of neutralization escape mutations selected by various monoclonal antibodies" on page 9.
Editor of portion(s)	Aoki, Scott T.; Trask, Shane D.; Coulson, Barbara S.; Greenberg, Harry B.; Dormitzer, Philip R.; Harrison, Stephen C.
Volume of serial or monograph	85
Page or page range of portion	10509-10517
Title of the article/chapter the portion is from	Cross-linking of rotavirus outer capsid protein VP7 by antibodies or disulfides inhibits viral entry.
Author of portion(s)	Aoki, Scott T.; Trask, Shane D.; Coulson, Barbara S.; Greenberg, Harry B.; Dormitzer, Philip R.; Harrison, Stephen C.
Issue, if republishing an article from a serial	20
Publication date of portion	2011-10-15

JOHN WILEY AND SONS LICENSE

TERMS AND CONDITIONS

This Agreement between Mr. Pierre Le Roux ("You") and John Wiley and Sons ("John Wiley and Sons") consists of your license details and the terms and conditions provided by John Wiley and Sons and Copyright Clearance Center.

License Number	5370070927694
License date	Aug 15, 2022
Licensed Content Publisher	John Wiley and Sons
Licensed Content Publication	Biotechnology & Bioengineering
Licensed Content Title	Impact of physicochemical parameters on in vitro assembly and disassembly kinetics of recombinant triple-layered rotavirus-like particles
Licensed Content Author	Paula M. Alves, Laura A. Palomares, Manuel J.T. Carrondo, et al
Licensed Content Date	Jul 21, 2009
Licensed Content Volume	104
Licensed Content Issue	4
Licensed Content Pages	13
Type of use	Dissertation/Thesis
Requestor type	University/Academic
Format	Print and electronic
Portion	Figure/table
Number of figures/tables	1
Will you be translating?	No
Title	Investigating the feasibility of generating chimeric intergroup rotavirus triple-layered virus-like particles on SA11 double-layered particles.
Institution name	North-West University
Expected presentation date	Dec 2022
Portions	"Fig. 1: Schematic representation of TLP 2/6/7 (A) disassembly, (B) reassembly" on page 677.
Requestor Location	Mr. Pierre Le Roux Building F3, Room 211 North-West University 11 Hoffman St Potchefstroom, North-West Province 2531 South Africa Attn: Mr. Pierre Le Roux
Publisher Tax ID	EU826007151
Total	0.00 USD

Reference list:

Adams, W.R. & Kraft, L.M. 1967. Electron-microscopic study of the intestinal epithelium of mice infected with the agent of epizootic diarrhea of infant mice (EDIM Virus). *American Journal of Pathology*, 51(1):39-60.

Alam, M., Kobayashi, N., Ishino, M., Ahmed, M., Ahmed, M., Paul, S., ... Naik, T. 2007. Genetic analysis of an ADRV-N-like novel rotavirus strain B219 detected in a sporadic case of adult diarrhea in Bangladesh. *Archives of Virology*, 152(1):199-208.

Alloway, J. 1932. The transformation in vitro of R pneumococci into S forms of different specific types by the use of filtered pneumococcus extracts. *The Journal of Experimental Medicine*, 55:91-99.

Almeida, J.D., Hall, T., Banatvala, J.E., Totterdell, B.M. & Chrystie, I.L. 1978. The Effect of trypsin on the growth of rotavirus. *Journal of General Virology*, 40(1):213-218.

Altenburg, B.C., Graham, D.Y. & Estes, M.K. 1980. Ultrastructural study of rotavirus replication in cultured cells. *Journal of General Virology*, 46(1):75-85.

Aoki, S.T., Settembre, E.C., Trask, S.D., Greenberg, H.B., Harrison, S.C. & Dormitzer, P.R. 2009. Structure of rotavirus outer-layer protein VP7 bound with a neutralizing fab. *Science*, 324(5933):1444-1447.

Aoki, S.T., Trask, S.D., Coulson, B.S., Greenberg, H.B., Dormitzer, P.R. & Harrison, S.C. 2011. Cross-linking of rotavirus outer capsid protein VP7 by antibodies or disulfides inhibits viral entry. *Journal of Virology*, 85(20):10509-10517.

Attoui, H., Becnel, J., Belaganahalli, S., Bergoin, M., Brussaard, C.P., Chappell, J.D., ... Zhou, H. 2012. Family - Reoviridae. In: King, A.M.Q., Adams, M.J., Carstens, E.B. & Lefkowitz, E.J., eds*. Virus Taxonomy*. San Diego: Elsevier. pp. 541-637.

Au, K.S., Chan, W.K., Burns, J.W. & Estes, M.K. 1989. Receptor activity of rotavirus nonstructural glycoprotein NS28. *Journal of Virology*, 63(11):4553-4562.

Bányai, K., Kemenesi, G., Budinski, I., Földes, F., Zana, B., Marton, S., ... Jakab, F. 2017. Candidate new rotavirus species in Schreiber's bats, Serbia. *Infection, Genetics and Evolution*, 48:19-26.

Bekker, S., Huismans, H. & van Staden, V. 2022. Generation of a soluble African horse sickness virus vp7 protein capable of forming core-like particles. *Viruses*, 14(1624):1-22.

Belyaev, A.S., Hails, R.S. & Roy, P. 1995. High-level expression of five foreign genes by a single recombinant baculovirus. *Gene*, 156(2):229-233.

Berger, I., Fitzgerald, D.J. & Richmond, T.J. 2004. Baculovirus expression system for heterologous multiprotein complexes. *Nature Biotechnology*, 22(12):1583-1587.

Bertolotti-Ciarlet, A., Ciarlet, M., Crawford, S.E., Conner, M.E. & Estes, M.K. 2003. Immunogenicity and protective efficacy of rotavirus 2/6-virus-like particles produced by a dual baculovirus expression vector and administered intramuscularly, intranasally, or orally to mice. *Vaccine*, 21(25):3885-3900.

Bhan, M.K., Lew, J.F., Sazawal, S., Das, B.K., Gentsch, J.R. & Glass, R.I. 1993. Protection conferred by neonatal rotavirus infection against subsequent rotavirus diarrhea. *The Journal of Infectious Diseases*, 168(2):282-287.

Bhandari, N., Rongsen-Chandola, T., Bavdekar, A., John, J., Antony, K., Taneja, S., ... Bhan, M.K. 2014. Efficacy of a monovalent human-bovine (116E) rotavirus vaccine in Indian infants: a randomised, double-blind, placebo-controlled trial. *The Lancet*, 383(9935):2136-2143.

Bican, P., Cohen, J., Charpilienne, A. & Scherrer, R. 1982. Purification and characterization of bovine rotavirus cores. *Journal of Virology*, 43(3):1113-1117.

Birnboim, H.C. & Doly, J. 1979. A rapid alkaline extraction procedure for screening recombinant plasmid DNA. *Nucleic Acids Research*, 7(6):1513-1523.
Bishop, R., Davidson, G.P., Holmes, I.H. & Ruck, B.J. 1973. Virus particles in epithelial cells of duodenal mucosa from children with acute non-bacterial gastroenteritis. *The Lancet*, 302(7841):1281-1283.
Bishop, S. 2016. *Recovery of an African horsesickness virus VP2 chimera using reverse genetics.* North-West University (South Africa), Potchefstroom Campus: North-West University.
Blazevic, V., Malm, M., Arinobu, D., Lappalainen, S. & Vesikari, T. 2016. Rotavirus capsid VP6 protein acts as an adjuvant in vivo for norovirus virus-like particles in a combination vaccine. *Human Vaccines & Immunotherapeutics*, 12(3):740-748.
Bridger, J. 1980. Detection by electron microscopy of caliciviruses, astroviruses and rotavirus-like particles in the faeces of piglets with diarrhea. *Veterinary Record*, 107:532-533.
Brunet, J.P., Cotte-Laffitte, J., Linxe, C., Quero, A.M., Geniteau-Legendre, M. & Servin, A. 2000. Rotavirus infection induces an increase in intracellular calcium concentration in human intestinal epithelial cells: role in microvillar actin alteration. *Journal of Virology*, 74(5):2323-2332.
Brussow, H., Bruttin, A. & Marc-Martin, S. 1990. Polypeptide composition of rotavirus empty capsids and their possible use as a subunit vaccine. *Journal of Virology*, 64(8):3635-3642.
Bryden, A., Thouless, M. & Flewett, T. 1976. A rabbit rotavirus. *Vet. Rec*, 99:323.
Buchs, M., Kim, E., Pouliquen, Y., Sachs, M., Geisse, S., Mahnke, M. & Hunt, I. 2009. High-throughput insect cell protein expression applications. In: Doyle, S.A., ed. *High Throughput Protein Expression and Purification: Methods and Protocols*. Totowa, NJ: Humana Press. pp. 199-227.
Burnett, E., Parashar, U.D. & Tate, J.E. 2020. Real-world effectiveness of rotavirus vaccines, 2006–19: a literature review and meta-analysis. *The Lancet Global Health*, 8(9):1195-1202.
Burnette, W.N. 1981. “Western blotting”: electrophoretic transfer of proteins from sodium dodecyl sulfate-polyacrylamide gels to unmodified nitrocellulose and radiographic detection with antibody and radioiodinated protein A. *Analytical biochemistry*, 112(2):195-203.
Burns, J.W., Siadat-Pajouh, M., Krishnaney, A.A. & Greenberg, H.B. 1996. Protective effect of rotavirus VP6-specific IgA monoclonal antibodies that lack neutralizing activity. *Science*, 272(5258):104-107.
Burstone, M.S. 1960. Histochemical demonstration of cytochrome oxidase with new amine reagents. *Journal of Histochemistry & Cytochemistry*, 8(1):63-70.
Charlton Hume, H.K., Vidigal, J., Carrondo, M.J.T., Middelberg, A.P.J., Roldão, A. & Lua, L.H.L. 2019. Synthetic biology for bioengineering virus-like particle vaccines. *Biotechnology and Bioengineering*, 116(4):919-935.
Chasey, D. 1980. Investigation of Immunoperoxidase-labelled Rotavirus in Tissue Culture by Light and Electron Microscopy. 50(1):195-200.
Chen, G.-M., Hung, T., Bridger, J.C. & McCrae, M.A. 1985. Chinese adult rotavirus is a group B rotavirus. *The Lancet*, 326(8464):1123-1124.
Christy, C., Offit, P., Clark, H.F. & Treanar, J. 1993. Evaluation of a bovine-human rotavirus reassortant vaccine in infants. *Journal of Infectious Diseases*, 168(6):1598-1599.

Chung, C.T., Niemela, S.L. & Miller, R.H. 1989. One-step preparation of competent Escherichia coli: transformation and storage of bacterial cells in the same solution. *Proceedings of the National Academy of Sciences*, 86(7):2172-2175.
Ciarlet, M., Crawford, S.E., Barone, C., Bertolotti-Ciarlet, A., Ramig, R.F., Estes, M.K. & Conner, M.E. 1998. Subunit rotavirus vaccine administered parenterally to rabbits induces active protective immunity. *Journal of virology*, 72(11):9233-9246.
Ciccarone, V.C., Polayes, D.A. & Luckow, V.A. 1998. Generation of recombinant baculovirus DNA in E.coli using a baculovirus shuttle vector. In: Reischl, U., ed. *Molecular Diagnosis of Infectious Diseases*. Totowa, NJ: Humana Press. pp. 213-235.
Clark, A., van Zandvoort, K., Flasche, S., Sanderson, C., Bines, J., Tate, J., ... Jit, M. 2019. Efficacy of live oral rotavirus vaccines by duration of follow-up: a meta-regression of randomised controlled trials. *The Lancet Infectious Diseases*, 19(7):717-727.
Clarke, E. & Desselberger, U. 2015. Correlates of protection against human rotavirus disease and the factors influencing protection in low-income settings. *Mucosal immunology*, 8(1):1-17.
Cohen, J., Laporte, J., Charpilienne, A. & Scherrer, R. 1979. Activation of rotavirus RNA polymerase by calcium chelation. *Archives of Virology*, 60(3):177-186.
Cortes-Perez, N.G., Sapin, C., Jaffrelo, L., Daou, S., Grill, J.P., Langella, P., ... Trugnan, G. 2010. Rotavirus-like particles: a novel nanocarrier for the gut. *Journal of Biomedicine and Biotechnology*, 2010:1-10.
Crawford, S.E., Labbé, M., Cohen, J., Burroughs, M.H., Zhou, Y.J. & Estes, M.K. 1994. Characterization of virus-like particles produced by the expression of rotavirus capsid proteins in insect cells. *Journal of Virology*, 68(9):5945-5952.
Crawford, S.E., Estes, M.K., Ciarlet, M., Barone, C., O'Neal, C.M., Cohen, J. & Conner, M.E. 1999. Heterotypic protection and induction of a broad heterotypic neutralization response by rotavirus-like particles. *Journal of Virology*, 73(6):4813-4822.
Crawford, S.E., Mukherjee, S.K., Estes, M.K., Lawton, J.A., Shaw, A.L., Ramig, R.F. & Prasad, B.V. 2001. Trypsin cleavage stabilizes the rotavirus VP4 spike. *Journal of Virology* , 75(13):6052-6061.
Crouse, J. & Amorese, D. 1987. Ethanol precipitation: ammonium acetate as an alternative to sodium acetate. *Focus*, 9:3-5.
Davis, B.J. 1964. Disc electrophoresis. II. Method and application to human serum proteins. *Annals of the New York Academy of Sciences Journal*, 121(2):404-427.
Desselberger, U. 2014. Rotaviruses. *Virus Research*, 190:75-96.
Desselberger, U. 2017. Differences of rotavirus vaccine effectiveness by country: likely causes and contributing factors. *Pathogens*, 6(4):65.
Dhama, K., Chauhan, R.S., Mahendran, M. & Malik, S.V.S. 2009. Rotavirus diarrhea in bovines and other domestic animals. *Veterinary Research Communications*, 33(1):1-23.
Dormitzer, P.R., Nason, E.B., Venkataram Prasad, B.V. & Harrison, S.C. 2004. Structural rearrangements in the membrane penetration protein of a non-enveloped virus. *Nature*, 430(7003):1053-1058.
El-Attar, L., Oliver, S.L., Mackie, A., Charpilienne, A., Poncet, D., Cohen, J. & Bridger, J.C. 2009. Comparison of the efficacy of rotavirus VLP vaccines to a live homologous rotavirus vaccine in a pig model of rotavirus disease. *Vaccine*, 27(24):3201-3208.
Elliott, W. 1963. The effects of antimicrobial agents on deoxyribonucleic acid polymerase. *Biochemical Journal*, 86(3):562-567.

Espejo, R.T., López, S. & Arias, C. 1981. Structural polypeptides of simian rotavirus SA11 and the effect of trypsin. *Journal of Virology*, 37(1):156-160.
Estes, M.K., Graham, D.Y. & Mason, B.B. 1981. Proteolytic enhancement of rotavirus infectivity: molecular mechanisms. *Journal of Virology*, 39(3):879-888.
Estes, M.K., Mason, B.B. & Cohen, J. 1984. Cloning and nucleotide sequence of the simian rotavirus gene 6 that codes for the major inner capsid protein. *Nucleic Acids Research*, 12(4):1875-1887.
Estes, M.K., Graham, D.Y., Ramig, R.F. & Ericson, B.L. 1982. Heterogeneity in the structural glycoprotein (VP7) of simian rotavirus SA11. *Virology*, 122(1):8-14.
Ferrari, E., Salogni, C., Martella, V., Alborali, G.L., Scaburri, A. & Boniotti, M.B. 2022. Assessing the epidemiology of rotavirus A, B, C and H in diarrheic pigs of different ages in northern Italy. *Pathogens*, 11(4):467.
Fields, B.N., Knipe, D.M. & Howley, P.M. 1996. *Fields virology*. Lippincott-Raven.
Flewett, T.H., Bryden, A.S. & Davies, H. 1975. Letter: Virus diarrhoea in foals and other animals. *The Veterinary Record*, 96(21).
Flewett, T.H., Bryden, A.S., Davies, H., Woode, G.N., Bridger, J.C. & Derrick, J.M. 1974. Relation between viruses from acute gastroenteritis of children and newborn calves. *Lancet*, 2(7872):61-63.
Flores, J., Perez, I., White, L., Perez, M., Kalica, A.R., Marquina, R., ... Chanock, R.M. 1982. Genetic Relatedness among human rotaviruses as determined by RNA hybridization. *Infection and Immunity*, 37(2):648-655.
Fuenmayor, J., Gòdia, F. & Cervera, L. 2017. Production of virus-like particles for vaccines. *New Biotechnology*, 39:174-180.
Gallagher, S.R. & Desjardins, P.R. 2006. Quantitation of DNA and RNA with absorption and fluorescence spectroscopy. *Current Protocols in Molecular Biology*, 76(1):A.3D.1-A.3D.21.
Gardet, A.S., Breton, M., Fontanges, P., Trugnan, G. & Chwetzoff, S. 2006. Rotavirus spike protein VP4 binds to and remodels actin bundles of the epithelial brush border into actin bodies. *Journal of Virology*, 80(8):3947-3956.
Gentsch, J.R., Glass, R.I., Woods, P., Gouvea, V., Gorziglia, M., Flores, J., ... Bhan, M.K. 1992. Identification of group A rotavirus gene 4 types by polymerase chain reaction. *Journal of Clinical Microbiology*, 30(6):1365-1373.
Ginn, D.I., Ward, R.L., Hamparian, V.V. & Hughes, J.H. 1992. Inhibition of rotavirus in vitro transcription by optimal concentrations of monoclonal antibodies specific for rotavirus VP6. *Journal of General Virology*, 73(11):3017-3022.
Glasel, J. 1995. Validity of nucleic acid purities monitored by 260nm/280nm absorbance ratios. *Biotechniques*, 18(1):62-3.
Gouvea, V., Glass, R.I., Woods, P., Taniguchi, K., Clark, H.F., Forrester, B. & Fang, Z.Y. 1990. Polymerase chain reaction amplification and typing of rotavirus nucleic acid from stool specimens. *Journal of Clinical Microbiology*, 28(2):276-282.
Graham, D.Y. & Estes, M.K. 1985. Proposed working serologic classification system for rotaviruses. *Annales de l'Institut Pasteur / Virologie*, 136(1):5-12.
Graham, R.C., Lundholm, U. & Karnovsky, M.J. 1965. Cytochemical demonstration of peroxidase activity with 3-amino-9-ethylcarbazole. *Journal of Histochemistry & Cytochemistry*, 13(2):150-152.
Gray, J. & Desselberger, U. 2000. *Rotaviruses: methods and protocols*. Springer Science & Business Media.
Green, M.R. & Sambrook, J. 2016. Precipitation of DNA with Ethanol. *Cold Spring Harbor Protocols*, 2016(12).

Greenberg, H.B. & Estes, M.K. 2009. Rotaviruses: From Pathogenesis to Vaccination. *Gastroenterology*, 136(6):1939-1951.
Hanahan, D. 1983. Studies on transformation of Escherichia coli with plasmids. *Journal of Molecular Biology*, 166(4):557-580.
Hawtin, R.E., Zarkowska, T., Arnold, K., Thomas, C.J., Gooday, G.W., King, L.A., ... Possee, R.D. 1997. Liquefaction of autographa californica nucleopolyhedrovirus-infected insects is dependent on the integrity of virus-encoded chitinase and cathepsin genes. *Virology*, 238(2):243-253.
Heaton, P.M., Goveia, M.G., Miller, J.M., Offit, P. & Clark, H.F. 2005. Development of a pentavalent rotavirus vaccine against prevalent serotypes of rotavirus gastroenteritis. *The Journal of Infectious Diseases*, 192(Supplement_1):S17-S21.
Heinimäki, S., Hankaniemi, M.M., Sioofy-Khojine, A.-B., Laitinen, O.H., Hyöty, H., Hytönen, V.P., ... Blazevic, V. 2019. Combination of three virus-derived nanoparticles as a vaccine against enteric pathogens; enterovirus, norovirus and rotavirus. *Vaccine*, 37(51):7509-7518.
Henschke, N., Bergman, H., Hungerford, D., Cunliffe, N.A., Grais, R.F., Kang, G., ... Neuzil, K.M. 2022. The efficacy and safety of rotavirus vaccines in countries in Africa and Asia with high child mortality. *Vaccine*, 40(12):1707-1711.
Hia, F. & Takeuchi, O. 2021. The effects of codon bias and optimality on mRNA and protein regulation. *Cellular and Molecular Life Sciences*, 78(5):1909-1928.
Holland, R.E. 1990. Some infectious causes of diarrhea in young farm animals. *Clinical Microbiology Reviews*, 3(4):345-375.
Holmes, I.H., RUCK, B.J., BISHOP, R.F. & DAVIDSON, G.P. 1975. Infantile enteritis viruses: morphogenesis and morphology. *Journal of virology*, 16(4):937-943.
Horwitz, J.P., Chua, J., Curby, R.J., Tomson, A.J., Da Rooge, M.A., Fisher, B.E., ... Klundt, I. 1964. Substrates for cytochemical demonstration of enzyme activity. i. some substituted 3-indolyl-β-d-glycopyranosides. *Journal of Medicinal Chemistry*, 7(4):574-575.
Hu, L., Ramani, S., Czako, R., Sankaran, B., Yu, Y., Smith, D.F., ... Venkataram Prasad, B.V. 2015. Structural basis of glycan specificity in neonate-specific bovine-human reassortant rotavirus. *Nature Communications*, 6(1):8346.
Hyser, J.M., Collinson-Pautz, M.R., Utama, B. & Estes, M.K. 2010. Rotavirus disrupts calcium homeostasis by NSP4 Viroporin activity. *American Society for Microbiology*, 1(5):210-265.
Hyser, J.M., Utama, B., Crawford, S.E. & Estes, M.K. 2012. Genetic divergence of rotavirus nonstructural protein 4 results in distinct serogroup-specific viroporin activity and intracellular punctate structure morphologies. *Journal of Virology*, 86(9):4921-4934.
Hyser, J.M., Utama, B., Crawford, S.E., Broughman, J.R. & Estes, M.K. 2013. Activation of the endoplasmic reticulum calcium sensor stim1 and store-operated calcium entry by rotavirus requires NSP4 viroporin activity. *Journal of Virology,* 87(24):13579-13588.
Isanaka, S., Langendorf, C., McNeal, M.M., Meyer, N., Plikaytis, B., Garba, S., ... Makarimi, R. 2021. Rotavirus vaccine efficacy up to 2 years of age and against diverse circulating rotavirus strains in Niger: Extended follow-up of a randomized controlled trial. *PLoS Medicine*, 18(7):e1003655.
Ish-Horowicz, D. & Burke, J.F. 1981. Rapid and efficient cosmid cloning. *Nucleic Acids Research*, 9(13):2989-2998.

Istrate, C., Hinkula, J., Charpilienne, A., Poncet, D., Cohen, J., Svensson, L. & Johansen, K. 2008. Parenteral administration of RF 8-2/6/7 rotavirus-like particles in a one-dose regimen induce protective immunity in mice. *Vaccine*, 26(35):4594-4601.

Iturriza-Gomara, M., Green, J., Brown, D.W.G., Desselberger, U. & Gray, J.J. 1999. Comparison of specific and random priming in the reverse transcriptase polymerase chain reaction for genotyping group A rotaviruses. *Journal of Virological Methods*, 78(1-2):93-103.

Iturriza-Gómara, M., Kang, G. & Gray, J. 2004. Rotavirus genotyping: keeping up with an evolving population of human rotaviruses. *Journal of Clinical Virology*, 31(4):259-265.

Jamur, M.C. & Oliver, C. 2010a. Permeabilization of cell membranes. *Methods in Molecular Biology*, 588:63-66.

Jamur, M.C. & Oliver, C. 2010b. Cell Fixatives for Immunostaining. In: Oliver, C. & Jamur, M.C., eds*. Immunocytochemical Methods and Protocols*. Totowa, NJ: Humana Press. pp. 55-61.

Jansen van Vuren, P. 2006. *Development of a recombinant antigen for the detection of antibodies against rift valley fever virus in humans and animals.* North-West University. (Dissertation).

Jason, Kinkela, Abebe, A., Enweronu-Laryea, C., Amina, I., McHomvu, J., ... A. 2010. Burden and epidemiology of rotavirus diarrhea in selected african countries: preliminary results from the African rotavirus surveillance network. *The Journal of Infectious Diseases*, 202(S1):S5-S11.

Jere, K.C. 2012. *Whole genome characterisation and engineering of chimaeric rotavirus–like particles using African rotavirus field strains.* North-West University.

Jere, K.C., O'Neill, H.G., Potgieter, A.C. & Van Dijk, A.A. 2014. Chimaeric virus-like particles derived from consensus genome sequences of human rotavirus strains co-circulating in Africa. *PLoS ONE*, 9(9):e105167.

Jere, K.C., Mlera, L., O'Neill, H.G., Potgieter, A.C., Page, N.A., Seheri, M.L. & Van Dijk, A.A. 2011. Whole genome analyses of African G2, G8, G9, and G12 rotavirus strains using sequence-independent amplification and 454® pyrosequencing. *Journal of Medical Virology,* 83(11):2018-2042.

Jiang, B., Barniak, V., Smith, R.P., Sharma, R., Corsaro, B., Hu, B. & Madore, H.P. 1998. Synthesis of rotavirus-like particles in insect cells: Comparative and quantitative analysis. *Biotechnology and Bioengineering*, 60(3):369-374.

Jiang, B., Estes, M., Barone, C., Barniak, V., O'Neal, C., Ottaiano, A., ... Conner, M. 1999. Heterotypic protection from rotavirus infection in mice vaccinated with virus-like particles. *Vaccine*, 17:1005-1013.

Jonesteller, C.L., Burnett, E., Yen, C., Tate, J.E. & Parashar, U.D. 2017. Effectiveness of rotavirus vaccination: A systematic review of the first decade of global postlicensure data, 2006–2016. *Clinical Infectious Diseases*, 65(5):840-850.

Kaba, S.A., Salcedo, A.M., Wafula, P.O., Vlak, J.M. & Van Oers, M.M. 2004. Development of a chitinase and v-cathepsin negative bacmid for improved integrity of secreted recombinant proteins. *Journal of Virological Methods*, 122(1):113-118.

Kaminjolo, J.S. & Adesiyun, A.A. 1994. Rotavirus infection in calves, piglets, lambs and goat kids in trinidad. *British Veterinary Journal*, 150(3):293-299.

Kim, I.S., Trask, S.D., Babyonyshev, M., Dormitzer, P.R. & Harrison, S.C. 2010. Effect of mutations in VP5* hydrophobic loops on rotavirus cell entry. *Journal of Virology,* 84(12):6200-6207.

Kim, Y., Chang, K.O., Kim, W.Y. & Saif, L.J. 2002. Production of hybrid double- or triple-layered virus-like particles of group A and C rotaviruses using a baculovirus expression system. *Virology*, 302(1):1-8.
Koretz, K., Leman, J., Brandt, I. & Möller, P. 1987. Metachromasia of 3-amino-9-ethylcarbazole (AEC) and its prevention in immunoperoxidase techniques. *Histochemistry*, 86(5):471-478.
Kumar, B., Hawkins, G.M., Kicmal, T., Qing, E., Timm, E. & Gallagher, T. 2021. Assembly and entry of severe acute respiratory syndrome coronavirus 2 (SARS-CoV2): evaluation using virus-like particles. *Cells*, 10(4):853.
Kurokawa, N., Lavoie, P.-O., D'aoust, M.-A., Couture, M.M.-J., Dargis, M., Trépanier, S., ... Tsutsui, N. 2021. Development and characterization of a plant-derived rotavirus-like particle vaccine. *Vaccine*, 39(35):4979-4987.
Labbé, M., Charpilienne, A., Crawford, S.E., Estes, M.K. & Cohen, J. 1991. Expression of rotavirus VP2 produces empty corelike particles. *Journal of Virology*, 65(6):2946-2952.
Laemmli, U.K. 1970. Cleavage of Structural Proteins during the Assembly of the Head of Bacteriophage T4. *Nature*, 227(5259):680-685.
Laimbacher, A.S., Esteban, L.E., Castello, A.A., Abdusetir Cerfoglio, J.C., Argüelles, M.H., Glikmann, G., ... Fraefel, C. 2012. HSV-1 amplicon vectors launch the production of heterologous rotavirus-like particles and induce rotavirus-specific immune responses in mice. *Molecular Therapy*, 20(9):1810-1820.
Lecatsas, G. 1972. Electron microscopic and serological studies on simian virus S.A. 11 and the "related" O agent. *Onderstepoort Journal of Veterinary Research*, 39(3):133-137.
Lecce, J.G., King, M.W. & Mock, R. 1976. Reovirus-like agent associated with fatal diarrhea in neonatal pigs. *Infection and Immunity*, 14(3):816-825.
Lepault, J., Petitpas, I., Erk, I., Navaza, J., Bigot, D., Dona, M., ... Rey, F.A. 2001. Structural polymorphism of the major capsid protein of rotavirus. *The EMBO Journal*, 20(7):1498-1507.
LePecq, J.B. & Paoletti, C. 1967. A fluorescent complex between ethidium bromide and nucleic acids. Physical-chemical characterization. *Journal of Molecular Biology,* 27(1):87-106.
Li, Z., Michael, I.P., Zhou, D., Nagy, A. & Rini, J.M. 2013. Simple piggyBac transposon-based mammalian cell expression system for inducible protein production. *Proceedings of the National Academy of Sciences*, 110(13):5004-5009.
Lu, X., McDonald, S.M., Tortorici, M.A., Tao, Y.J., Vasquez-Del Carpio, R., Nibert, M.L., ... Harrison, S.C. 2008. Mechanism for coordinated RNA packaging and genome replication by rotavirus polymerase VP1. *Structure*, 16(11):1678-1688.
Luckow, V.A., Lee, S.C., Barry, G.F. & Olins, P.O. 1993. Efficient generation of infectious recombinant baculoviruses by site-specific transposon-mediated insertion of foreign genes into a baculovirus genome propagated in Escherichia coli. *Journal of Virology*, 67(8):4566-4579.
Ludert, J.E., Ruiz, M.C., Hidalgo, C. & Liprandi, F. 2002. Antibodies to rotavirus outer capsid glycoprotein VP7 neutralize infectivity by inhibiting virion decapsidation. *Journal of Virology*, 76(13):6643-6651.
Maass, D.R. & Atkinson, P.H. 1990. Rotavirus proteins VP7, NS28, and VP4 form oligomeric structures. *Journal of Virology*, 64(6):2632-2641.
Madore, H.P., Estes, M.K., Zarley, C.D., Hu, B., Parsons, S., Digravio, D., ... Conner, M.E. 1999. Biochemical and immunologic comparison of virus-like particles for a rotavirus subunit vaccine. *Vaccine*, 17(19):2461-2471.

Malherbe, H.H. & Strickland-Cholmley, M. 1967. Simian virus SA11 and the related 0 agent. *Archiv Für die Gesamte Virusforschung*, 22(1):235-245.
Malik, S.V.S., Kumar, A. & Bhilegaonkar, K. 1996. Rotavirus an emerging enteropathogen of man and animals: an overview. *The Journal of Communicable Diseases*, 27:199-207.
Malm, M., Heinimäki, S., Vesikari, T. & Blazevic, V. 2017. Rotavirus capsid VP6 tubular and spherical nanostructures act as local adjuvants when co-delivered with norovirus VLPs. *Clinical and Experimental Immunology*, 189(3):331-341.
Mandel, M. & Higa, A. 1970. Calcium-dependent bacteriophage DNA infection. *Journal of Molecular Biology*, 53(1):159-162.
Martin, S., Lorrot, M., El Azher, M.A. & Vasseur, M. 2002. Ionic strength- and temperature-induced K Ca shifts in the uncoating reaction of rotavirus strains RF and SA11: Correlation with Membrane Permeabilization. *Journal of Virology*, 76(2):552-559.
Mason, B.B., Graham, D.Y. & Estes, M.K. 1980. In vitro transcription and translation of simian rotavirus SA11 gene products. *Journal of virology*, 33(3):1111-1121.
Mathieu, M. 2001. Atomic structure of the major capsid protein of rotavirus: implications for the architecture of the virion. *The EMBO Journal*, 20(7):1485-1497.
Matson, D.O. 2006. The Pentavalent Rotavirus Vaccine, RotaTeq™. *Seminars in Pediatric Infectious Diseases*, 17(4):195-199.
Matsuno, S., Inouye, S. & Kono, R. 1977. Plaque assay of neonatal calf diarrhea virus and the neutralizing antibody in human sera. *Journal of Clinical Microbiology*, 5(1):1-4.
Matthijnssens, E., Johne, R., Patton, J. & Bányai, K. 2019. *Remove one species (Rotavirus E) from the genus Rotavirus*. https ://ictv.globa l/ICTV/proposals/2019.023M.zip Date of access: 19 August 2022.
Matthijnssens, J., Ciarlet, M., Heiman, E., Arijs, I., Delbeke, T., McDonald, S.M., ... Van Ranst, M. 2008. Full genome-based classification of rotaviruses reveals a common origin between human Wa-Like and porcine rotavirus strains and human DS-1-Like and Bovine rotavirus strains. *Journal of Virology*, 82(7):3204-3219.
Matthijnssens, J., Attoui, H., Bányai, K., Brussaard, C.P.D., Danthi, P., Del Vas, M., ... Wei, T. 2022. ICTV virus taxonomy profile: Sedoreoviridae 2022. *Journal of General Virology*, 103(10).
Matthijnssens, J., Ciarlet, M., Rahman, M., Attoui, H., Bányai, K., Estes, M.K., ... Van Ranst, M. 2008. Recommendations for the classification of group A rotaviruses using all 11 genomic RNA segments. *Archives of Virology*, 153(8):1621-1629.
McClain, B., Settembre, E., Temple, B.R., Bellamy, A.R. & Harrison, S.C. 2010. X-ray crystal structure of the rotavirus inner capsid particle at 3.8 A resolution. *Journal of Molecular Biology*, 397(2):587-599.
McNulty, M.S., Curran, W.L. & McFerran, J.B. 1976. The morphogenesis of a cytopathic bovine rotavirus in madin-darby bovine kidney cells. *Journal of General Virology*, 33(3):503-508.
McNulty, M.S., Todd, D., Allan, G.M., McFerran, J.B. & Greene, J.A. 1984. Epidemiology of rotavirus infection in broiler chickens: Recognition of four serogroups. *Archives of Virology*, 81(1-2):113-121.
Mebus, C.A., Wyatt, R.G. & Kapikian, A.Z. 1977. Intestinal Lesions Induced in Gnotobiotic Calves by the Virus of Human Infantile Gastroenteritis. *Veterinary Pathology*, 14(3):273-282.

Mebus, C.A., Kono, M., Underdahl, N.R. & Twiehaus, M.J. 1971. Cell culture propagation of neonatal calf diarrhea (scours) virus. *Canadian Veterinary Journal*, 12(3):69-72.
Mebus, C.A., Stair, E.L., Rhodes, M.B. & Twiehaus, M.J. 1973. Pathology of neonatal calf diarrhea induced by a coronavirus-like agent. *Veterinary Pathology*, 10(1):45-64.
Mebus, C.A., Underdahl, N.R., Rhodes, M.B. & Twiehaus, M.J. 1969. Calf diarrhea (Scours): Reproduced with a virus from a field outbreak. *Research Bulletin: Bulletin of the Agricultural Experiment Station of Nebraska*, (No. 233),
Mebus, C.A., Wyatt, R.G., Sharpee, R.L., Sereno, M.M., Kalica, A.R., Kapikian, A.Z. & Twiehaus, M.J. 1976. Diarrhea in gnotobiotic calves caused by the reovirus-like agent of human infantile gastroenteritis. *Infection and immunity*, 14(2):471-474.
Mellado, M.C.M., Mena, J.A., Lopes, A., Ramírez, O.T., Carrondo, M.J.T., Palomares, L.A. & Alves, P.M. 2009. Impact of physicochemical parameters on in vitro assembly and disassembly kinetics of recombinant triple-layered rotavirus-like particles.
Mihalov-Kovács, E., Gellért, Á., Marton, S., Farkas, S.L., Fehér, E., Oldal, M., ... Bányai, K. 2015. Candidate new rotavirus species in sheltered dogs, Hungary. *Emerging Infectious Diseases*, 21(4):660-663.
Mohsen, M.O., Zha, L., Cabral-Miranda, G. & Bachmann, M.F. 2017. Major findings and recent advances in virus–like particle (VLP)-based vaccines. In. Seminars in immunology. *Elsevier*. pp. 123-132.
Naik, S.P., Zade, J.K., Sabale, R.N., Pisal, S.S., Menon, R., Bankar, S.G., ... Dhere, R.M. 2017. Stability of heat stable, live attenuated Rotavirus vaccine (ROTASIIL®). *Vaccine*, 35(22):2962-2969.
Nakagomi, O., Nakagomi, T., Akatani, K. & Ikegami, N. 1989. Identification of rotavirus genogroups by RNA-RNA hybridization. *Molecular and Cellular Probes*, 3(3):251-261.
Nakagomi, O., Nakagomi, T., Hoshino, Y., Flores, J. & Kapikian, A.Z. 1987. Genetic analysis of a human rotavirus that belongs to subgroup I but has an RNA pattern typical of subgroup II human rotaviruses. *Journal of Clinical Microbiology*, 25(7):1159-1164.
Nelson, E.A.S., Widdowson, M.-A., Kilgore, P.E., Steele, D. & Parashar, U.D. 2009. A decade of the Asian rotavirus surveillance network: Achievements and future directions. *Vaccine*, 27:F1-F3.
Neumann, E. & Rosenheck, K. 1972. Permeability changes induced by electric impulses in vesicular membranes. *The Journal of Membrane Biology*, 10(1):279-290.
Norton, I.T., Goodall, D.M., Austen, K.R.J., Morris, E.R. & Rees, D.A. 1986. Dynamics of molecular organization in agarose sulphate. *Biopolymers*, 25(6):1009-1029.
O'Ryan, M.L., Matson, D.O., Estes, M.K. & Pickering, L.K. 1994. Acquisition of serum isotype-specific and G type-specific antirotavirus antibodies among children in day care centers. *The Pediatric infectious Disease Journal*, 13(10):890-895.
Ogden, K.M., Johne, R. & Patton, J.T. 2012. Rotavirus RNA polymerases resolve into two phylogenetically distinct classes that differ in their mechanism of template recognition. *Virology,* 431(1-2):50-57.
Ornstein, L. 1964. Disc electrophoresis. I. Background and theory. *Annals of the New York Academy of Sciences journal*, 121(2):321-349.
Page, N.A., Seheri, L.M., Groome, M.J., Moyes, J., Walaza, S., Mphahlele, J., ... Madhi, S.A. 2018. Temporal association of rotavirus vaccination and genotype circulation in South Africa: Observations from 2002 to 2014. *Vaccine*, 36(47):7231-7237.

Palomares, L.A. & Ramírez, O.T. 2009. Challenges for the production of virus-like particles in insect cells: The case of rotavirus-like particles. *Biochemical Engineering Journal*, 45(3):158-167.

Palomares, L.A., López, S. & Ramírez, O.T. 2002. Strategies for manipulating the relative concentration of recombinant rotavirus structural proteins during simultaneous production by insect cells. *Biotechnology and Bioengineering*, 78(6):635-644.

Parez, N., Fourgeux, C., Mohamed, A., Dubuquoy, C., Pillot, M., Dehee, A., ... Garbarg-Chenon, A. 2006. Rectal immunization with rotavirus virus-like particles induces systemic and mucosal humoral immune responses and protects mice against rotavirus infection. *Journal of Virology*, 80(4):1752-1761.

Patton, J.T., Chizhikov, V., Taraporewala, Z. & Chen, D. 2000. Virus Replication. In: Gray, J. & Desselberger, U., eds*. Rotaviruses: Methods and Protocols*. Totowa, NJ: Humana Press. pp. 33-66.

Pedley, S., Bridger, J.C., Chasey, D. & McCrae, M.A. 1986. Definition of Two New Groups of Atypical Rotaviruses. *Journal of General Virology*, 67(1):131-137.

Peixoto, C., Sousa, M.F.Q., Silva, A.C., Carrondo, M.J.T. & Alves, P.M. 2007. Downstream processing of triple layered rotavirus like particles. *Journal of Biotechnology*, 127(3):452-461.

Petrie, B.L., Graham, D.Y., Hanssen, H. & Estes, M.K. 1982. Localization of Rotavirus Antigens in Infected Cells by Ultrastructural Immunocytochemistry. *Journal of General Virology*, 63(2):457-467.

Petrie, B.L., Greenberg, H.B., Graham, D.Y. & Estes, M.K. 1984. Ultrastructural localization of rotavirus antigens using colloidal gold. *Virus Research*, 1(2):133-152.

Pham, T., Perry, J.L., Dosey, T.L., Delcour, A.H. & Hyser, J.M. 2017. The rotavirus NSP4 viroporin domain is a calcium-conducting ion channel. *Scientific Reports*, 7(1):43487.

Pisanelli, G., Martella, V., Pagnini, U., De Martino, L., Lorusso, E., Iovane, G. & Buonavoglia, C. 2005. Distribution of G (VP7) and P (VP4) genotypes in buffalo group A rotaviruses isolated in Southern Italy. *Veterinary Microbiology*, 110(1-2):1-6.

Poruchynsky, M.S., Maass, D.R. & Atkinson, P.H. 1991. Calcium depletion blocks the maturation of rotavirus by altering the oligomerization of virus-encoded proteins in the ER. *The Journal of Cell Biology*, 114(4):651-656.

Prasad, B.V., Rothnagel, R., Jiang, X. & Estes, M.K. 1994. Three-dimensional structure of baculovirus-expressed Norwalk virus capsids. *Journal of Virology*, 68(8):5117-5125.

Prasad, B.V.V., Wang, G.J., Clerx, J.P.M. & Chiu, W. 1988. Three-dimensional structure of rotavirus. *Journal of Molecular Biology*, 199(2):269-275.

Prasad, B.V.V., Burns, J.W., Marietta, E., Estes, M.K. & Chiu, W. 1990. Localization of VP4 neutralization sites in rotavirus by three-dimensional cryo-electron microscopy. *Nature*, 343(6257):476-479.

Rathi, R., Kadian, K., Khurana, B., Grover, Y. & Gulati, B. 2007. Evaluation of immune response to bovine rotavirus following oral and intraperitoneal inoculation in mice. *Indian Journal of Experimental Biology*, 45:212-216.

Ready, K.F.M., Sabara, M.I.J. & Babiuk, L.A. 1988. In vitro assembly of the outer capsid of bovine rotavirus is calcium-dependent. *Virology*, 167(1):269-273.

Redmond, M.J., Ijaz, M.K., Parker, M.D., Sabara, M.I., Dent, D., Gibbons, E. & Babiuk, L.A. 1993. Assembly of recombinant rotavirus proteins into virus-like particles and assessment of vaccine potential. *Vaccine*, 11(2):273-281.

Richard & David. 2009. Rotarix: A Rotavirus Vaccine for the World. *Clinical Infectious Diseases*, 48(2):222-228.
Rodger, S.M., Schnagl, R.D. & Holmes, I.H. 1977. Further biochemical characterization, including the detection of surface glycoproteins, of human, calf, and simian rotaviruses. *Journal of Virology*, 24(1):91-98.
Roest, S., Kapps-Fouthier, S., Klopp, J., Rieffel, S., Gerhartz, B. & Shrestha, B. 2016. Transfection of insect cell in suspension for efficient baculovirus generation. *MethodsX*, 3:371-377.
Roldão, A., Mellado, M.C.M., Lima, J.C., Carrondo, M.J.T., Alves, P.M. & Oliveira, R. 2012. On the effect of thermodynamic equilibrium on the assembly efficiency of complex multi-layered virus-like particles (VLP): the case of rotavirus VLP. *PLOS Computational Biology*, 8(2):e1002367.
Roldão, A., Vieira, H.L.A., Charpilienne, A., Poncet, D., Roy, P., Carrondo, M.J.T., ... Oliveira, R. 2007. Modeling rotavirus-like particles production in a baculovirus expression vector system: Infection kinetics, baculovirus DNA replication, mRNA synthesis and protein production. *Journal of Biotechnology*, 128(4):875-894.
Roy, P. 2004. Baculovirus solves a complex problem. *Nature Biotechnology*, 22(12):1527-1528.
Roy, P., Mikhailov, M. & Bishop, D.H. 1997. Baculovirus multigene expression vectors and their use for understanding the assembly process of architecturally complex virus particles. *Gene*, 190(1):119-129.
Ruiz, M.C., Cohen, J. & Michelangeli, F. 2000. Role of Ca^{2+} in the replication and pathogenesis of rotavirus and other viral infections. *Cell Calcium*, 28(3):137-149.
Saif, L.J. & Fernandez, F.M. 1996. Group a Rotavirus Veterinary Vaccines. *The Journal of Infectious Diseases*, 174:S98-S106.
Saif, L.J., Theil, K.W. & Bohl, E.H. 1978. Morphogenesis of porcine rotavirus in porcine kidney cell cultures and intestinal epithelial cells. *Journal of General Virology*, 39(2):205-217.
Saif, L.J., Bohl, E.H., Theil, K.W., Cross, R.F. & House, J.A. 1980. Rotavirus-like, calicivirus-like, and 23-nm virus-like particles associated with diarrhea in young pigs. *Journal of Clinical Microbiology*, 12(1):105-111.
Salgado, E.N., Garcia Rodriguez, B., Narayanaswamy, N., Krishnan, Y. & Harrison, S.C. 2018. Visualization of Ca^{2+} loss from rotavirus during cell entry. *Journal of Virology*.
Sambrook, J.F. & Russell, D.W. 2001. *Molecular cloning: A laboratory manual*. 1. 3rd. Cold Spring Harbor Laboratory Press.
Seheri, L.M., Magagula, N.B., Peenze, I., Rakau, K., Ndadza, A., Mwenda, J.M., ... Mphahlele, M.J. 2018. Rotavirus strain diversity in Eastern and Southern African countries before and after vaccine introduction. *Vaccine*, 36(47):7222-7230.
Settembre, E.C., Chen, J.Z., Dormitzer, P.R., Grigorieff, N. & Harrison, S.C. 2011. Atomic model of an infectious rotavirus particle. *The EMBO Journal*, 30(2):408-416.
Shagin, D.A., Barsova, E.V., Yanushevich, Y.G., Fradkov, A.F., Lukyanov, K.A., Labas, Y.A., ... Matz, M.V. 2004. GFP-like proteins as ubiquitous metazoan superfamily: evolution of functional features and structural complexity. *Molecular Biology and Evolution*, 21(5):841-850.
Sharp, P.A., Sugden, B. & Sambrook, J. 1973. Detection of two restriction endonuclease activities in Haemophilus parainfluenzae using analytical agarose-ethidium bromide electrophoresis. *Biochemistry*, 12(16):3055-3063.
Shaw, R.D., Vo, P.T., Offit, P.A., Coulson, B.S. & Greenberg, H.B. 1986. Antigenic mapping of the surface proteins of rhesus rotavirus. *Virology*, 155(2):434-451.

Singh, A. & Pandey, R. 1988. Analysis of electropherotypes of rotavirus from diarrheic feces of neonatal buffalo calves in India. *Acta Virologica*, 32:156-159.
Smith, G.E., Summers, M.D. & Fraser, M.J. 1983. Production of human beta interferon in insect cells infected with a baculovirus expression vector. *Molecular and Cellular Biology*, 3(12):2156-2165.
Snodgrass, D.R., Smith, W., Gray, E.W. & Herring, J.A. 1976. A rotavirus in lambs with diarrhoea. *Research in Veterinary Science*, 20(1):113-114.
Stencel-Baerenwald, J.E., Reiss, K., Reiter, D.M., Stehle, T. & Dermody, T.S. 2014. The sweet spot: defining virus–sialic acid interactions. *Nature Reviews Microbiology*, 12(11):739-749.
Sternberger, L.A., Hardy JR, P.H., Cuculis, J.J. & Meyer, H.G. 1970. The unlabeled antibody enzyme method of immunohistochemistry preparation and properties of soluble antigen-antibody complex (horseradish peroxidase-antihorseradish peroxidase) and its use in identification of spirochetes. *Journal of Histochemistry & Cytochemistry*, 18(5):315-333.
Tamminen, K., Heinimäki, S., Gröhn, S. & Blazevic, V. 2020. Internalization and antigen presentation by mouse dendritic cells of rotavirus VP6 preparations differing in nanostructure. *Molecular Immunology*, 123:26-31.
Tamminen, K., Heinimäki, S., Gröhn, S. & Blazevic, V. 2021. Fusion protein of rotavirus VP6 and SARS-CoV-2 receptor binding domain induces T cell responses. *Vaccines*, 9(7):733.
Tate, J.E., Burton, A.H., Boschi-Pinto, C. & Parashar, U.D. 2016. Global, regional, and national estimates of rotavirus mortality in children <5 years of age, 2000–2013. *Clinical Infectious Diseases*, 62(suppl 2):S96-S105.
Tate, J.E., Burton, A.H., Boschi-Pinto, C., Steele, A.D., Duque, J. & Parashar, U.D. 2012. 2008 estimate of worldwide rotavirus-associated mortality in children younger than 5 years before the introduction of universal rotavirus vaccination programmes: a systematic review and meta-analysis. *The Lancet Infectious Diseases*, 12(2):136-141.
Taylor, J.A., O'Brien, J.A. & Yeager, M. 1996. The cytoplasmic tail of NSP4, the endoplasmic reticulum-localized non-structural glycoprotein of rotavirus, contains distinct virus binding and coiled coil domains. *The EMBO Journal*, 15(17):4469-4476.
Theart, L.J.C. 2022. *Expression of rotavirus proteins and virus-like particles in bacterial and insect cells.* North-West University. (Dissertation).
Tian, P., Hu, Y., Schilling, W.P., Lindsay, D.A., Eiden, J. & Estes, M.K. 1994. The nonstructural glycoprotein of rotavirus affects intracellular calcium levels. *Journal of Virology*, 68(1):251-257.
Torres-Medina, A., Wyatt, R.G., Mebus, C.A., Underdahl, N.R. & Kapikian, A.Z. 1976. Diarrhea caused in gnotobiotic piglets by the reovirus-like agent of human infantile gastroenteritis. *The Journal of Infectious Diseases*, 133(1):22-27.
Towbin, H. & Gordon, J. 1984. Immunoblotting and dot immunobinding—current status and outlook. *Journal of Immunological Methods*, 72(2):313-340.
Towbin, H., Staehelin, T. & Gordon, J. 1979. Electrophoretic transfer of proteins from polyacrylamide gels to nitrocellulose sheets: procedure and some applications. *Proceedings of the National Academy of Sciences*, 76(9):4350-4354.
Trask, S.D. & Dormitzer, P.R. 2006. Assembly of highly infectious rotavirus particles recoated with recombinant outer capsid proteins. *Journal of Virology*, 80(22):11293-11304.

Trask, S.D., McDonald, S.M. & Patton, J.T. 2012. Structural insights into the coupling of virion assembly and rotavirus replication. *Nature Reviews Microbiology*, 10(3):165-177.
Troeger, C., Khalil, I.A., Rao, P.C., Cao, S., Blacker, B.F., Ahmed, T., ... Reiner, R.C. 2018. Rotavirus Vaccination and the Global Burden of Rotavirus Diarrhea Among Children Younger Than 5 Years. *JAMA Pediatrics*, 172(10):958.
Troeger, C., Blacker, B.F., Khalil, I.A., Rao, P.C., Cao, S., Zimsen, S.R., ... Reiner, R.C. 2018. Estimates of the global, regional, and national morbidity, mortality, and aetiologies of diarrhoea in 195 countries: a systematic analysis for the Global Burden of Disease Study 2016. *The Lancet Infectious Diseases*, 18(11):1211-1228.
Van Gennip, R.G.P., Van De Water, S.G.P., Potgieter, C.A., Wright, I.M., Veldman, D. & Van Rijn, P.A. 2012. Rescue of recent virulent and avirulent field strains of bluetongue virus by reverse genetics. *PLoS ONE*, 7(2):e30540.
Varghese, T., Kang, G. & Steele, A.D. 2022. Understanding rotavirus vaccine efficacy and effectiveness in countries with high child mortality. *Vaccines*, 10(3):346.
Vaughn, J.L., Goodwin, R.H., Tompkins, G.J. & McCawley, P. 1977. The establishment of two cell lines from the insect Spodoptera frugiperda (Lepidoptera; Noctuidae). *In Vitro*, 13(4):213-217.
Vesikari, T., Isolauri, E., Delem, A., D'Hondt, E., André, F. & Zissis, G. 1983. Immunogenicity and safety of live oral attenuated bovine rotavirus vaccine strain RIT 4237 in adults and young children. *The Lancet*, 322(8354):807-811.
Vesikari, T., Isolauri, E., D'Hondt, E., Delem, A., André, F. & Zissis, G. 1984. Protection of infants against rotavirus diarrhoea by RIT 4237 attenuated bovine rotavirus strain vaccine. *The Lancet*, 323(8384):977-981.
Vieira, H., Estêvão, C., Roldão, A., Peixoto, C., Sousa, M., Cruz, P. & Alves, P. 2005. Triple layered rotavirus VLP production: Kinetics of vector replication, mRNA stability and recombinant protein production. *Journal of Biotechnology*, 120:72-82.
Walker, P.J., Siddell, S.G., Lefkowitz, E.J., Mushegian, A.R., Adriaenssens, E.M., Dempsey, D.M., ... Davison, A.J. 2020. Changes to virus taxonomy and the statutes ratified by the International Committee on Taxonomy of Viruses (2020). *Archives of Virology*, 165(11):2737-2748.
Wang, Q., Bosch, B.-J., Vlak, J.M., van Oers, M.M., Rottier, P.J. & van Lent, J.W.M. 2016. Budded baculovirus particle structure revisited. *Journal of Invertebrate Pathology*, 134:15-22.
Warburg, O. 1942. Isolation and crystallization of enolase. *Biochemische Zeitschrift*, 310:384-421.
Ward, R.L., Knowlton, D.R. & Pierce, M.J. 1984. Efficiency of human rotavirus propagation in cell culture. *Journal of Clinical Microbiology*, 19(6):748-753.
Ward, R.L., Knowlton, D.R. & Greenberg, H.B. 1988. Phenotypic mixing during coinfection of cells with two strains of human rotavirus. *Journal of Virology*, 62(11):4358-4361.
Ward, R.L., Knowlton, D.R., Greenberg, H.B., Schiff, G.M. & Bernstein, D.I. 1990. Serum-neutralizing antibody to VP4 and VP7 proteins in infants following vaccination with WC3 bovine rotavirus. *Journal of virology*, 64(6):2687-2691.
Ward, R.L., McNeal, M.M., Sander, D.S., Greenberg, H.B. & Bernstein, D.I. 1993. Immunodominance of the VP4 neutralization protein of rotavirus in protective natural infections of young children. *Journal of Virology*, 67(1):464-468.
Ward, R.L., Clemens, J.D., Sack, D.A., Knowlton, D.R., McNeal, M.M., Huda, N., ... Schiff, G.M. 1991. Culture adaptation and characterization of group A rotaviruses

causing diarrheal illnesses in Bangladesh from 1985 to 1986. *J Clin Microbiol*, 29(9):1915-1923.
Waring, M.J. 1965. Complex formation between ethidium bromide and nucleic acids. *Journal of Molecular Biology*, 13(1):269-282.
Wilfinger, W.W., Mackey, K. & Chomczynski, P. 1997. Effect of pH and ionic strength on the spectrophotometric assessment of nucleic acid purity. *Biotechniques*, 22(3):474-481.
Wyatt, R.G., Sly, D.L., London, W.T., Palmer, A.E., Kalica, A.R., Van Kirk, D.H., ... Kapikian, A.Z. 1976. Induction of diarrhea in colostrum-deprived newborn rhesus monkeys with the human reovirus-like agent of infantile gastroenteritis. *Archives of Virology*, 50(1-2):17-27.
Wyatt, R.G., Kapikian, A.Z., Greenberg, H.B., Kalica, A.R., Flores, J., Hoshino, Y., ... Levine, M.M. 1983. Development of vaccines against rotavirus disease. *Progress in Food & Nutrition Science*, 7(3-4):189-192.
Yao, L., Wang, S., Su, S., Yao, N., He, J., Peng, L. & Sun, J. 2012. Construction of a baculovirus-silkworm multigene expression system and its application on producing virus-like particles. *PLoS ONE*, 7(3):e32510.
Zeng, C.Q.Y., Labbé, M., Cohen, J., Prasad, B.V.V., Chen, D., Ramig, R.F. & Estes, M.K. 1994. Characterization of rotavirus VP2 particles. *Virology*, 201(1):55-65.
Zeugin, A. & Hartley, J.L. 1985. Ethanol precipitation of DNA. *Focus*, 7:1-2,
Zhou, H., Guo, L., Wang, M., Qu, J., Zhao, Z., Wang, J. & Hung, T. 2011. Prime immunization with rotavirus VLP 2/6 followed by boosting with an adenovirus expressing VP6 induces protective immunization against rotavirus in mice. *Virology Journal*, 8:3-3.